UNIVERSITY OF SOUTH FLORIDA

Department of Civil and Environmental Engineering

EFFECT OF POLYMER SLURRY STABILIZATION ON DRILLED SHAFT SIDE SHEAR OVER TIME

BDV25 TWO977-19

FINAL REPORT

Gray Mullins, Ph.D., P.E.
Principal Investigator
And
Graduate Researchers
Lucas Caliari, Ph.D.,
Kelly Costello, E.I., Ph.D. Candidate

Disclaimer

The opinions, findings, and conclusions expressed in this publication are those of the authors and not necessarily those of the State of Florida Department of Transportation.

APPROXIMATE CONVERSIONS TO SI UNITS

SYMBOL	WHEN YOU KNOW	MULTIPLY BY	TO FIND	SYMBOL
		LENGTH		
in	inches	25.4	millimeters	mm
ft	feet	0.305	meters	m
yd	yards	0.914	meters	m
mi	miles	1.61	kilometers	km

SYMBOL	WHEN YOU KNOW	MULTIPLY BY	TO FIND	SYMBOL
		AREA		
in^2	square inches	645.2	square millimeters	mm^2
ft^2	square feet	0.093	square meters	m^2
yd^2	square yard	0.836	square meters	m^2
ac	acres	0.405	hectares	ha
mi^2	square miles	2.59	square kilometers	km^2

SYMBOL	WHEN YOU KNOW	MULTIPLY BY	TO FIND	SYMBOL
		VOLUME		
fl oz	fluid ounces	29.57	milliliters	mL
gal	gallons	3.785	liters	L
ft^3	cubic feet	0.028	cubic meters	m^3
yd^3	cubic yards	0.765	cubic meters	m^3
		NOTE: volumes greater than 1000 L shall be shown in m^3		

SYMBOL	WHEN YOU KNOW	MULTIPLY BY	TO FIND	SYMBOL
		MASS		
oz	ounces	28.35	grams	g
lb	pounds	0.454	kilograms	kg
T	short tons (2000 lb)	0.907	megagrams (or "metric ton")	Mg (or "t")

SYMBOL	WHEN YOU KNOW	MULTIPLY BY	TO FIND	SYMBOL
TEMPERATURE (exact degrees)				
°F	Fahrenheit	5 (F-32)/9 or (F-32)/1.8	Celsius	°C

SYMBOL	WHEN YOU KNOW	MULTIPLY BY	TO FIND	SYMBOL
ILLUMINATION				
fc	foot-candles	10.76	lux	lx
fL	foot-Lamberts	3.426	candela/m^2	cd/m^2

SYMBOL	WHEN YOU KNOW	MULTIPLY BY	TO FIND	SYMBOL
FORCE and PRESSURE or STRESS				
lbf	poundforce	4.45	newtons	N
lbf/in^2	poundforce per square inch	6.89	kilopascals	kPa
kip	kilopound	4.45	kilonewtons	kN

APPROXIMATE CONVERSIONS TO SI UNITS

SYMBOL	WHEN YOU KNOW	MULTIPLY BY	TO FIND	SYMBOL
LENGTH				
mm	millimeters	0.039	inches	in
m	meters	3.28	feet	ft
m	meters	1.09	yards	yd
km	kilometers	0.621	miles	mi

SYMBOL	WHEN YOU KNOW	MULTIPLY BY	TO FIND	SYMBOL
AREA				
mm^2	square millimeters	0.0016	square inches	in^2
m^2	square meters	10.764	square feet	ft^2
m^2	square meters	1.195	square yards	yd^2
ha	hectares	2.47	acres	ac
km^2	square kilometers	0.386	square miles	mi^2

SYMBOL	WHEN YOU KNOW	MULTIPLY BY	TO FIND	SYMBOL
VOLUME				
mL	milliliters	0.034	fluid ounces	fl oz
L	liters	0.264	gallons	gal
m³	cubic meters	35.314	cubic feet	ft³
m³	cubic meters	1.307	cubic yards	yd³

YMBOL	HEN YOU KNOW	MULTIPLY BY	TO FIND	YMBOL
MASS				
g	grams	0.035	ounces	oz
kg	kilograms	2.202	pounds	lb
Mg (or "t")	igrams (or "metric ton")	1.103	hort tons (2000 lb)	T

SYMBOL	WHEN YOU KNOW	MULTIPLY BY	TO FIND	SYMBOL
TEMPERATURE (exact degrees)				
°C	Celsius	1.8C+32	Fahrenheit	°F

SYMBOL	WHEN YOU KNOW	MULTIPLY BY	TO FIND	SYMBOL
ILLUMINATION				
lx	lux	0.0929	foot-candles	fc
cd/m²	candela/m²	0.2919	foot-Lamberts	fl

SYMBOL	WHEN YOU KNOW	MULTIPLY BY	TO FIND	SYMBOL
FORCE and PRESSURE or STRESS				
N	newtons	0.225	poundforce	lbf
kPa	kilopascals	0.145	dforce per square inch	lbf/in²
kN	kilonewtons	0.225	kilopound	kip

*SI is the symbol for the International System of Units. Appropriate rounding should be made to comply with Section 4 of ASTM E380.

Technical Report Documentation Page

1. Report No.	2. Government Accession No.	3. Recipient's Catalog No.

4. Title and Subtitle	5. Report Date
Effect of Polymer Slurry Stabilization on Drilled Shaft Side Shear Over Time	January 2018
	6. Performing Organization Code

7. Author(s)	8. Performing Organization Report No.
G. Mullins and L. Caliari	

9. Performing Organization Name and Address	10. Work Unit No. (TRAIS)
University of South Florida Department of Civil and Environmental Engineering 4202 E. Fowler Avenue, ENB 118s Tampa, FL 33620	
	11. Contract or Grant No. BDV25 977-19

12. Sponsoring Agency Name and Address	13. Type of Report and Period Covered
Florida Department of Transportation 605 Suwannee Street, MS 30 Tallahassee, FL 32399	Final Report 04/15-03/18
	14. Sponsoring Agency Code

15. Supplementary Notes
FDOT Project Manager:
Juan Castellanos

16. Abstract

Slurry supported construction of drilled shafts requires highly engineered fluid made from mineral clay or polymer powder mixed with water. In the state of Florida the present open excavation time limit / specification is directed at the use of mineral slurry that forms a layer of clay along the excavation walls and thereby can affect the as-built concrete / soil interface bond. As use of polymer slurry is relatively new in the state, there is no definitive specification that addresses the slurry exposure time of open excavations supported by polymer slurry.

The primary objective of this study was to quantify the effects on side shear (if any) from prolonged open excavation times where polymer slurry is present. To this end, both small and large scale field evaluations of shafts constructed with polymer slurry were performed. Bentonite supported shafts were also cast and tested as means for comparison.

Small scale field tests involved casting 32, 1/10th scale shafts constructed with four different slurry products including bentonite and three different commercially available polymer products. Exposure times were varied from 0 to 96 hours. Results of the small scale tests showed a clear reduction in capacity over time for bentonite constructed shafts where up to a 50% reduction was observed after 96hrs of exposure. but no affects were noted for polymer constructed shafts. On average, polymer shafts exhibited 26% higher side shear than bentonite shafts.

Full scale field testing entailed casting 5, 2ft diameters shafts with exposure times of 2 and 48 hours with both bentonite and polymer slurry. In this series of tests no reduction in capacity was noted with prolonged slurry exposure times. However, like the small scale testing, polymer shafts performed better (15%) in side shear resistance than bentonite shafts.

Finally, automated slurry testing performed at several sites indicated that polymer slurry viscosity was often lower than manufacturer recommendations throughout the length of the shaft despite meeting the minimum acceptance criteria at the bottom of the shaft where testing is always performed. The results of these tests showed that side wall stability was drastically reduced as the polymer slurry viscosity fell below 40 sec/qt. Where slurry was mixed in the casing, large variations in slurry viscosity was noted. Given these findings three recommendations were made: (1) slurry should be tested at bottom, middle and top of the shaft regardless of shaft length, (2) all slurry should be premixed and meet specifications prior to being introduction, and (3) polymer slurry should always target a minimum viscosity of 50sec/qt. This minimum slurry viscosity would not necessarily be suitable for all soil conditions but falling below it presents opportunity for sidewall collapse.

17. Key Words	18. Distribution Statement
Drilled shaft, polymer slurry, bentonite slurry, load test	No restrictions.

19. Security Classif. (of this report)	20. Security Classif. (of this page)	21. No. of Pages	22. Price
Unclassified.	Unclassified.	205	

Form DOT F 1700.7 (8-72) Reproduction of completed page authorized

Acknowledgments

Executive Summary

Slurry supported construction of drilled shafts requires highly engineered fluid made from mineral clay or polymer powder mixed with water. In the state of Florida the present open excavation time limit / specification is directed at the use of mineral slurry that forms a layer of clay along the excavation walls and thereby can affect the as-built concrete / soil interface bond. As use of polymer slurry is relatively new in the state, there is no definitive specification that addresses the slurry exposure time of open excavations supported by polymer slurry.

The primary objective of this study was to quantify the effects on side shear (if any) from prolonged open excavation times where polymer slurry is present. To this end, both small and large scale field evaluations of shafts constructed with polymer slurry were performed. Bentonite supported shafts were also cast and tested as means for comparison.

Small scale field tests involved casting 32, $1/10^{th}$ scale shafts constructed with four different slurry products including bentonite and three different commercially available polymer products. Exposure times were varied from 0 to 96 hours. Results of the small scale tests showed a clear reduction in capacity over time for bentonite constructed shafts where up to a 50% reduction was observed after 96hrs of exposure. but no affects were noted for polymer constructed shafts. On average, polymer shafts exhibited 26% higher side shear than bentonite shafts.

Full scale field testing entailed casting 5, 2ft diameters shafts with exposure times of 2 and 48 hours with both bentonite and polymer slurry. In this series of tests no reduction in capacity was noted with prolonged slurry exposure times. However, like the small scale testing, polymer shafts performed better (15%) in side shear resistance than bentonite shafts.

Finally, automated slurry testing performed at several sites indicated that polymer slurry viscosity was often lower than manufacturer recommendations throughout the length of the shaft despite meeting the minimum acceptance criteria at the bottom of the shaft where testing is always performed. The results of these tests showed that side wall stability was drastically reduced as the polymer slurry viscosity fell below 40 sec/qt. Where slurry was mixed in the casing, large variations in slurry viscosity was noted. Given these findings three recommendations were made: (1) slurry should be tested at bottom, middle and top of the shaft regardless of shaft length, (2) all slurry should be premixed and meet specifications prior to being introduction, and (3) polymer slurry should always target a minimum viscosity of 50sec/qt. This minimum slurry viscosity would not necessarily be suitable for all soil conditions but falling below it presents opportunity for sidewall collapse.

Table of Contents

List of Tables

List of Figures

Intentionally Left Blank

Chapter One: Introduction

Wet construction of drilled shafts in the state of Florida requires the excavation to be stabilized by either mechanical (casing) or fluid pressure (slurry) systems due to high water elevations encountered. Therein, lateral pressure / support is radially applied to the excavation walls by the lateral compressive strength of the casing or by the net fluid pressure of a slurry level maintained above the ground water table. Depending on the slurry type (mineral, polymer, or natural), a lower to higher differential fluid level is required, respectively.

1.1   Background

Until recently, FDOT allowed only mineral slurry to be used to stabilize the drilled shaft excavations during the installation of drilled shafts foundations (FDOT, 2007). Specification changes made in July 2008 allowed the use of polymer slurry but limited its use to drilled shaft excavations up to 60 inches in diameter installed to support mast arms, cantilever signs, overhead truss signs, high mast light poles or other miscellaneous structures (FDOT, 2009).

Although both mineral and polymer slurry have been shown to be effective in stabilizing an excavation (and now both permitted in certain cases), the mechanisms by which each provides stability are quite different. Mineral slurries depend on minimum clay mineral concentration to for an impervious barrier (filter cake) that quickly forms along the sidewalls; this works in conjunction with the lateral pressure from a slurry head differential relative to the ground water level. As literature is not conclusive, the time required to form a mineral filter cake is not certain. The window of shown effect ranges from 1 to 24hrs where 1hr showed the least effect and 24hrs showed more effect. Beyond 24hrs, the effect is not well documented and the exact time at which adverse effects cease to increase (between 1 and 24hrs) is similarly poorly documented. However, polymer slurries work completely differently.

Polymer slurry binds the soil in a quasi-cohesive manner making it less susceptible to low pressure sloughing behind the tool. However, the principle is not exactly the same as mineral slurries: for polymer slurry to stabilize the hole, it must constantly flow as no filter cake is formed. But similar to mineral slurry, this causes radially outward pressure on the walls. Figure 1.1 shows the soil around a model shaft that became wetted by mineral slurry and where the amount of radial flow was uniform in thickness due to filter cake formation regardless of depth. It also shows the same size shaft excavation where polymer slurry was used and that a larger zone around the shaft was stabilized proportional to higher net fluid pressure and more volume that flowed into the soil at higher pressure. There was no water table around either shaft.

Figure 1.1 Bentonite filter cake and wetted soil around model shaft (left), polymer stabilized soil around same size model excavation (right).

While the effects of exposure time for mineral slurry have been partially quantified in literature, the time-dependent effects of polymer slurry exposure have not. At present the FDOT 2018 Specifications, subarticle 455-15.11.5 state:

> *Any unclassified excavation work lasting more than 36 hours (measured from the beginning of excavation for all methods except the Permanent Casing Method, which begins at the time excavation begins below the casing) before placement of the concrete requires overreaming the sidewalls to the depth of softening or removing excessive slurry cake buildup. Ensure that the minimum depth of overreaming the shaft sidewall is 1/2inches and the maximum depth is 3 inches. . .*
>
> *. . . When using mineral slurry, adjust excavation operations so that the maximum time that slurry is in contact with the bottom 5ft of the shaft (from time drilling to concreting) does not exceed 12 hours. If exceeding the 12 hour time limit, overream the bottom 5ft of shaft . . .*

The primary motivation for this specification appears to be that mineral slurry is known to have adverse effects in a shorter time frame. To a lesser extent or by extension one might conclude, that polymer slurry does not have the same concerns and that a second threshold of adverse effects commences at exposure times beyond 36 hours. (Note: based on results observed during

this study, the July 2018 version of this specification will remove the 12 and 36 hours limitations for polymer slurries).

It was the focus of this research study to identify if there is a time limit after which adverse effects from polymer slurry exposure may exist. The primary objective of this study was to quantify the effects on side shear (if any) from prolonged open excavation times where polymer slurry is present. To this end, both laboratory and field evaluations of shafts constructed with polymer slurry were performed.

1.2 Organization of the Report

This study entailed four experimentally based tasks in the process of quantifying the effects of prolonged exposure time to polymer slurries on the resulting side shear of drilled shafts. These are presented in the four ensuing chapters. Chapter 2 provides a background for slurry types, shaft stability using slurry, and design methods. Chapter 3 evaluates past studies involving slurry supported excavations and the effects on capacity. Chapter 4 presents the experimental approach to isolate the effects of slurry exposure (and slurry type) on the side shear resistance from 32, 1/10 scale shafts constructed under field conditions. Based on the results of Chapter 4, Chapter 5 outlines the construction, testing and performance of selected full scale shafts constructed with both short and prolonged exposure times (both mineral and polymer slurry). Finally, the results of the entire study are summarized in Chapter 6; recommendations are provided based on the study findings.

Chapter Two: Literature Review

This study focuses on the effects that construction methods can have on shaft performance. Specifically, this chapter discusses the wet construction technique that uses hydrostatic / slurry stabilization and how it may negatively affect the side shear capacity of drilled shafts. State and federal specifications intended to limit these adverse effects are discussed along with previous investigative studies addressing the effects on side shear resistance.

2.1   Background

A drilled shaft is a cylindrical column of concrete, constructed by pouring fluid concrete into an excavated hole for the purpose of supporting a structure (O'Neill and Reese, 1999). These deep foundation elements also referred to as drilled piers, caissons, cast-in-drilled-hole piles, and bored piles are typically constructed in three main steps: (1) excavation, (2) reinforcement placement and (3) concreting (Figure 2.1). In this process, large diameter augers are used to excavate the soil/rock therefore the surrounding in situ material is used as formwork for the shaft. Hence, proper construction process is critical to the performance of the shaft (Deese, 2014). Once excavated, the placement of steel reinforcement is followed by the concreting process. Though the process seems quite simple, logistical issues exist within this process; the most prevalent being borehole stabilization. It is essential that collapse or sloughing of the boring walls is avoided during the construction process. Stabilization issues can be circumvented mechanically, hydrostatically or by a combination of both methods (Mullins et al., 2014).

Figure 2.1 Drilled shaft construction: excavation (left), reinforcement cage placement (middle), concreting (right) (Mullins et al., 2014).

Mechanical stabilization involves using a full length casing to support the walls of the boring during excavation. The casing is hollow to facilitate the removal of material within the walls of the casing once advanced to the appropriate depth. If the casing is temporary, the casing is extracted after concreting but before the concrete cures whereas in the permanent casing method, the casing remains in place. For the temporary casing method, the concrete must maintain enough slump to push against the walls of the boring once the casing has been extracted. This is necessary to ensure sufficient side shear is generated at the interface of concrete and soil or rock.

Hydrostatic stabilization (wet construction) uses a fluid (slurry) to support the boring. Slurry levels are maintained at greater elevations (4-8ft) than the excavation resulting in a net pressure on the walls of the boring. The net pressure direction is outward and must at all times overcome active soil pressures pushing into the excavation. Hence, instead of material entering the excavation, slurry flows from the excavation into the in situ soils.

Prior to concreting, the bottom of the excavation is cleaned to remove loose soil or debris that may have settled during the construction process. Once excavation has been cleaned, the reinforcement cage is placed within the excavated hole. Concrete is then introduced with a tremie placed at the bottom of the borehole. This is to ensure all of the slurry is displaced during the concreting process and mixture of the two materials is avoided (FHWA, 2010). Surface casings are often required to: (1) stabilize surface soils and prevent collapse near the top of the shaft, (2) aid in tool alignment and position and (3) increase the allowable level of slurry (FDOT, 2016). The wet / slurry method of construction (Figure 2.2) is the method used for the testing discussed later in this report.
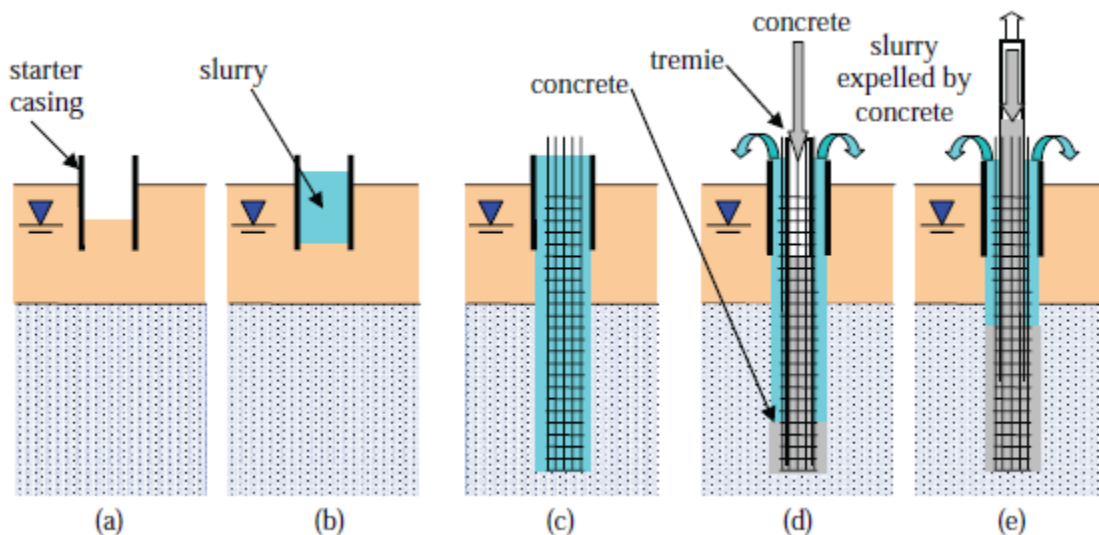
Figure 2.2 Wet construction method: surface casing (a), slurry introduction (b), completed excavation and reinforcement placement (c), concrete introduction through tremie (d), tremie removal and slurry expulsion during concreting (FHWA, 2010).

5

2.2   Drilling Fluids (Slurries)

Slurry can be classified as either natural, mineral or polymer. Natural slurry refers to water (salt or fresh) and is typically used with casing methods to counterbalance the influx of water through the tip of the excavation. Mineral slurries have been used historically and are most commonly used in wet construction when full length temporary casing is not used for stability. They are formed by mixing water with dry clay powder, bentonite (sodium montmorillonite) or attapulgite (calcium montmorillonite), to form a slurry. Polymer slurries are typically formed by mixing polyacrylamides with water (Mullins et al., 2014).

2.2.1   Mineral Slurries

The mineral montmorillonite, of the smectite group, which has an enormous absorption capacity serves as the foundation for mineral slurries. Montmorillonite is processed into the powdered clays, bentonite, attapulgite and sepiolite which are then mixed with water to form mineral slurries. Bentonite is the most common of powdered clay used for most excavations while attapulgite and sepiolite are used for saline excavation. When mixed with water, the clay forms plate-like particles which are suspended in solution. These plates give mineral slurries the ability to suspended solids but must first be fully hydrated. It is common practice to give mineral slurries, bentonite in particular, 24 hours to fully hydrate and achieve the desired viscosity (FHWA, 2010). Bentonite slurries are permitted to contain 4% suspended sand by volume at the time of concreting and if excess solids are encountered in the slurry, de-sanding is required to avoid concrete contamination.

Bentonite slurry stabilizes the excavation by first providing positive fluid pressure on the borehole walls and secondly by forming a filter cake to "seal" the excavation and slow slurry loss. The filter cake forms when water from the slurry seeps into the pores of the in situ soil leaving the suspended clay lodged in the voids. As this process continues, the clay continues to build up and form a thin layer on the walls of the borehole. Once the filter cake is formed, it is essential to maintain the positive pressure on the walls of the borehole to prevent back flushing of the filter cake (FHWA, 2010). Unfortunately, the filter cake, essential to the stabilization of the borehole, has been proven to degrade the soil to concrete interface with increased exposure times and hence, reduce side shear resistance. Figure 2.3 illustrates how bentonite slurry works to stabilize excavations.
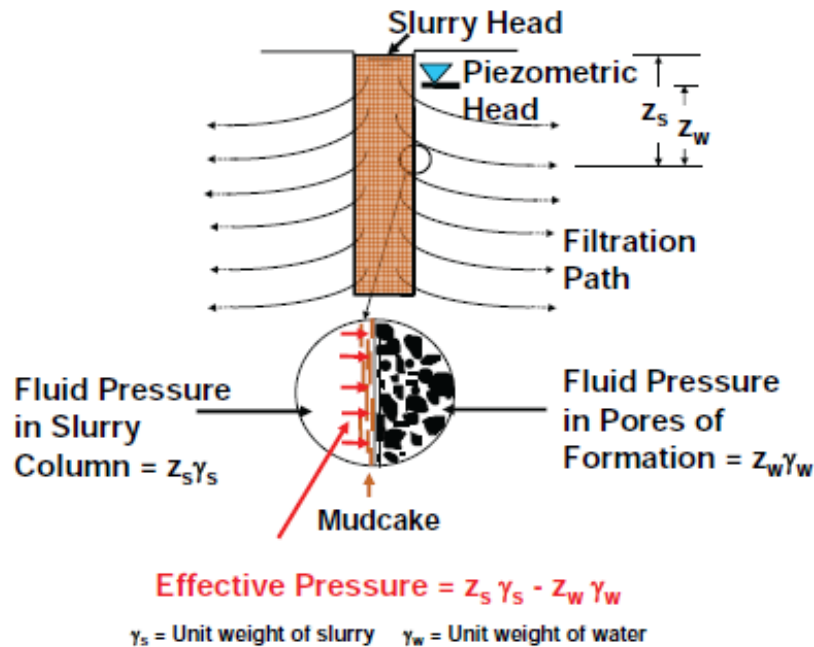
Figure 2.3 Filtration and filter cake formation with bentonite slurries (FHWA, 2010).

Bentonite slurry has a density slightly greater than water and develops gel strength that allows for transport of suspended cuttings throughout the excavation and during concreting. These suspended solids increase the density (and sometimes the viscosity) of the slurry which may be problematic as slurry too dense or viscous cannot be easily displaced by fluid concrete. Therefore, slurry viscosity, density must be monitored throughout the excavation and prior to concreting sand content is also tested to ensure the slurry is acceptable.

Due to filter cake formation, environmental agencies have required special disposal of bentonite slurry. This has become an additional cost for contractors as proper training to handle the fluids is necessary. Mineral slurries must be maintained in a closed system, where slurry removed from the borehole is reclaimed (and often reused) to ensure no slurry contaminates surface water or clogs sewers (FHWA, 2010).

While the filter cake formation is the primary source of effectiveness relative to other slurry types, the infiltration rate into the soil slows drastically as the filter cake forms. This means that at some point, the filter cake ceases to increase in thickness as no further infiltration can occur. Therefore, there is a time after which no further side shear degradation will occur; this time has been poorly identified and was investigated as a secondary objective of this study.

2.2.2   Polymer Slurries

Due to the disposal issue with mineral slurries, polymer slurries have become popular among contractors because they can be readily disposed into sewer systems or at waste water treatment plants, with approval. Alternately, the polymer can be broken down with calcium hypochlorite or

7

simply diluted with water and disposed of on site. Polymer slurries can be either natural or synthetic in nature. The term polymer is very broad and encompasses various compounds, all having a high molecular weight and repeating chains of individual units (monomers). Generally, the synthetic slurries used for excavation consist of long, chain-like hydrocarbon molecules which form a three-dimensional lattice or web-like structure (FHWA, 2010).

The most common polymers are polyacrylamides (PAMs) formed from the monomers, acrylamides and acrylic acid. These chains have similar electrical charges and repel each other to remain in suspension. When polymer slurries were first developed, partial hydrolyzation was used to adjust the charge on the backbone of the chain, resulting in a partially-hydrolyzed polyacrylamide or "PHPA". Today, highly engineered polymeric materials are also used as polymer slurries and are produced by combining acrylamides with other chemicals. Natural polymers such as cellulose have also been combined with synthetic polymers to improve their performance (FHWA, 2010).

Polymer slurries stabilize the excavation by infiltrating soils throughout the excavation process which requires that (like mineral slurry) the slurry column remain above the piezometric level. Where mineral slurries are suspensions, polymer slurries are solutions with a dry powder concentration $1/100^{th}$ that of mineral slurry. As a result, no suspended solids other than cuttings are present. Assuming cuttings are not appreciably different from the surrounding soils (source of cuttings) no filter cake is formed. Therefore, polymer slurries continuously infiltrate the soil and attention must be given to maintaining slurry level in the excavation especially in extended overnight periods.

As seen in Figure 2.4, polymer chains wrap around soil particles and tend to result in particles that clump together. These agglomerated particles fall out of suspension easily and settle on the bottom of the borehole. For this reason, de-sanding of the slurry is not typically required with polymer slurries but the fallen particles must be removed from the borehole after a sufficient wait time. Therefore, polymer slurries can be quickly re-used for subsequent shafts without substantial processing; slurry contaminated with concrete must be removed and discarded.
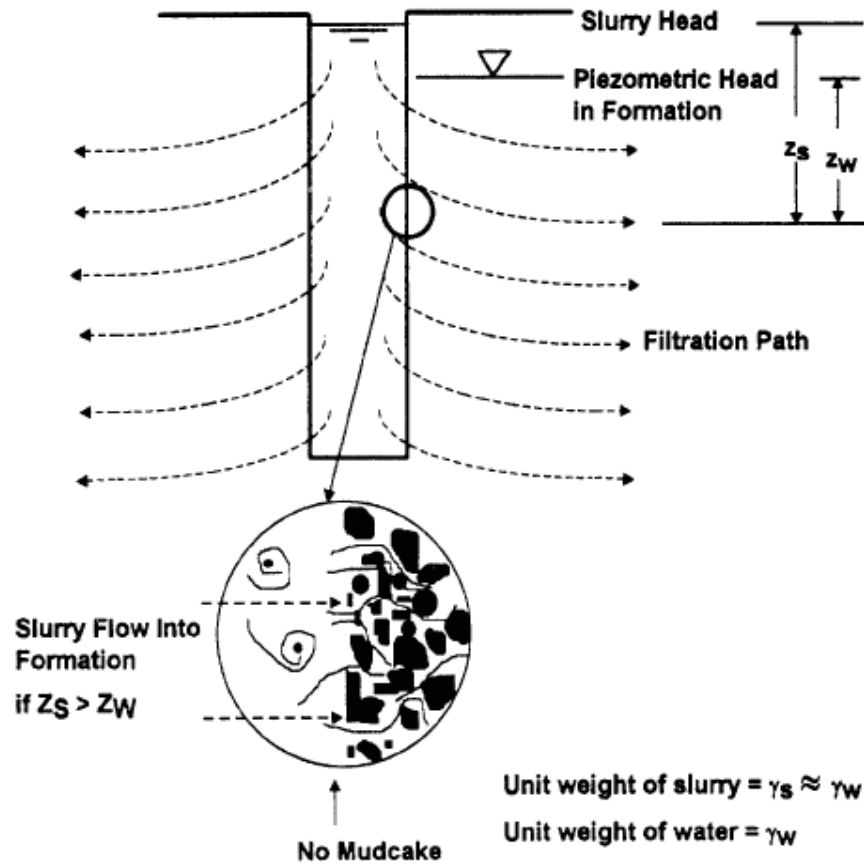
Figure 2.4 Mechanism of borehole stabilization using polymer slurry (FHWA, 2010).

Polymer products are commercially available as dry powders, granules or liquids. These products should be introduced to water with a pH greater than 9 for mixing. It is at this pH level that the polyacrylamide is soluble in water. At pH levels less than 2.5, polyacrylamides are not water soluble and at pH levels between 2.5 and 9 become water-swollen instead of water soluble (Leibert, 1991). Hard water and chlorides have also been known to have a negative effect on polymer slurries therefore sodium carbonate (soda ash) is added to water to raise the pH prior to mixing to reduce these effects. When mixing polymer slurries, the product should be introduced to a moving stream of water to avoid clumping. Recirculation should employ diaphragm pumps and/or air bubbling instead of centrifugal pumps. However, the research team and principal investigator have found that mixing may require a shear-type centrifugal pump at the onset to ensure that clumps of poorly mixed polymer are broken apart making the slurry more uniform. Sufficient time is then required for the polymer chains to reform (e.g. 1 to 4hr).

2.3 Drilling Fluid Specifications

Drilling fluids must have certain characteristics to effectively stabilize excavations. Therefore, key properties must be achieved and maintained at the construction site. These characteristics are identified by state and federal entities but it is important to realize that the specifications are merely guidelines developed based on collective experience in the drilled shaft industry and that

no specific set of slurry properties or characteristics are applicable to all conditions and soil types encountered during construction (FHWA, 2010). Drilling fluid manufacturers also recommend slurry properties for various types of subsurface conditions that should also be met during excavation.

Slurry specifications detail the tests to be performed, the allowable test methods and the minimum and maximum property requirements. The characteristics required to be monitored by contractors are slurry density, viscosity, pH and sand content. Contractors should have in place a slurry quality control plan that details, the test performed, the testing method used, and the value for each of the required properties (FDOT, 2018). Figure 2.5 shows the result of a shaft constructed with poor slurry and/or concrete properties. Notice how concrete flow through the rebar cage was inhibited due to either slurry too viscous, concrete without sufficient slump or a combination of both. If slurry properties are not monitored, shafts such as the one in Figure 2.5 can possibly be constructed and result in poor foundation performance. Tables 2.1 and 2.2 show the slurry property requirements for mineral slurries and polymer slurries, respectively. Table 2.3 shows the minimum required tests for the slurry quality control.

Figure 2.5 exhumed shaft showing poor concrete flow resulting from poor slurry/concrete properties (Mullins et al., 2014).

Table 2.1 Required mineral slurry properties.

Property	Required range of values	
	AASHTO (2016); FHWA (2010)	FDOT (2018)
Density (lb/ft^3)	64.3 to 72	64 to 73 (fresh water) 66 to 75 (salt water)
Viscosity (s/qt)	28 to 50	30 to 40
pH	8 to 11	8 to 11
Sand Content (%)	≤ 4.0	≤ 4.0

Table 2.2 Required polymer slurry properties.

Property	Required range of values	
	AASHTO (2016); FHWA (2010)	FDOT (2018)
Density (lb/ft^3)	≤ 64	62 to 64 (fresh water) 64 to 66 (salt water)
Viscosity (s/qt)	32 to 135	Manufacturer range
pH	8 to 11.5	Manufacturer range
Sand Content (%)	≤ 1.0	≤ 0.5

Table 2.3 Required testing method for slurry quality control.

Property	Test Method	
	AASHTO (2016); FHWA (2010)	FDOT (2018)
Density (lb/ft^3)	Mud weight (density), API 13B-1, Section 1	Mud density balance: FM 8-RP13B-1
Viscosity (s/qt)	Marsh funnel and cup, API 13B-1, Section 2.2	Marsh cone method: FM 8-RP13B-2
pH	Glass electrode, pH meter or pH paper	Electric pH meter or pH paper strips: FM 8-RP13B-4
Sand Content (%)	Sand, API 13B-1, Section 5	FM 8-RP13B-3

A survey of US Department of Transportation Specifications was performed to determine the allowance of bentonite and polymer slurry for drilled shafts. The results are displayed in Tables 2.4-2.8, below. Figures 2.6 and 2.7, graphically show allowable viscosity ranges for each state.

Table 2.4 Ten (10) states provide no drilled shaft specifications.

US States	References
AK, AR, DE, ID, IN, MN, NH, ND, TN, VT	AKDOT (2015), AHTD (2014), DELDOT (2001), ITD (2012), INDOT (2016), MNDOT (2014), NHDOT (2010), NDDOT (2014), TDOT (2015), Vermont DOT (2011)

Table 2.5 Eleven (11) states specify no drill slurry, but allow use if approved by the engineer.

US States	References
CO, GA, IL, KS, KY, MD, MT, PA, WV, WI, WY	CDOT (2011), GDOT SSP 524 (2013), IDOT (2012), KSDOT (2015), KYTC Special Note 11C (2012), MDOT (2008), MDT (2014), PENNDOT (2008), WVDOH (2010), WisDOT (2014); **, WYDOT (2010)

** wisconsindot.gov/dtsdManuals/strct/spec-provs/drldshft.doc

Table 2.6. Seventeen (17) states allow both mineral and polymer slurries and have specifications/recommendations.

US States	References
AL, AZ, CA, CT, FL, IA, LA, MA, MS, MO, NV, NJ, NM, NC, OH, OK, OR, WA	ALDOT (2012), ADOT (2008), CALTRANS (2010), ConnDOT (2005), FDOT (2018), Iowa DOT (2012), DOTD (2006), MassDOT (2012), MDOT (2004), MODOT (2011), NDOT (2014), NJDOT (2007), NMDOT (2014), NCDOT (2012), Ohio DOT (2013), ODOT (2009), Oregon DOT (2015), WSDOT (2014)

Table 2.7. Two (2) states allow only mineral slurry for drilled shafts of major structures.

US States	References
SC	SCDOT (2007)

Table 2.8. US states that have conflicting or different restrictions on excavation stabilization.

US States		References
HI	Only water may be used as the drilling fluid.	HIDOT Section 511 (2013)
ME	Only accepts drilled shafts for foundation of miscellaneous structures.	MaineDOT (2014)
NE	Only allow borehole stabilization with permanent casing.	NDOR (2014)
NY	Only defines drilled shafts for overhead sign structures.	NYSDOT (2008)
RI	Only defines driven piles for bridge foundations	Baxter et al. (2005)
SD	Only allows dry or cased excavations	SDDOT (2015)
UT	The use of drilling fluids is not allowed.	UDOT (2012)
VA	Only accepts drilled "piers" overhead sign structures	VDOT (2007),
MI	Only polymer slurries are allowed as the drilling fluid.	MDOT (2012)
TX	Recommends the use mineral slurry, and do not allow the use partially hydrolyzed polyacrylamide (PHPA) polymeric slurry or any blended mineral-polymer slurry.	TXDOT (2014)

The tables and figures show that there is no consensus among governing officials on the allowance of drilled shafts, the allowable stabilization techniques and allowable slurries/ slurry

viscosities. This may be the result of a disconnect between these agencies, or the result of local geological issues, or the result of conflicting literature regarding construction effects on side shear resistance of drilled shafts. Though it is known that the filter cake formed by bentonite slurries adversely affect side shear resistance, there is insufficient evidence to determine if the same effects are witnessed with polymer slurries. The effect of bentonite is formally addressed in FDOT (2016) Section 455-15.11.5, where it states,

Any unclassified excavation work lasting more than 36 hours (measured from the beginning of excavation for all methods except the Permanent Casing Method, which begins at the time excavation begins below the casing) before placement of the concrete requires overreaming the sidewalls to the depth of softening or removing excessive slurry cake buildup. Ensure that the minimum depth of overreaming the shaft sidewall is 1/2inches and the maximum depth is 3 inches. . .

. . . When using mineral slurry, adjust excavation operations so that the maximum time that slurry is in contact with the bottom 5ft of the shaft (from time of drilling to concreting) does not exceed 12 hours. If exceeding the 12 hour time limit, overream the bottom 5ft of shaft . . .

The above excerpt clearly acknowledges that the filter cake produced by mineral slurries is known to: (1) adversely affect side shear of drilled shafts and (2) amplify the adverse effects the longer exposed to sidewalls. Hence, the limitations of 12 hours exposure in the bottom 5ft of shaft and 36 hours for the rest of the shaft, else, over-reaming sidewalls to remove filter cake buildup being required. No analogous statement regarding the effect of polymer slurries on side shear exists due to the absence of a filter cake formation; hence the motivation for this study.

There has been some evidence to suggest that polymer slurries have little to no effect on side shear with increased exposure time but there are some cases in which bentonite slurry has outperformed polymer slurries or there was no distinguishable difference between the performances of the two fluids for similar exposure periods. Along with this, some believe the slippery feel of polymer slurries can reduce friction and has resulted in skepticism among industry officials to their effect on side shear resistance. For these reasons, it seems as if the traditional bentonite slurry is preferred over polymer slurry as suggested by the Tables, Figures and excerpt presented above. Therefore, further investigation is required to establish a definitive relationship, if one exists, between polymer exposure and side shear resistance. Previous studies exploring these effects have been performed and are discussed herein.
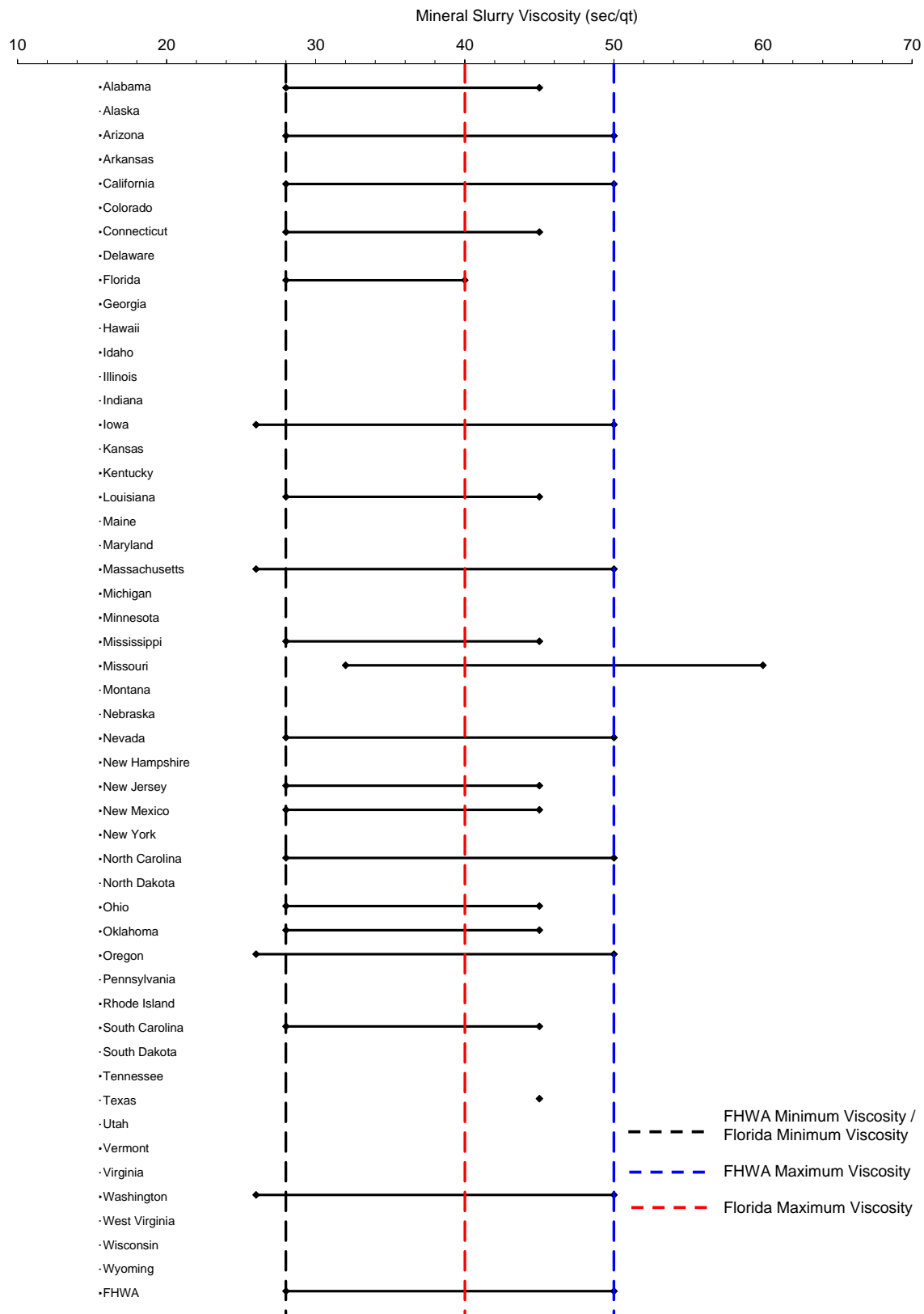
Figure 2.6 Recommended viscosity limits for mineral slurries (Mullins et al., 2014).
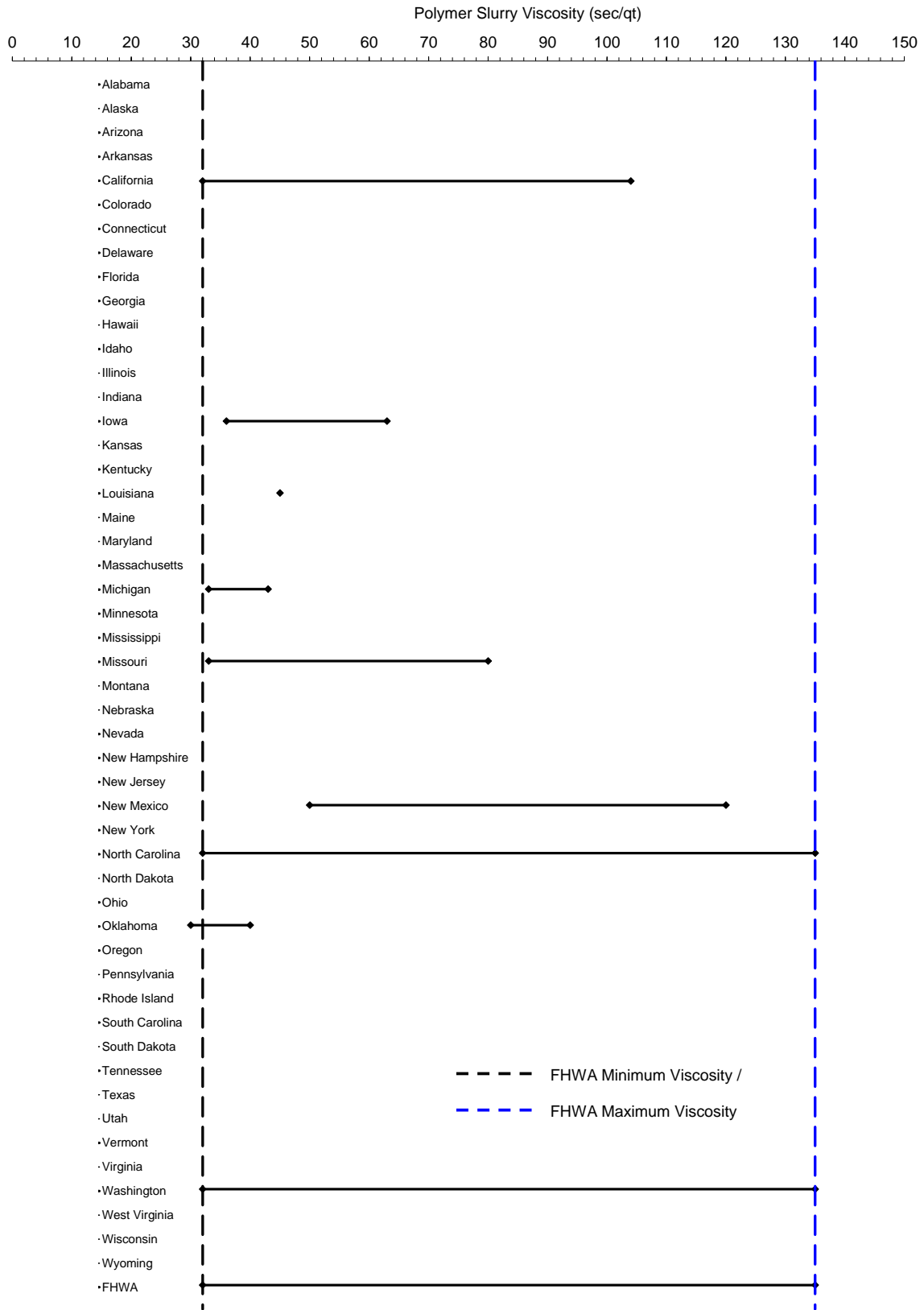
Figure 2.7 Recommended viscosity limits for polymer slurries (Mullins et al., 2014).

2.4   Past Studies

2.4.1   Majano, 1992 and Majano and O'Neill, 1994

Small scale laboratory extraction tests were performed on model shafts constructed with various type of slurries, slurry concentrations and exposure times at the University of Houston. The model shafts were cast into sand from the San Jacinto River with 2% silt and clay content. The five slurries tested, along with their dosage concentrations, exposure times, pH and slurry viscosities can be found in Table 2.9 (Majano, 1992).

Table 2.9 Properties of slurry and exposure times for model shafts (Majano, 1992)

Method of Construction	Slurry Dosage	Contact Time			pH	Slurry Viscosity (sec/qt)
		0.5h	4h	24h		
Casing	None	3	-	-	-	-
Bentonite	0.15ppg	3	2	2	9	29.8
	0.30ppg	5	2	3	9	32.7
	0.60ppg	5	2	3	8	267.8
Attapulgite	0.15ppg	3	2	-	9	28.5
	0.30ppg	5	3	-	9	30.6
	0.60ppg	4	2	-	9	69.8
Emulsified Polymer	1/800 by volume	3	2	-	9	30.2
	1/400 by volume	6	3	-	9	33.6
	1/200 by volume	5	2	-	9	42.8
Solid Vinyl Polymer	0.0035ppg	6	4	3	7	45
	0.0080ppg	6	4	4	7	75
	0.0180ppg	4	3	3	7	125

The testing procedure involved casting 1in diameter, 6in long specimens in an extraction cell 3in wide and 6.5in deep. The extraction cell consisted of an impermeable membrane placed on a base cell and supported by a membrane stretcher. In situ conditions were recreated by placing a filter paper membrane inside the impermeable membrane and on the top and bottom of plates. The sand was then placed within the cell and compacted to a relative density of 0.6 to 0.7. The cell was then sealed and the confining pressure was set to 1.44ksf for at least one hour prior to saturation. Saturation was achieved by filling a standpipe placed on the top cap and leaving to drain overnight (Majano, 1992).

After saturation, the pressure was dropped to 0.72ksf and the borehole was excavated. Most of the borehole excavation was performed with a 6in long wooden auger tip, but a 1in tip was also used. The wooden tips were attached to a stainless steel bar with slotted spacers that were responsible for centering the auger within the excavated hole and removing suction effects

during the withdrawal of auger. Before excavation, the standpipe on the top cell was filled with the candidate slurry up to 7in so that the excavated hole would be filled with slurry once the hole was advanced. Once the hole was completed, the slurry level was maintained at a level that kept the differential pressure at 0.72ksf. After the adjustment, the exposure time began (Majano, 1992).

After the exposure time expired, the tremie, made of 0.4in outer diameter plexiglass, was placed in the borehole and the slurry was displaced through concreting. The specimens were cast with concrete having a water to cement (w/c) ratio of 0.5, consisting of both fine (0.088mm) and coarse (2.00mm) aggregates, along with a chemical plasticizer to improve the flow. This mixture yielded concrete with a slump of 10in. After concreting, a ¼in diameter steel bar was placed into the freshly concreted hole. The concrete was allowed to harden for 72 hours and one hour before the extraction test was performed, the pressure was raised back to 1.44ksf. Just before the cell was installed in the loading frame, a small tube was inserted into the bottom of the sand specimen to relieve pressures and reduce suction at the base of the shaft by adding water that percolated through the soil sample. The cell was then placed in the extraction frame and the shaft was extracted at constant displacement rate of 0.2in/min (0.5mm/min) from the pressurized chamber. The extraction frame can be seen in Figure 2.8 (Majano, 2002).
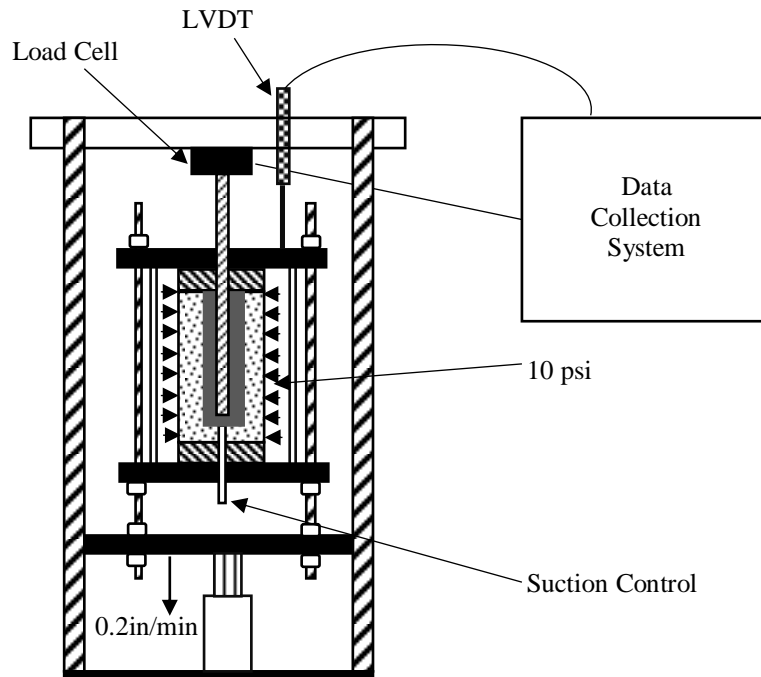
Figure 2.8 Model shaft for extraction cell (adapted from Majano, 1992).

Upon extraction, shaft dimensions were recorded and filter cake thickness (if any) was measured (Figure 2.9). The results of the extraction test were converted into dimensionless quantities by the authors for standard comparisons across all tests performed. From the load, side shear (f_s) was calculated, and divided by the confining pressure (σ_c) which was constant throughout all extraction testing. Displacement on the other hand was presented in terms of a dimensionless parameter depending on shaft area, length, diameter, maximum side shear and concrete modulus.

The necessary values to obtain load vs. displacement plots were not presented by the authors and hence will not be included. Instead, the "f_s/σ_c" value presented by the authors was multiplied by the confining pressure of 1.44ksf and shown in Table 2.10 as side shear corrected for as built dimensions and uncorrected for the intended nominal dimension (1in). No "filter cake" effects were noted on the polymer shafts, therefore they are omitted from Figure 2.9 as no geometric corrections were necessary. Figure 2.10 shows the effect of exposure time on shaft side shear for each fluid tested. Both the corrected and uncorrected values are displayed in Figure 2.10 (Majano, 1992). It should be noted that significant sedimentation was observed at low dosages of the emulsified polymer shafts but the uncorrected side shear values could not be calculated due because no information on these thicknesses being reported.
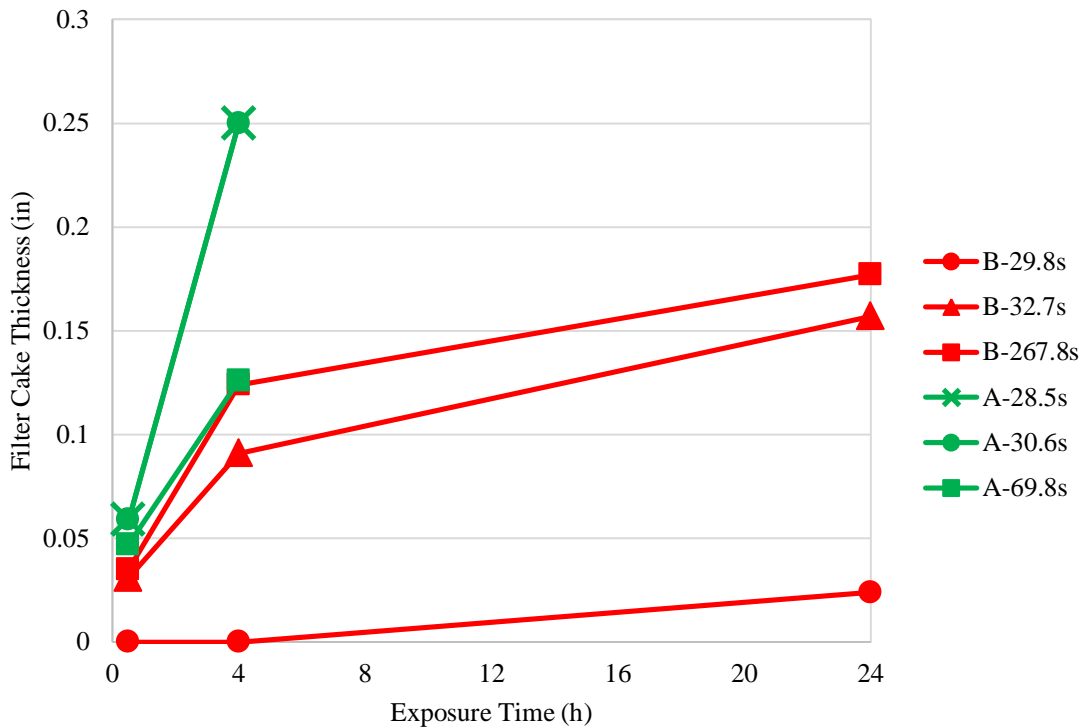
Figure 2.9 Time dependent effect of filter cake thickness on mineral slurry (data from Majano, 1992).

Table 2.10 Average side shear and filter cake thickness (Majano, 1992).

Slurry Type	Slurry Dosage	f_{max} (ksf) - as built diameter			Measured Cake Thickness (in)			f_{max} (ksf) – intended diameter		
		Contact Time (h)								
		0.5	4	24	0.5	4	24	0.5	4	24
Casing	None	1.54	-	-	-	-	-			
Bentonite	0.15ppg	0.70	0.37	0.92	-	-	0.024	0.70	0.37	0.88
	0.30ppg	0.76	0.52	0.72	0.031	0.091	0.157	0.71	0.43	0.49
	0.60ppg	0.67	0.56	0.55	0.035	0.124	0.177	0.62	0.42	0.35
Attapulgite	0.15ppg	0.81	0.35	-	0.059	0.250	-	0.72	0.18	-
	0.30ppg	0.86	0.34	-	0.059	0.250	-	0.76	0.17	-
	0.60ppg	0.59	0.49	-	0.047	0.126	-	0.53	0.37	-
Emulsified Polymer	1/800 vol.	0.63	0.96	-	-	-	-	0.63	0.96	-
	1/400 vol.	0.81	0.95	-	-	-	-	0.81	0.95	-
	1/200 vol.	0.90	1.06	-	-	-	-	0.90	1.06	-
Solid Vinyl Polymer	0.0035ppg	0.62	0.65	0.81	-	-	-	0.62	0.65	0.81
	0.0080ppg	0.99	1.14	1.08	-	-	-	0.99	1.14	1.08
	0.0180ppg	1.01	0.98	0.92	-	-	-	1.01	0.98	0.92
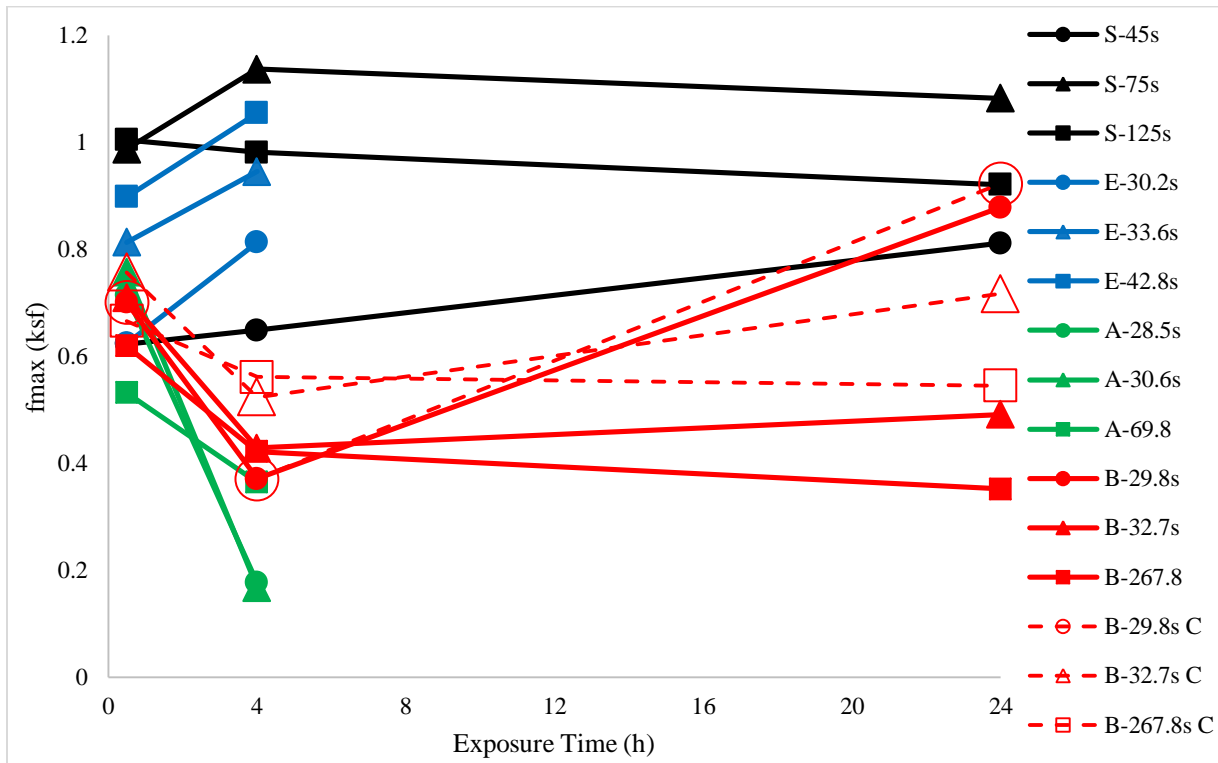
Figure 2.10 Effect of exposure time and viscosity on side shear for various slurries (data from Majano, 1992).

As expected, the results showed that filter cake thickness of mineral slurries increased as exposure time increased. The deviations from the expected results displayed in Figures 2.9 and 2.10 were both explained by the authors. In Figure 2.9, the lower measured filter cake thickness in the highest concentration of attapulgite was attributed to the attapulgite cake being much more compressible than bentonite cakes. Also, the increase of side shear witnessed after 4 hours in the bentonite shafts (Figure 2.10) was due to a decrease in the diameter of the shaft; resulting in inflated shear stresses due to forces being divided by smaller a smaller areas (Majano, 1992). Majano went on to say:

"Although the perimeter shear values yielded by some slurries showed an improvement in the load transfer with time (e.g., low bentonite dosages), it is erroneous to assume that longer exposure times produce better drilled shafts. Visual analysis of the model shafts indicated a deterioration in their geometrical dimensions, which can be extrapolated to field practice to suggest a detrimental effect on structural integrity of the foundation."

Hence, the filter cake produced by mineral slurries proved detrimental to the side shear and care should be taken when applying the results of the laboratory tests to field tests. Nonetheless, polymer slurries still outperformed mineral slurries which supports further exploration into the interface created with the polymer slurries and how it is affected by time. The authors believe that the polymer slurries may have penetrated the pore spaces of the model shafts and reacted with the cement to provide superior perimeter bond (Majano, 1992, Majano and O'Neill 1993). Ata and O'Neill (2000)

2.4.2   Ata and O'Neill

This study was also conducted at the University of Houston and involved performing shear tests on the interface of soil samples and concrete exposed to high-molecular-weight polymer slurry. The samples were collected from the test sites of two full-scale drilled shafts and were classified as NGES-UH (stiff silty clay) and NGES-TAMU (medium dense silty sand). The results of the interface shear tests were also compared against the maximum unit side shear obtained from full-scale load tests that were constructed using the same slurry. The slurry tested was a PHPA polymer that had a marsh funnel viscosity of 48sec/qt. The authors noted that the polymer also had a relatively high molecular weight and more negative charge than most drilling polymers but these qualities are fairly common in today's commercial available polymers. The results of the load test revealed that the resistances produced by the polymer stabilizing fluid was comparable to the anticipated resistances if the shafts had been constructed using bentonite slurry (Ata and O'Neill, 2000).

The soil samples were gathered from pre-determined points along the depth of the full-scale shafts by a Shelby tube from the NGES-UH site (undisturbed samples) and by a split spoon sampler from the NGES-TAMU site (disturbed samples). A 2.5in diameter ring was pushed into the Shelby tube to obtain the cohesive test specimens. The cohesionless soil was washed over a #200 sieve, oven dried for 24h and then compacted in a standard Proctor mold. The cohesionless

test specimens were then cored directly from the Proctor mold (Ata and O'Neill, 2000). During preparation, the moisture content was maintained between 16 and 18% which was the natural range for the test site. Prepared soil samples were then placed in the lower half of the direct shear box and a plexiglass cylinder that fit perfectly onto the lower half above it. Once securely attached and sealed, porous plates were placed at both ends of the soil sample (for free drainage) and the plexiglass cylinder was filled with 12in of slurry. Slurry was exposed to the soil samples for 3h (Ata and O'Neill, 2000).

After the exposure time had expired, the cement mortar was then placed in the top portion of the shear box. The mortar used type I cement, had a w/c ratio of 0.55 and sand to cement ratio of 3:1. Spacing screws were used to separate the halves of the shear box and once set, the shear box was clamped together using set screws. The shear box was then placed into a consolidation loading frame and a normal pressure equal to the theoretical effective fluid pressure of concrete at the depth of sample extraction was applied. Concrete was allowed to cure for either 3 or 7 days, after which the direct shear test was performed under the applied normal pressure. Specimens were allowed to drain from both the top and the bottom while a constant shear displacement rate of 0.08mm/min (approximately 3.15mils/min) was applied to perform the interface test. The results of the interface tests for cohesive and cohesionless soils are shown Figures 2.11 and 2.12, respectively. Both the specimens that were exposed and unexposed to the test polymer for 3 and 7 days are displayed below. Uniform shear distribution was assumed across a planar failure surface to calculate the resulting side shear (Ata and O'Neill, 2002).
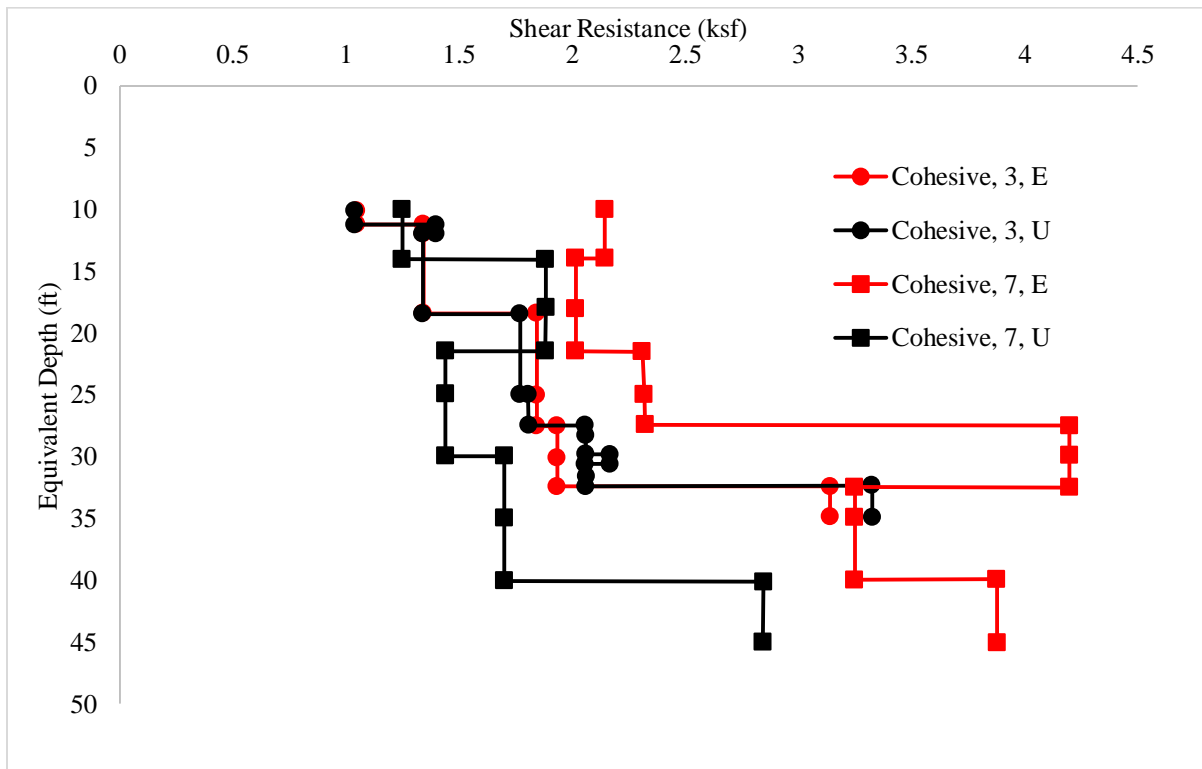
Figure 2.11 Laboratory shear resistance profile in cohesive soils (data from Ata and O'Neill).
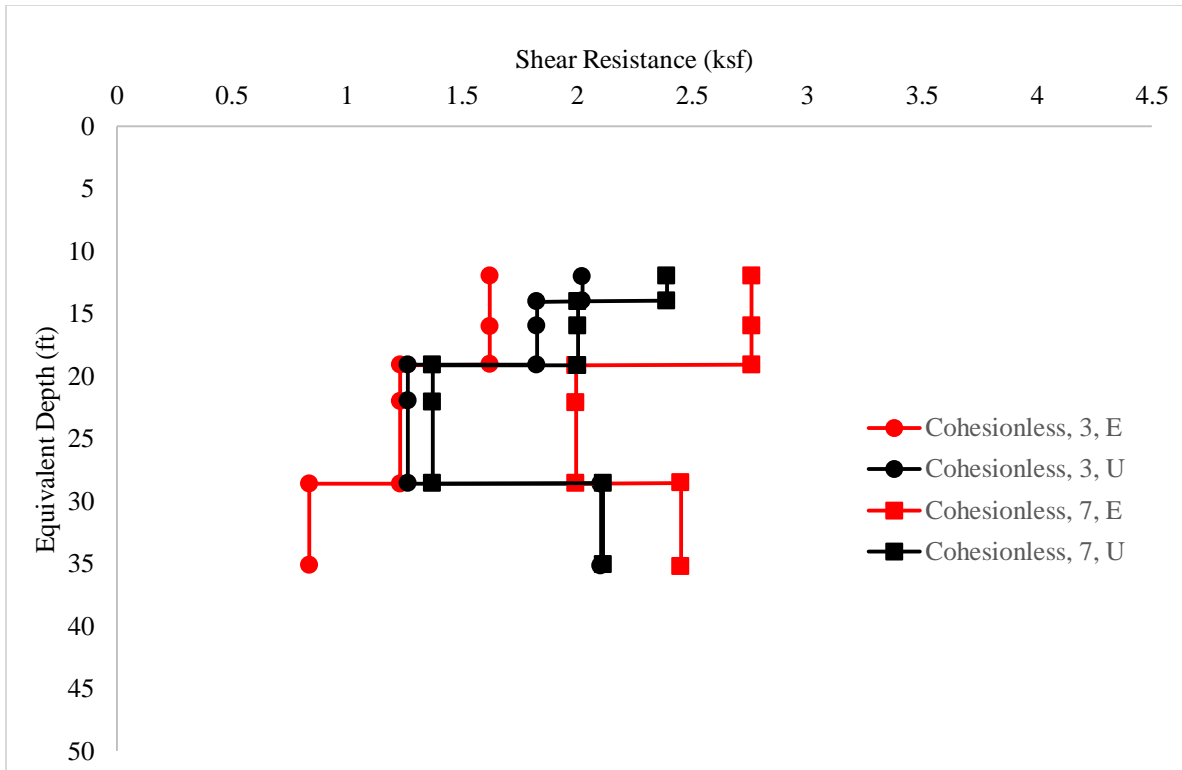
Figure 2.12 Laboratory shear resistance profile in cohesionless soils (data from Ata and O'Neill).

In Figures 2.11 and 2.12, the numbers 3 and 7 correspond to the concrete cure time while the letters E and U correspond to samples exposed and unexposed to polymer slurry. The 3 day specimens produced resistances that were either identical or similar to the unexposed samples while the resistances of the 7 day specimens were significantly higher than both the 3 day and unexposed specimens. After observing the failure surface of the soil samples, the authors determined that the unexposed specimen always failed along the soil-concrete interface while the failure plane of the exposed samples was between 0.04-0.08in (1-2mm) away from the sand-concrete interface. This suggests that the shear strength of the soil-concrete interface improved by being exposed to the polymer slurry (Figures 2.13 and 2.14). The authors stated that the strength increase of the interface between the 3 and 7 day exposure periods was due to either a chemical improvement of surface adhesion or mechanical improvement resulting from the roughening of the concrete surface (Ata and O'Neill, 2002).
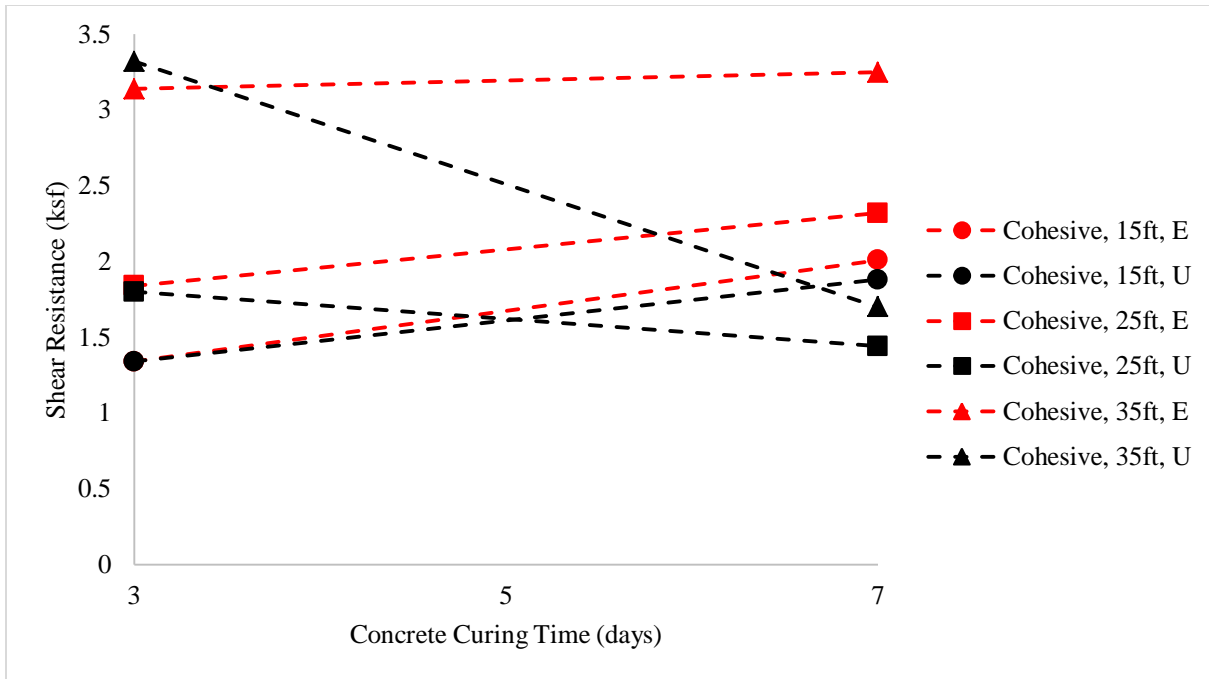
Figure 2.13 Shear resistance vs. concrete curing time for cohesive soils (data from Ata and O'Neill, 2002).
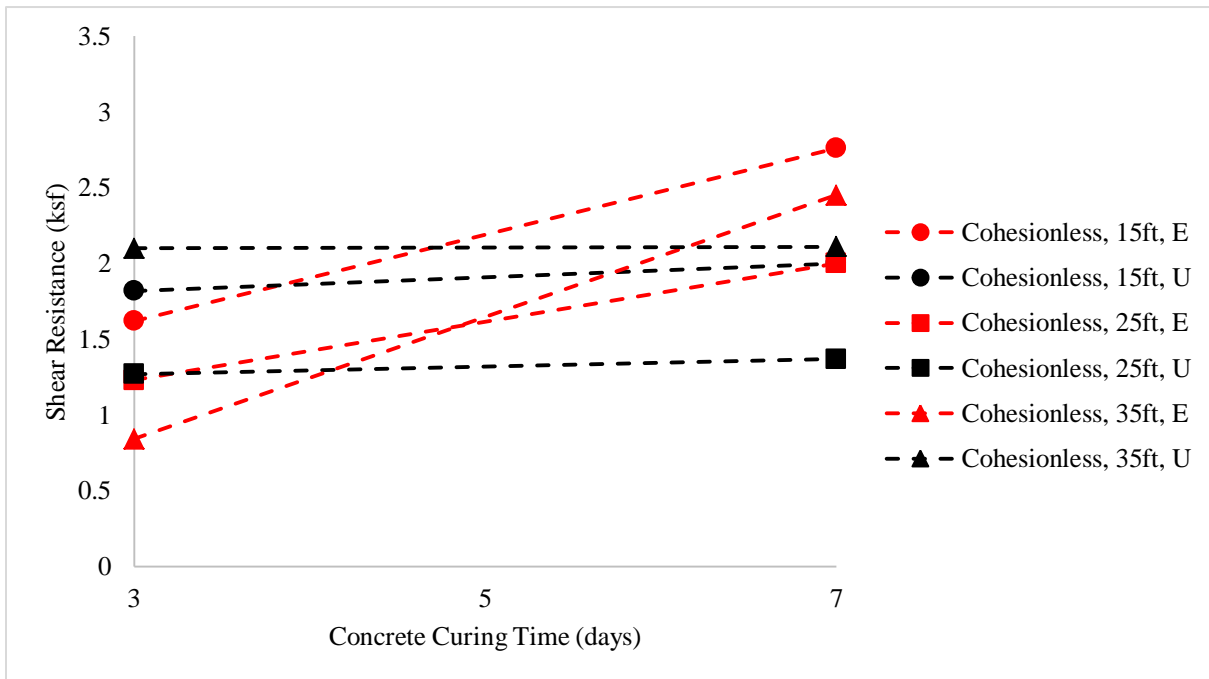
Figure 2.14 Shear resistance vs. concrete curing time for cohesionless soils (data from Ata and O'Neill, 2002).

Results of the direct shear tests were presented against the unit side shear of the full-scale load tests. Osterberg cells were used to perform the load tests on the 3ft diameter shafts constructed using the same polymer slurry as that tested in the laboratory. The shafts at the NGES-UH and

23

NGES-TAMU sites were tested 56 and 28 days after casting, respectively. No information was provided regarded the exposure time of the polymer to the respective soils. The test data is presented in Figures 2.15 and 2.16 along with the exposed soil samples for the respective site (Ata and O'Neill, 2000).

As seen in the figures below, the laboratory tests followed the general trend of the field tests, though they were substantially larger at shallower depths (20ft or less). This anomaly was attributed it to the lateral effective stresses not being equal to the fluid pressure at these depth. Also, the failure plane of the direct shear test was slightly cupped, resulting in a larger failure stress in the laboratory tests. Hence, it was concluded that the laboratory tests only provided information on the behavior soils exposed to polymer slurry and not on the numerical resistances of these soils (Ata and O'Neill, 2000).
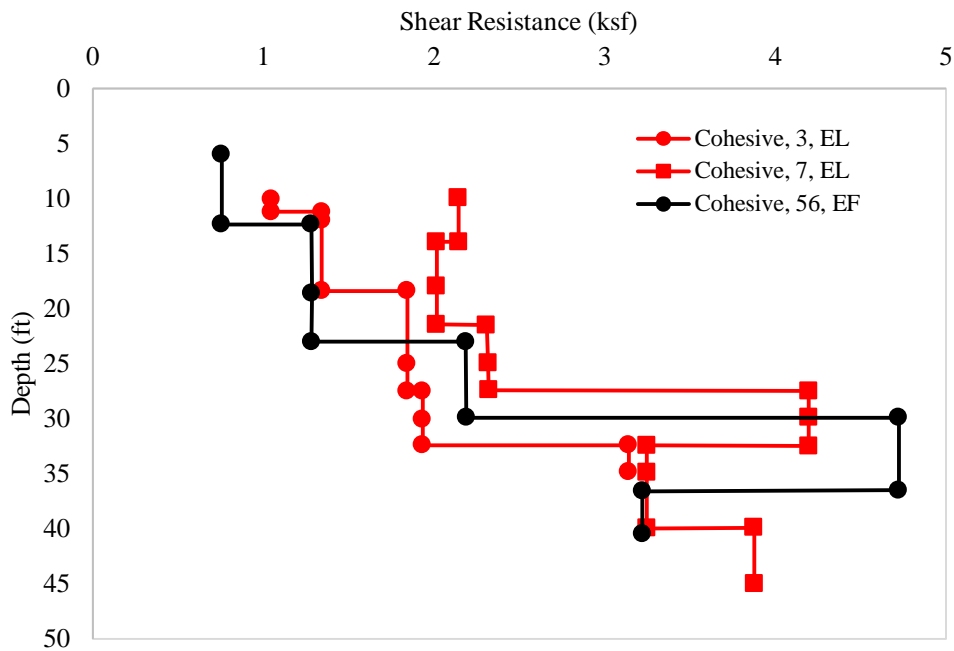
Figure 2.15 Field vs lab shear in cohesive soils (data from Ata and O'Neill, 2000).

24
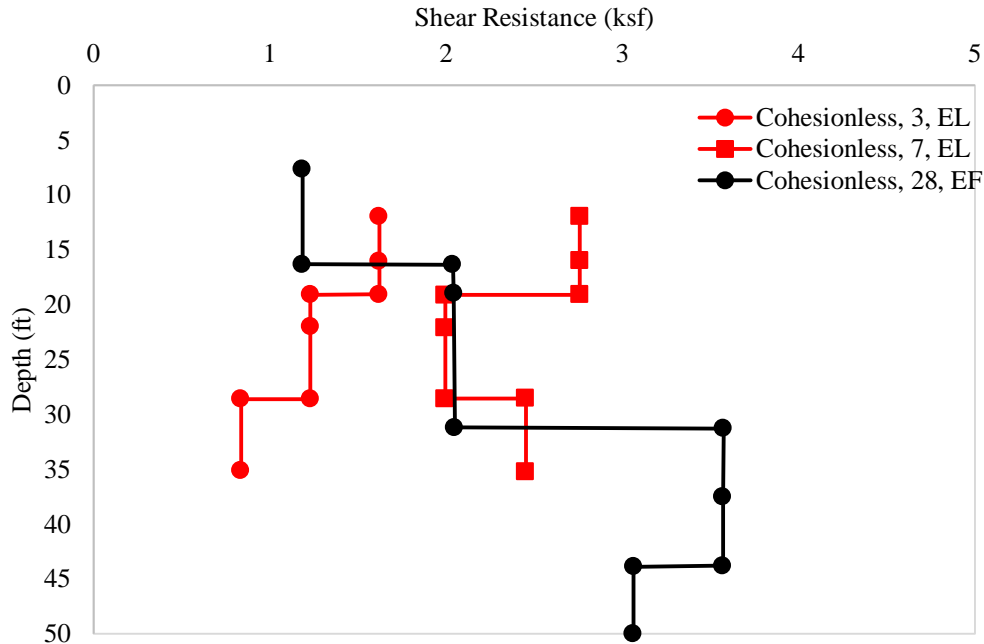
Figure 2.16 Field vs. laboratory side shear in cohesionless soils (data from Ata and O'Neill, 2000).

Overall, the direct shear tests performed by Ata and O'Neill (2000) gave insight to the influence of polymer slurries on the soil-concrete interface. The noted shear increase between the unexposed samples and 3 day samples against the 7 day samples suggest that polymer slurries may actually improve the bond between soil and concrete rather than deteriorate it as with bentonite slurries. Unfortunately, this study only addressed one type of polymer, (solid PHPA), therefore it is unknown if similar results are witnessed with polyacrylamide polymers. If multiple polymer products were tested, the effect of polymer slurries on the soil-concrete interface could be better understood. Though not through direct shear testing, the laboratory testing (small scale field testing) of this study is aimed to achieve this goal.

2.4.3   Brown (2002)

The primary purpose of this study was to determine the effect of drilled shaft construction techniques on axial performance in Piedmont soils. These soils have high silt contents (ML-CL and ML-SM classifications) and are can be found across the southeast United States. The test site was the Auburn University National Geotechnical Experimentation Site which has consistent soil over a larger area for the first 50ft below ground level (Brown, 2002).

Ten drilled shafts, 3ft diameter and 36ft long, were constructed and reinforced with ten #9 bars with #4 hoops on 1ft centers. Two of the shafts were constructed with bentonite slurry, four with polymer slurry and four with a temporary casing advanced prior to excavation. The concrete used had a design strength of 4ksi, with a slump of 7-9in and maximum aggregate size of ½in. Concrete for slurry shafts was place by bucket using a 10" tremie pipe while casing shafts were placed by free fall (Brown, 2002).

The bentonite slurry was a high grade commercially available Wyoming product while both dry and liquid polymers were used. Both polymer products were PHPA but an emulsifying agent was added to the liquid to assist with mixing. All of the slurries used for excavation were mixed 24h before its use and were added to the excavation prior to encountering the water table. The exposure times of each shaft along with slurry viscosity measurements can be found in Table 2.3. Exposure time "1h" ranges between 1 and 2 hours while exposure time "24h" ranges between 18 and 24 hours (Brown, 2002).

Table 2.11 Exposure Time and Slurry Viscosity for Each Shaft

Shaft ID	Slurry Type	Exposure Times (h)	Slurry Viscosity (sec/qt)
1B	Bentonite	1	52
24B	Bentonite	24	52
1DP	Dry Polymer	1	57
24DP	Dry Polymer	24	44
1LP	Emulsified Liquid Polymer	1	46
24LP	Emulsified Liquid Polymer	24	47

For the casing shafts, the soil was always approximately 5.5ft above the bottom of the casing. The casing for the shaft was rotated to advance the excavation and after advancing several feet, the soils inside the casing were removed. Casing shafts had similar "exposure" times to the slurry shafts, being "1h" and "24h". Two shaft for each "exposure" time were constructed. The "24h" shaft had a soil plug approximately 6-10ft left inside which would be removed prior to concreting. After the 24 hours had expired, approximately 20ft of groundwater (that had percolated through the soil plug) was found within the casing (Brown, 2002). The intrusion of groundwater through the soil plug identifies a concern with the casing method of construction as seepage can occur at increased rates in more porous soils and result in a poorly constructed shaft tip. Other than the economic advantage of wet construction, this serves as another reason that greater understanding of wet construction effects on shaft performance is required.

Compression static load test were performed to evaluate the performance of each shaft. Load was applied in increments ranged between 45 to 67kips and were held for 5 minutes each. Load data was recorded electronically, as well as manually for redundancy. Instrumentation of the shafts included a load cell, two linear displacement potentiometers and 12 strain gauges with the test shaft. The strain gauges were attached to the #4 stirrups at six different levels. The strain gauges data was used to estimate the soil resistance at each particular level. Measurements showed that the majority of the applied load was carried by side shear. Shafts were loaded until plunging occurred and the load vs displacement results are displayed in Figure 2.17 (Brown, 2002).

Figure 2.17 shows that the polymer shafts clearing outperformed bentonite shafts. The liquid polymer performed best out of all shafts tested. Note, that the 24h bentonite shaft (commonly accepted among industry) only reached around 225kips while the 24h polymer shafts reached around 450kips (dry) and 500kips (liquid) before plunging. Even the 1h bentonite shaft was substantially outperformed by all other shafts. Therefore, it is obvious that the presence of the

bentonite slurry adversely affects the side shear of drilled shafts. It is interesting to see that there is some time dependent effect of all shafts regardless of slurry type. Not only this, but there is no clear trend in the data as the 24hr dry polymer outperformed the 1hr dry polymer as seen in Figure 2.18. Upon closer observation, Figure 2.18 shows similar differences in magnitudes between the 1h and 24h shafts for each product. This suggests that the difference in capacity with each product series may not have resulted from slurry exposure time but rather soil relaxation as cited by Chang and Zhu (2004) and Bernal and Reese (1983).

After a few months, Brown excavated approximately 10ft of the 24 hour shafts and inspected the interface of between soil and concrete (2002). On the bentonite shaft, a distinct bentonite filter cake separated the surface of the concrete from the soil. The cake clearly affected the formation of a soil to concrete interface as Brown noted, "soil was easily dislodged from the face of the concrete with a small shove to reveal the concrete surface" (2002). According to Brown, the bentonite cake was up to 0.1in thick. No such layer between soil and concrete on the polymer shafts was noted. Actually, Brown noted that cement paste had penetrated into the pores of the soil and that it was extremely difficult to distinguish between soil and concrete, even after scraping with a sharp tool (2002). Hence, it is reasonable to assume that this superior bond results in increased capacities seen when using polymer slurries. In regards to the time dependent effects noticed within this study, further research is necessary to make definitive statements on how exposure time affects the side shear resistance of drilled shafts.

A point not discussed by Brown was the soil type and that the infiltration rate of bentonite slurry into the soil would have been very slow. Therefore the capacity reduction for the bentonite observed at one hour (relative to the other slurries) could not have been caused by filter cake, but rather by the mere presence of the bentonite. This suggests that the radial flow of concrete coming from the cage simply pressed against the soil and trapped the bentonite layer. Excavation and similar review of the 1hr shafts would have helped to better understand this phenomenon.
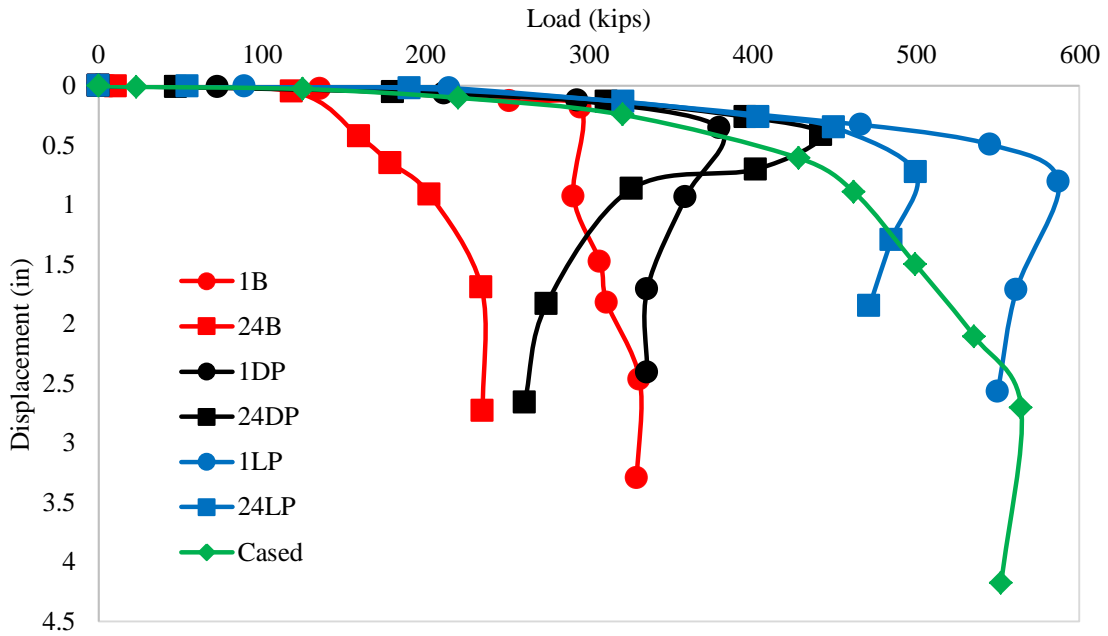
Figure 2.17 Load vs displacement curves (data from Brown, 2002).
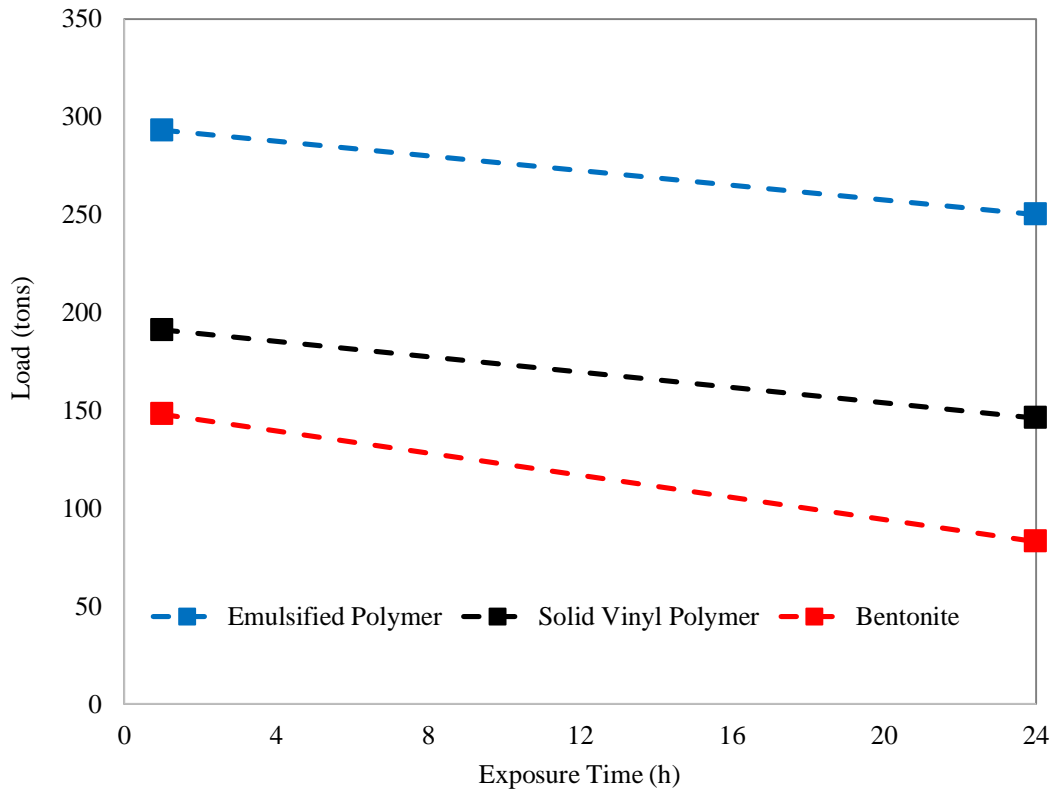
Figure 2.18 Time dependent effect on shaft performance (data from Brown, 2002).

2.4.4 Frizzi, et al. (2004)

A research study was conducted in Miami, Florida, to evaluate the performance of drilled shafts as a foundation for a high-rise building. The study encompassed, constructing and load testing three, 6ft diameter, 120ft long shafts in interbedded layers of limestone, sand and sandstone. Shafts were constructed using three different stabilization methods; polymer with temporary casing, polymer alone and bentonite alone. Each shaft also had an 80in diameter 15ft long surface casing while shaft PC had a 74in diameter, 80ft long temporary casing. Figure 2.19 shows the geologic subsurface of the full-scale shafts (Frizzi et al., 2004).
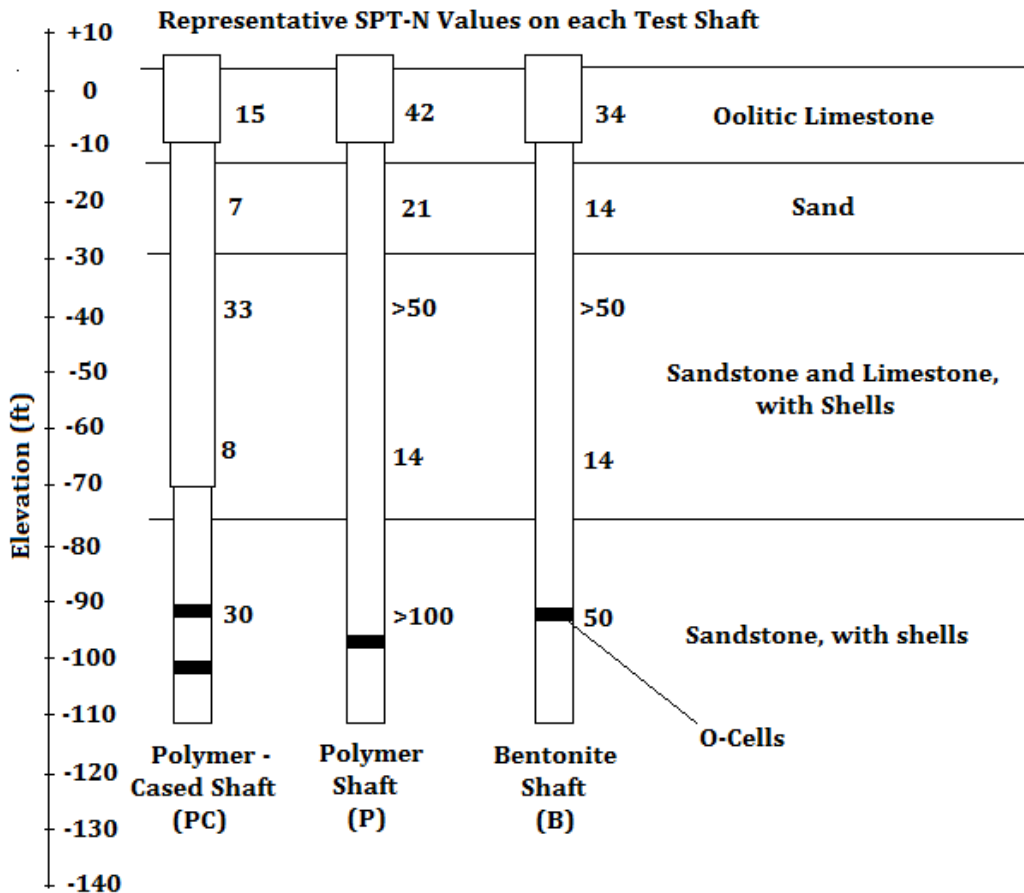
Figure 2.19 Geologic subsurface and shaft schematics.

Polymer shafts utilized proprietary polymer slurries along with their additives while high yield bentonite mixed with an additive was mixed with pH adjusted water for the bentonite shaft. According to Frizzi et al., additional bags of polymer slurry mix and other additives were added to the slurry column during drilling even though prepared polymer slurry was originally introduced to the excavation. Therefore, actual polymer dosages were difficult to estimate (Frizzi et al., 2004). No reason for the addition of polymer products to the column was given but it can only be assumed that there was inability to maintain a piezometric head due insufficient pre-mixed polymer or rapid soil infiltration. Hence, attempts were made to increase slurry volume or

29

slurry viscosity. No such adjustments were reported for the bentonite shaft which was allowed to hydrate prior to excavation. Polymer slurry viscosities ranged from 50 to 70 seconds while the bentonite slurry viscosity was 40 seconds. It is unclear at which point during the excavation process viscosity measurements were recorded but Frizzi et al., noted polymer information was recorded based on the available state of practice for polymer quality control (2004).

Prior to concreting, shaft inspection revealed sidewall undulations of 1-2in in shafts PC and B while shaft P measured 4-16in. Sidewall inspection was performed with a proprietary down-hole sidewall sampler. Samples from "soft rock" regions were taken for the bentonite shaft but it is unclear at which depths these as upper and lower regions are referred to but no classification is provided. Nonetheless, an 8mm thick filter cake, which was easily removed, was found in the upper rock strata. The surface of the soft rock was penetrated by had a 1mm thick filter cake and there was no filter cake in the lower rock region. Bottom sediment of each shaft was also recorded using a proprietary camera/caliper (Frizzi et al., 2004). Table 2.12 shows shaft construction times along with sediment thickness.

Table 2.12 Construction Times and Bottom Sediment (Frizzi et al., 2004)

Shaft ID	Construction Time (hours)				Bottom Sediment (in)
	Excavating	Reinforcing	Concreting	Total	
Bentonite (B)	31.5	1.25	2.75	35.5	0.7
Polymer (P)	21	2.42	2.17	25.59	2.8
Polymer w/ Casing (PC)	97	9.25	2.25	108.5	1.6

Load tests were performed with Osterberg jacks (O-cells) cast into the shaft at the approximate depths shown in Figure 2.19. O-cells allowed for independent but simultaneous testing of side shear and end bearing of the shafts. The quick loading procedure (ASTM D1143), was used to test the shafts and the results were reported in terms of unit side shear vs depth, unit end bearing load and equivalent top load (combination of both side shear and tip load) vs displacement (Frizzi et al., 2004).

Unit end bearing load was multiplied by the cross sectional area of the tip to attain the measured load. The resulting end bearing load was then subtracted from the equivalent top load to attain the side shear. Equivalent top and tip load vs displacement are shown in Figure 2.20 while Figure 2.21 displays the estimated side shear vs displacement (Frizzi et al., 2004). This method of side shear estimation was chosen to avoid accumulating error resulting from dimensionally anomalies along the length of the shaft.

As seen in Figure 2.21, substantial portions of the total load applied was resisted by side shear. Figure 2.21 shows that the polymer shaft outperformed both the bentonite and temporary cased shaft for loads up to 8000kips, in terms of side shear. At this point, the plunging occurred and the bentonite shaft then had the best response to additional loading. Plunging occurred around 9000kips and 7000kips within the bentonite and polymer cased shafts, respectively. The

corresponding displacement at plunging was approximately, 0.7in, 1in and 0.7in for the polymer bentonite and cased shaft, respectively.

In regards to total load and end bearing load, the bentonite shaft clearly performed the best out of all shafts tested. It should be noted though, overall shaft performance of the polymer shafts may have been affected by cited construction defects. As previously mentioned, additional product was added to the shaft P during excavation, therefore the quality of the polymer used is subject to question. Also, it is unclear to the extent of polymer interaction with the soil in shaft PC. Not only this, but shaft PC was also cast into a weaker subgrade than shaft P and B, as indicated in Figure 2.19 (Frizzi et al., 2004). All of these factors may have had some effect on the results of the load tests performed.
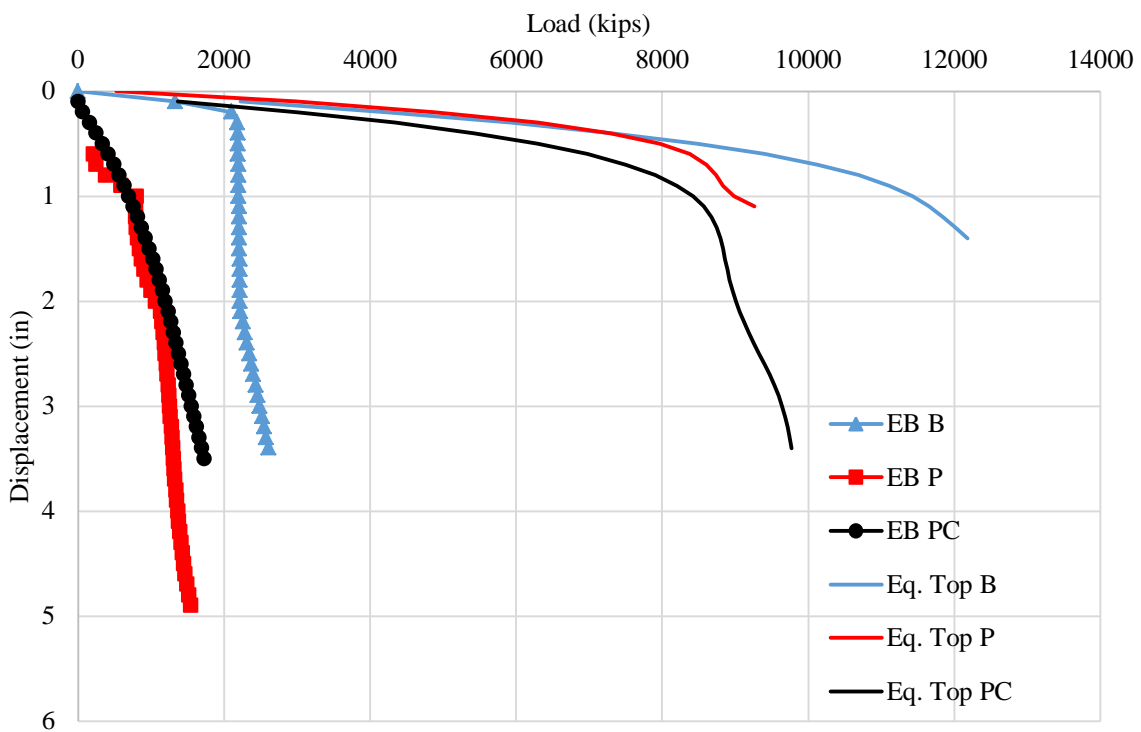
Figure 2.20 Estimated equivalent top load and end bearing load vs displacement (data from Frizzi et al., 2004)
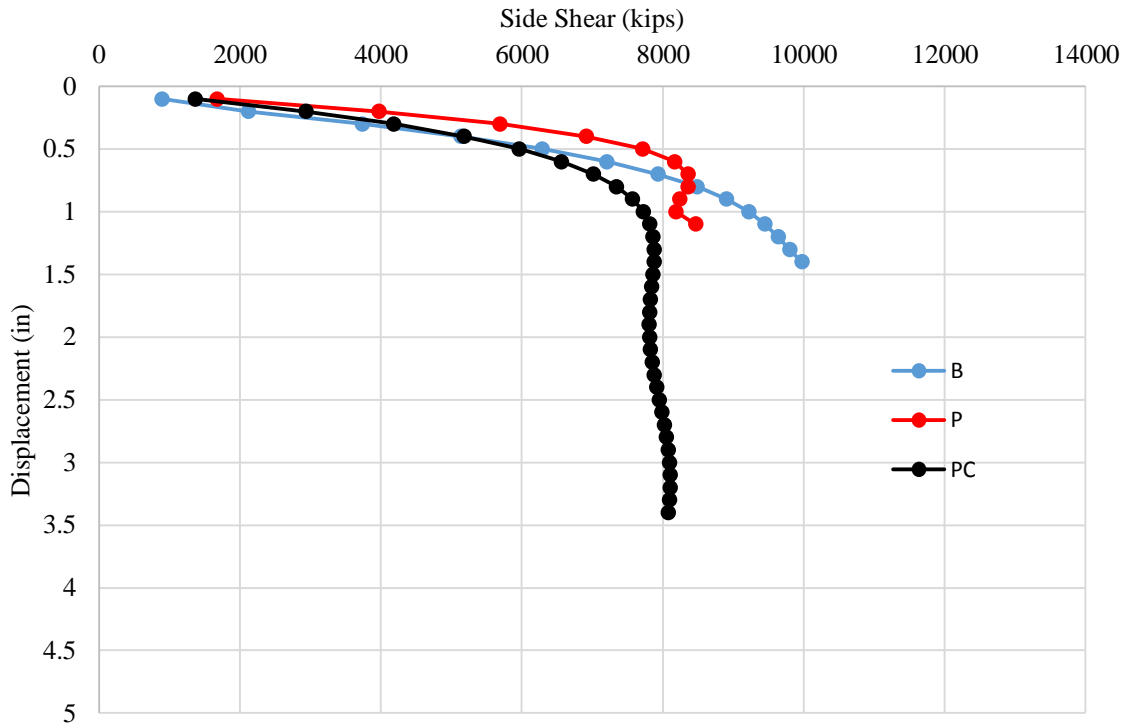
Figure 2.21 Estimated side shear vs. Displacement (data from Frizzi et al., 2004)

2.4.5 Lam et al., (2014)

This research study was aimed to explore the effects of slurries on the shear strength between sand and concrete when used to construct drilled shafts. The authors were aware of situations in which shafts constructed with bentonite fluids underperformed but once construction modifications were made to reduce filter cake thickness, shaft performance was increased by 30%. Hence, the authors questioned whether similar modifications are necessary for other shafts or if specifications are capable of minimizing such effects. Specification exploration by the authors found the recommendation of limiting bentonite exposure to 4h by (FHWA, 2010) while UK specifications called for 12h (Institution of Civil Engineers, 2007) and other countries had no such specification recommendations. Due to the inconsistencies and absence of specifications, the authors performed nine interface shear tests to investigate: (1) the effects of polymer slurries and concrete curing time, (2) the effects of bentonite fluid exposure times, (3) the effect of concrete aggregate protrusion (Lam et al., 2014).

The results of the two polymer and six bentonite slurries tested used water as a reference. The test performed were similar to those done by Ata and O'Neill (2002). A modified shear interface box with the dimensions being approximately 6.9in by 10.8in with the depths of 3.9in and 2.75in for the top and bottom halves, respectively was used for the tests. The modified system also incorporated a hydraulic accumulator to achieve field soil and concrete pressures. Once the test soils were washed with water, the respective stabilizing fluid was introduced. A hydraulic ram

32

was used to apply pressure to the system. Pressures of 34psi and 52psi were applied to the bentonite fluid and fluid concrete, respectively but the applied pressure for the polymer fluids was not provided. The marsh funnel viscosities were 70sec/qt and 34sec/qt for the polymer and bentonite slurry, respectively. Exposure times for each support fluid to the test soil can be found in Table 2.13. The number in each cell represent the number of tests performed for each drilling fluid and exposure time (Lam et al., 2014).

Table 2.13 Stabilizing Fluid Soil Exposure Time for Shear Interface Tests (Lam, et al., 2014).

Drilling Fluid	Exposure Times (h) and number of reported tests					
	0	0.5	3	7.5	12	24
Water	1	-	-	-	-	-
Bentonite	-	1	1	1	2	1
Polymer	-	-	-	2	-	-

After the slurry exposure time had expired, excess slurry was drained off and concrete was placed. A superplasticized fly ash-cement blend of concrete with a maximum aggregate size of 0.8in was used except for one of the 12h bentonite tests where 0.2in was the maximum aggregate size. Concrete was allowed to cure for 7 days in all tests except one of the polymer tests where the curing time was 3 days. Shearing tests were performed at a rate of 0.08in/min to an ultimate displacement of 0.6in was achieved. The results of the shear tests can be seen in Figure 2.22, below. The legend provides the respective drilling fluid (W-water, B-bentonite, P-polymer), exposure time and concrete curing time (Lam et al., 2013). The M on the 12h series represents the bentonite test performed using the 0.2in maximum aggregate size.

Little shear strength variation was seen between the polymer fluids and water supported tests while obvious deterioration in side shear was witnessed within the bentonite tests (Figure 2.23). As expected, shear stress decreased with bentonite exposure time. Notice, the bentonite 24h test only yielded 25% of the bentonite 0.5h shear stress which in and of itself was 90% of the polymer and water tests. This may be due to difference in shear strength but might actually be due to immediate shear stress deterioration in the tests performed by Lam et al (2014). It is interesting to note the effect of the smaller aggregate size in this study. The smaller maximum aggregate size reduced the shear stress to that of 24h bentonite (0.8in maximum aggregate) test. The author believed that this reduction was due to the absence of aggregates protruding from the filter cake which improved the interface bond in the other tests (Lam et al., 2014).
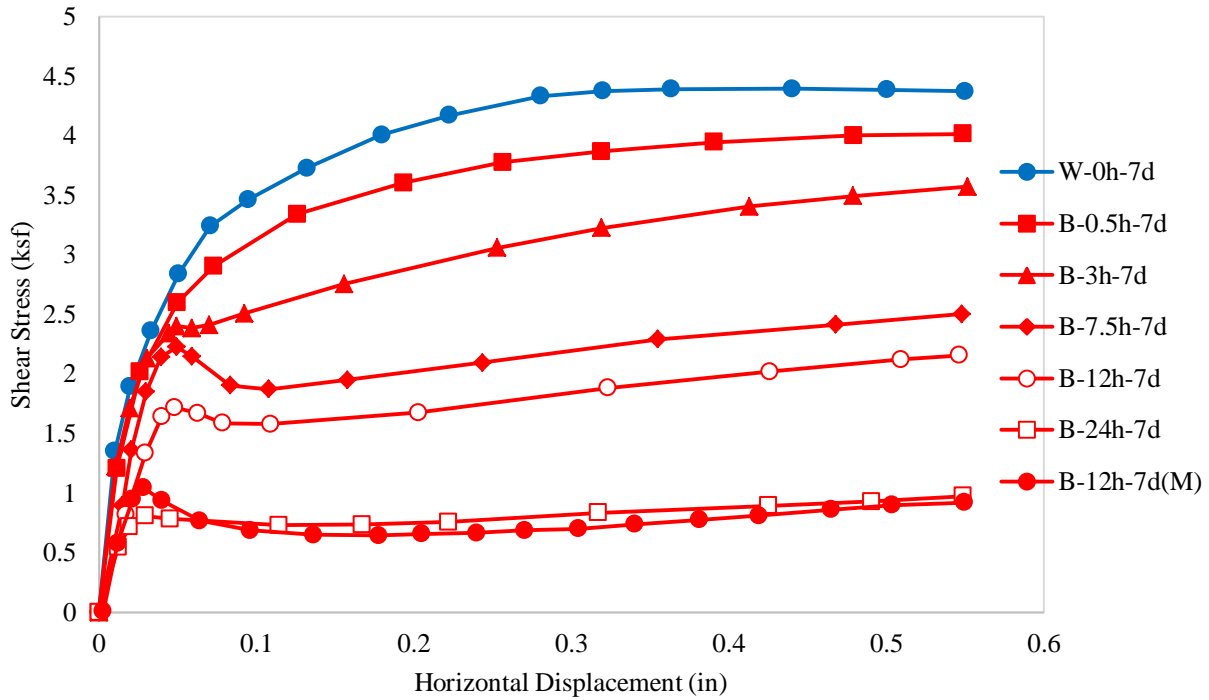
Figure 2.22 Shear interface results (data from Lam et al., 2014).
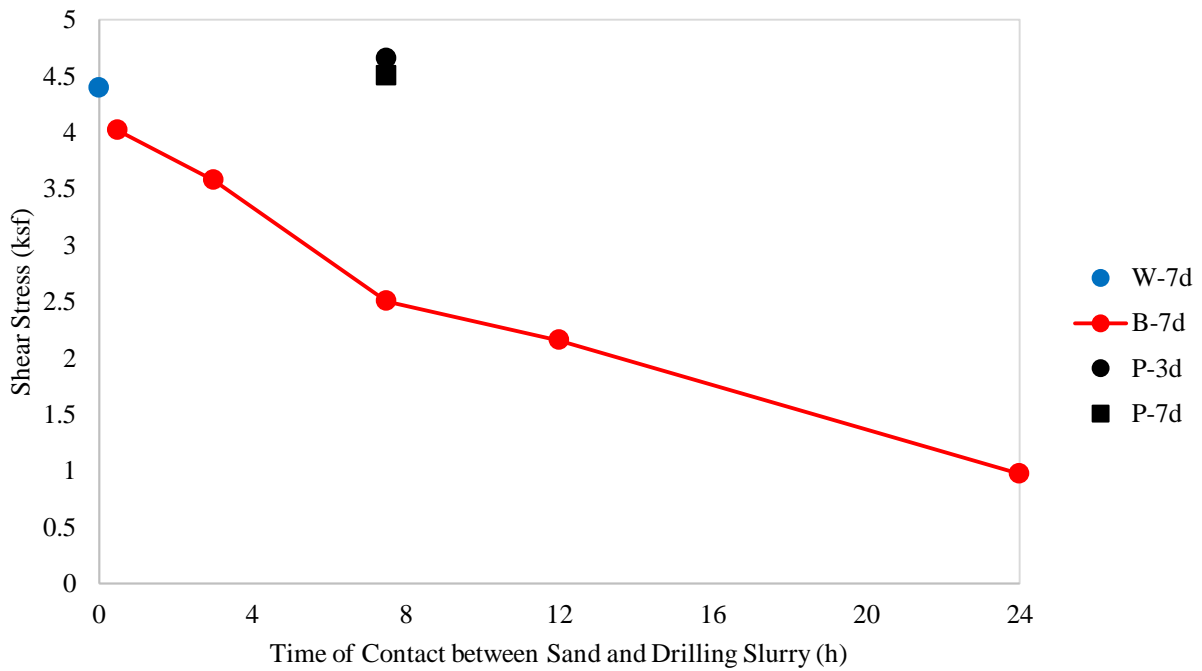
Figure 2.23 Effect of slurry exposure time on shear stress (data from Lam et al., 2014).

34

2.4.6   USF Upper Viscosity Project (2014)

A recent study performed at the University of South Florida investigated the effect of slurry viscosity on side shear resistance of drilled shafts. Viscosities of 40sec/qt and 74sec/qt were used for the bentonite tests while 50sec/qt and 131sec/qt were used for the polymer tests. The testing mentioned herein was performed on full-scaled shafts between 14.2ft and 17.4ft long having a nominal diameter of 2ft. A vinyl polymer product was used for the shafts which were constructed in Clearwater, FL. The subsurface consisted of 15ft of silty sand overlying clay and silty clay layers. The results showed no appreciable effects of viscosity or exposure time (Figures 2.24 and 2.25).
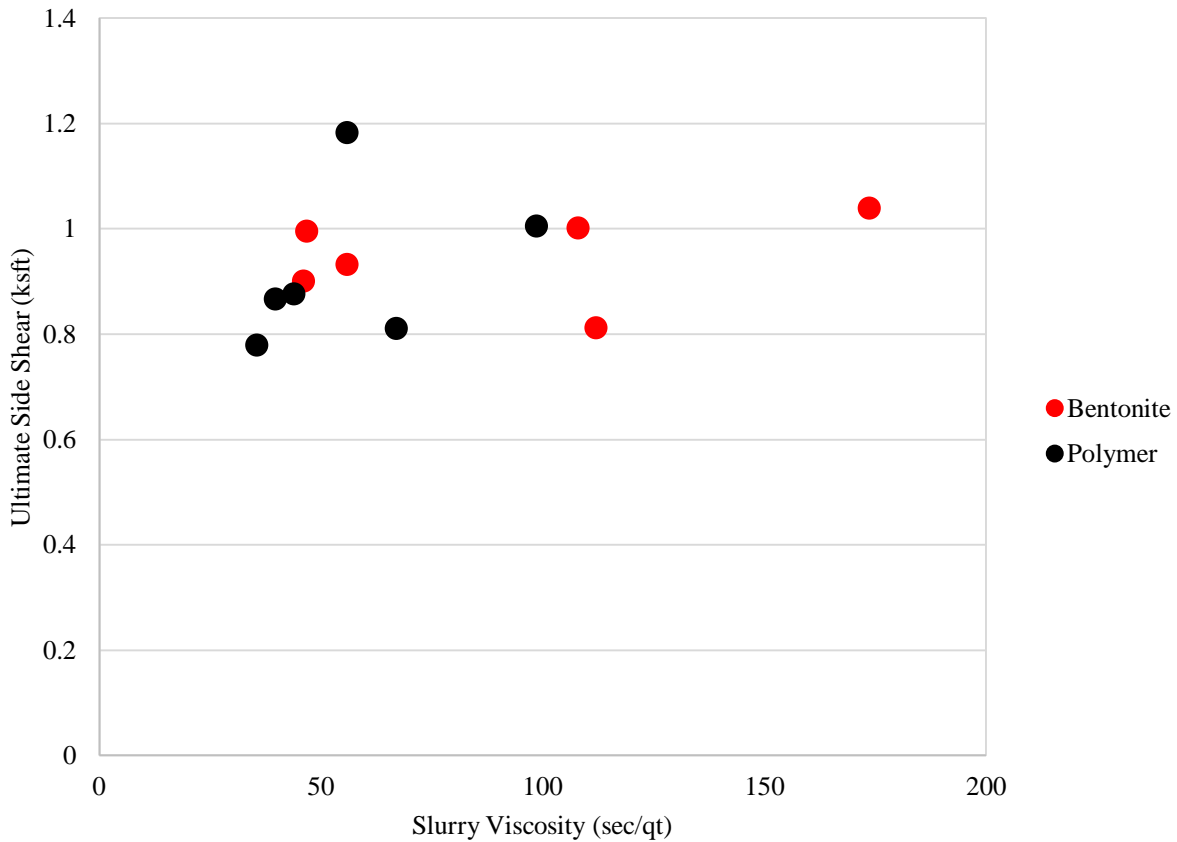
Figure 2.24 Ultimate side shear vs viscosity for each slurry type (data from Mullins and Winters, 2014).
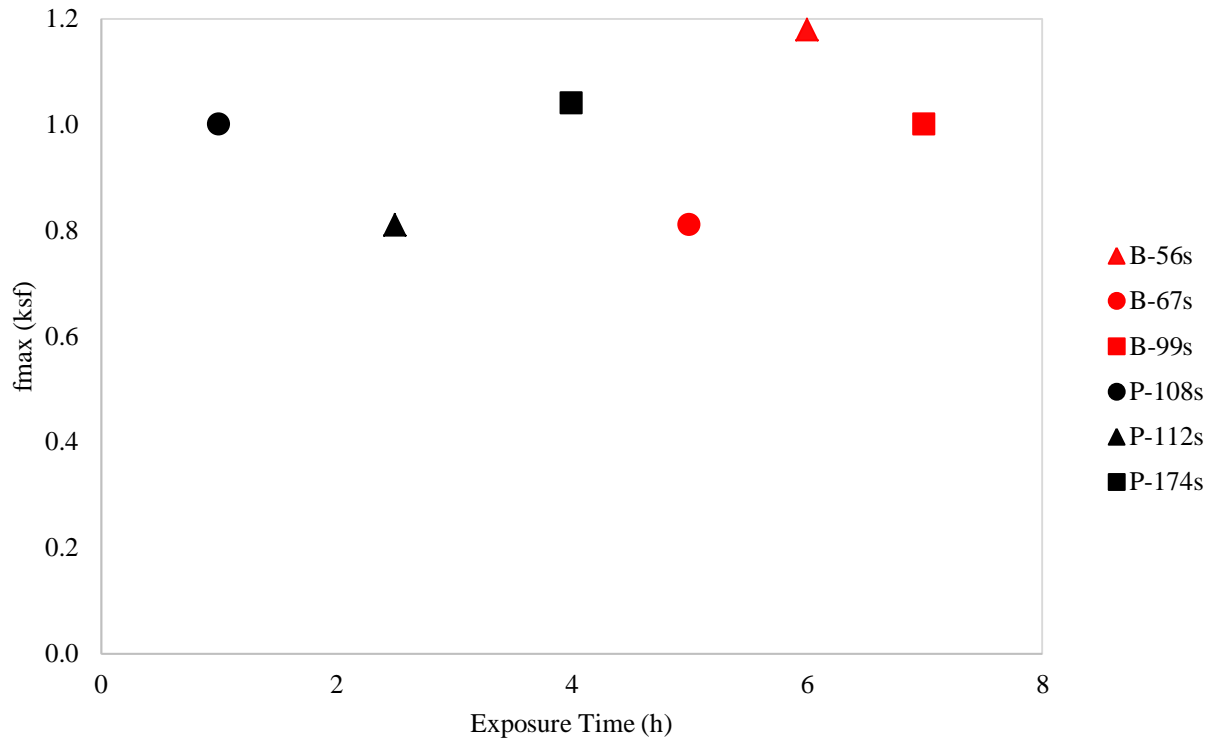
Figure 2.25 Effect of exposure time on side shear (data from Mullins and Winters, 2014).

In Figure 2.25, B and P used in the specimen names represent the bentonite and polymer shafts, respectively, and the numbers correspond to the slurry viscosity (sec/qt). Since the effects of exposure time on side shear were not the focus of this research, conclusions based solely on the presented results may not be immediately evident. Further, due to construction sequencing, all bentonite shafts were constructed first followed by polymer shafts. As a result, a somewhat longer open excavation time was experienced by the bentonite shafts (5 to 7hrs) when compared to the polymer shafts (1 to 4hrs).

Mullins and Winters (2014) noted that both bentonite and polymer slurries showed similar capabilities in maintaining excavation stability, and highlighted the importance of proper sequence/procedure of addition of slurry, regardless of the type. The authors also cited that comparative studies of exposure times of 1h and 24h bentonite slurry showed a reduction in the side shear, but much less information was available within that time span. It was believed that, based on the small amount of fluid loss, all the degradation of side shear from filter cake formation must occur shortly after contact initiates (Mullins and Winters, 2014). However, these findings concluded that more research is required to properly quantify such effects, if any.

2.4.7   Lam and Jefferis – Canary Wharf (2015)

In a recent ASCE publication, Lam and Jefferis reviewed various works presented throughout Europe regarding the performance of drilled shafts constructed using both bentonite and polymer fluids. The works performed in Canary Wharf, London evaluated the performance of four drilled

36

shafts, one 12h bentonite, two 12h polymer and one 37h polymer, to investigate if the specifications for bentonite could apply to polymer also. The shafts were roughly 2.5ft in diameter, 84ft long and cast into a subgrade of an interbedded clay and sand layer for the first 40ft followed by dense very dense sand. The polymer used was a PHPA (CDP) but no information was given regarding the bentonite used, slurry viscosities or mixing procedures. All of the shafts were tested to 220% of the design loads and showed little pile head movement as seen in Figure 2.26 (Lam and Jefferis, 2015).
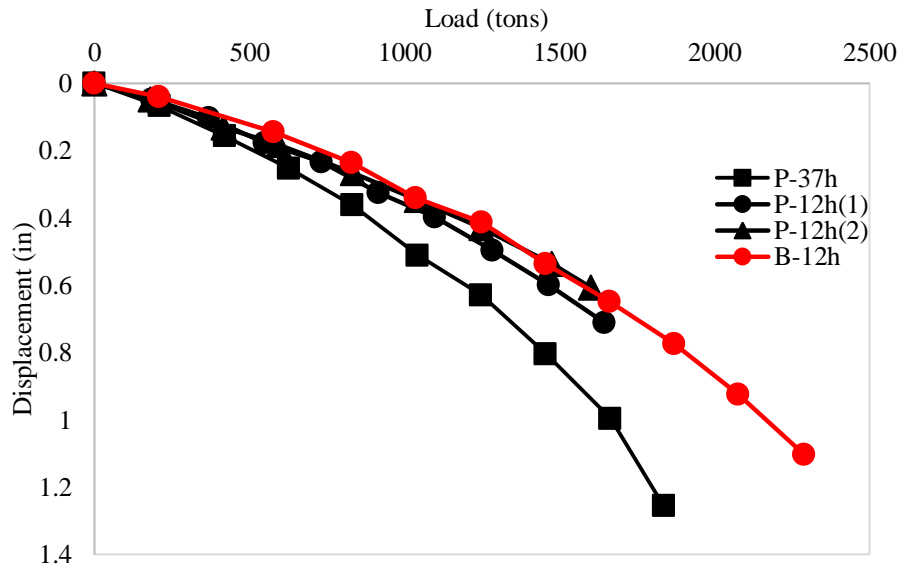
Figure 2.26 Canary Wharf load vs displacement curves (data from Lam and Jefferis, 2016).

Figure 2.26 shows that all shafts tested responded fairly similarly though displacements were slightly larger in the 37h polymer shaft. This was of no consequence though due to the fact that the working load (estimated to be 750) exhibited a maximum displacement of 0.3in. Based on this, the performance of all shafts was deemed acceptable. This performance also led to the conclusion that existing specifications and construction procedures that apply to bentonite could be adopted for polymer shafts. The authors also noted that the use of the polymer slurry was advantageous to the contractor as the excavation was allowed to remain open overnight and hence an extra half shaft per day was able to be constructed. This would have not been possible with bentonite fluids due to the performance decrease associated with increased exposure times (Lam and Jefferis, 2015).

The effect of exposure time on shaft performance is displayed in Figure 2.27, but no meaningful conclusions can be drawn from it since so little information was presented. To this measure, additional testing is necessary to determine how shaft performance is affected by polymer exposure time.
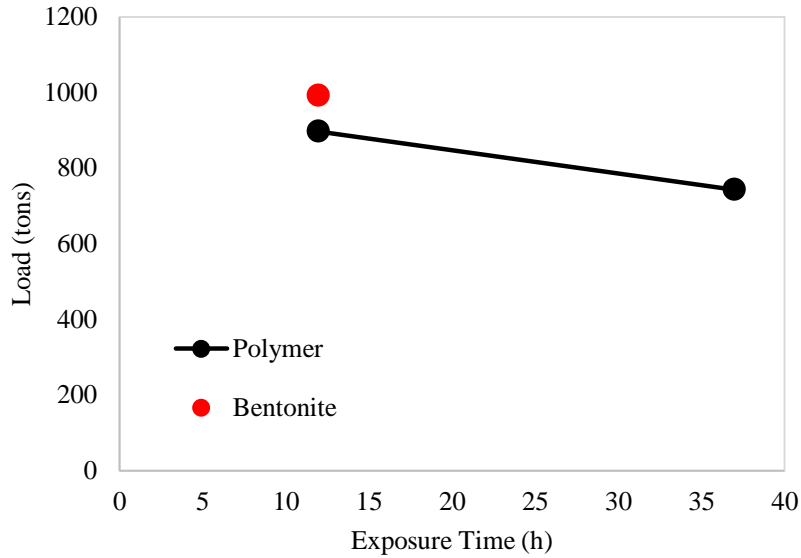
Figure 2.27. Effect of exposure time on sustained load (data from Lam and Jefferis, 2015).

2.4.8   Lam and Jefferis – Straford (2015)

Another study reviewed by Lam and Jefferis was conducted in Stratford, London to confirm the conclusions drawn by the study performed at Canary Wharf. This was achieved by constructing three 4ft diameter, 89ft drilled shafts into subsurface consisting of made ground (extending 20ft below the surface), very stiff clay (20-62ft) and dense sand (62-89ft). Two of the shafts were constructed using a CDP PHPA polymer while the other was constructed using bentonite. The marsh funnel viscosities and exposure time for each shaft can be found in Table 2.14 while the load vs displacement curves can be found in Figure 2.28.

Table 2.14. Marsh funnel viscosity and exposure times (Lam and Jefferis, 2016).

Shaft ID	Slurry Type	Viscosity (sec/qt)	Exposure Time (h)
P-7.5	Polymer	70	7.5
P-26	Polymer	69	26
B-7.5	Bentonite	34	7.5
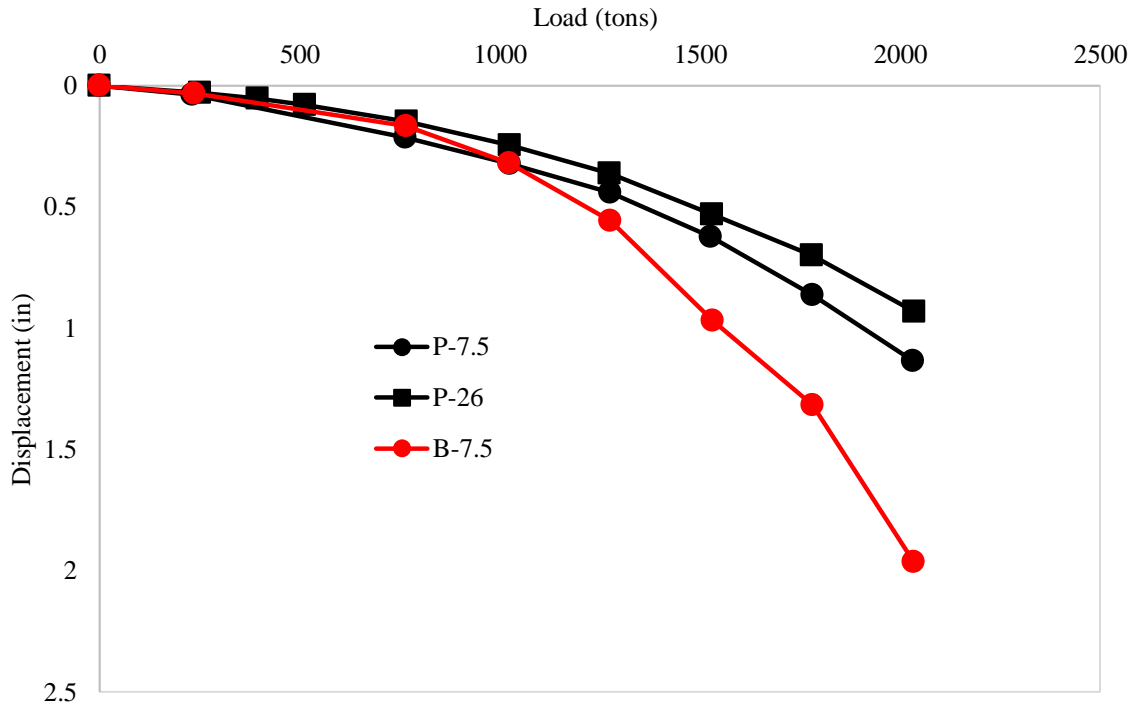
Figure 2.28. Load vs displacement curves for Stratford shafts (data from Lam and Jefferis, 2016).

Shafts were tested up to 2000tons where the maximum displacements were 1.1in, 0.9in and 2in for shafts P-7.5, P-26 and B-7.5, respectively. Though the polymer shafts significantly outperformed the bentonite shaft at extreme loads, at the working load (1000tons), there was hardly a difference in displacement. Due to this, the results of the Canary Wharf study was confirmed, in that polymer fluids do not affect the performance of drilled shafts no more than bentonite shafts. Also, the effect of increased exposure time to soil is negligible for polymer fluids which cannot be stated about bentonite fluids (Lam and Jefferis, 2015).

Based on the results of Lam and Jefferis, it can be said that the performance of both bentonite and polymer fluids are virtually indistinguishable at working loads as similar load-displacement characteristics are witnessed. The same is not true for extreme conditions where polymer shaft outperformed bentonite shafts. This finding may be irrelevant as production shafts may never experience such loading but it is important to note nonetheless. However, since this work was presented in terms total shaft resistance, it is impossible to determine how each drilling fluid affected side shear. Hence, further testing is required to determine the effect of polymer slurries on side shear.

2.5   Chapter Summary

The results of the previous studies presented in this chapter are evidence of the conflicting findings regarding the effect of polymer and bentonite slurries on shaft performance. Some studies indicate polymer slurry outperformed bentonite while anothers showed bentonite slurry outperform polymer. Yet another study showed no difference in shaft performance between the

two fluids. Hence, the need for further investigation into the slurry type effects along with the study focus, the time dependent effect of polymer slurry on shaft side shear, is needed.

It is unclear what led to the various results achieved in the reviewed studies. Differences in performance may have some dependence on varying soil strengths, construction procedures that were not cited, slurry viscosity, slurry mixing and addition to excavation, or on the polymer product itself. All of these variables can affect the side shear and should therefore be considered. Through the works presented above, it can be seen that two different exposures have been shown to affect the strength of the soil to concrete interface of drilled shafts, (1) exposure time of slurry to soil, (2) exposure of slurry laden soil to curing concrete. The shear strength increase resulting from the exposure of curing concrete to polymer laden soil is not expected to continue at the same rate as the cementitious reactions providing the increased shear strength will conclude within a few weeks. The work presented by Lam and Jefferis (2016) also suggests aggregate protrusion positively affects the interface bond due to an increased surface area. Though this may be true, this does not directly apply to polymer slurries since there is no filter cake build up to reduce aggregate protrusion. The studies above show no evidence to suggest polymer slurries adversely affect the side shear resistance of drilled shafts.

Chapter Three: Small Scale Field Testing of Side Shear Resistance

This chapter discusses the $1/10^{th}$ scale testing performed to investigate and quantify the effect of drilling fluid exposure time, primarily polymer systems, on the side shear resistance of drilled shafts. To achieve this goal, mini-shafts (4in diameter, 8ft long) were constructed using slurry stabilization with different slurry types, with varied slurry exposure times, and were extracted between 7-9 days later. The results of the test performed are presented herein, specifically, analysis of the CPT testing performed and the static load tests. Information gathered from "filter cake" measurements are also presented, analyzed and discussed. Based on the analysis of the test data, conclusions and recommendations are presented.

3.1 Small Scale Field Test Program

The objective of this study is to quantify the effects of slurry type and exposure time on drilled shaft performance. The most tangible aspect of performance is the load carrying capability but borehole stability (so that concreting can ensue) or slurry fluid loss into the soil are also important as the associated durability and constructability are just as important, although more difficult to quantify. To this end, $1/10^{th}$ scale (4in diameter x 96in long) shafts were cast, tested for pull out resistance, exhumed, and inspected for dimensional variations. In all, 32 shafts were cast with four different slurry types, where the slurry exposure against the soil was varied to provide six different exposure times (0, 1, 2, 4, 8, 24, 48 and 96hrs).

While polymer slurry was the main focus of the study, a series of shafts cast with bentonite slurry stabilization was used as a comparative baseline. Three commonly used polymer products were selected to form the field of products tested: (1) KB International Enhanced SlurryPro CDP, (2) Matrix Big-Foot and (3) Cetco ShorePac. The bentonite product was PureGold Gel from Cetco which is an API 13A, Section 10 pure bentonite product. This means it has no polymer additives as described by the American Petroleum Institute.

3.1.1 Testing Preparation

In preparation for testing, a test site was selected and characterized using CPT profiles, the test equipment was fabricated, slurry products were mixed in accordance with the manufacturer recommended procedures and a concrete mix was designed.

3.1.2 Subsurface Testing

The testing program was conducted in the Geo-Park, a geologic site on the University of South Florida Tampa Campus (Figure 3.1). The test site location was chosen to ensure that shaft construction would not be inhibited by large trees, roots or low hanging branches.

Figure 3.1 Geologic test site located within GeoPark.

Before casting could commence, it was necessary to first determine the underlying soil conditions of the test site. For the extents of this research project, it was desired to limit test soils to cohesionless soils as both bentonite and polymer slurries would have maximum soil permeattion in these soils. Cohesive soils on the other hand limit slurry infiltration and would minimize the formation of filter cake and the effects thereof. Hence, Cone Penetrometer Tests (CPT) were performed to determine the in-situ properties of the subsurface at the test locations which in turn dictated the acceptable shaft lengths.

The CPT tests were performed to depths of 14 – 25ft using the University of South Florida's miniature CPT rig (Figure 3.2) at the proposed test shaft locations. Analysis of the data showed that the test site was comprised mostly of silty sands from 0-8ft with interbedded clay layers at deeper depths. For this reason, the shaft lengths were reduced from the originally planned 10ft to 8ft to ensure the slurry and shafts would only interact with the cohesionless layers of the site.

Figure 3.2 Cone Penetration Testing.

Figure 3.3 shows the tip resistance, sleeve friction, friction ratio, equivalent SPT and soil classification from CPT tests performed for one of the bentonite test shaft locations. Note the classification plot shows the subsurface at the test site is mostly sands between 0-8ft. Subsequent CPT tests for the bentonite shafts yielded nearly identical results as the plots on each graph are practically on top of each other as seen in Figure 3.4. Subsequent subsurface profiles were comparable to the first bentonite shaft test location. Similar results were seen with each of the polymer shaft locations except in the bottom 2ft, where some variations were seen in tip resistances.
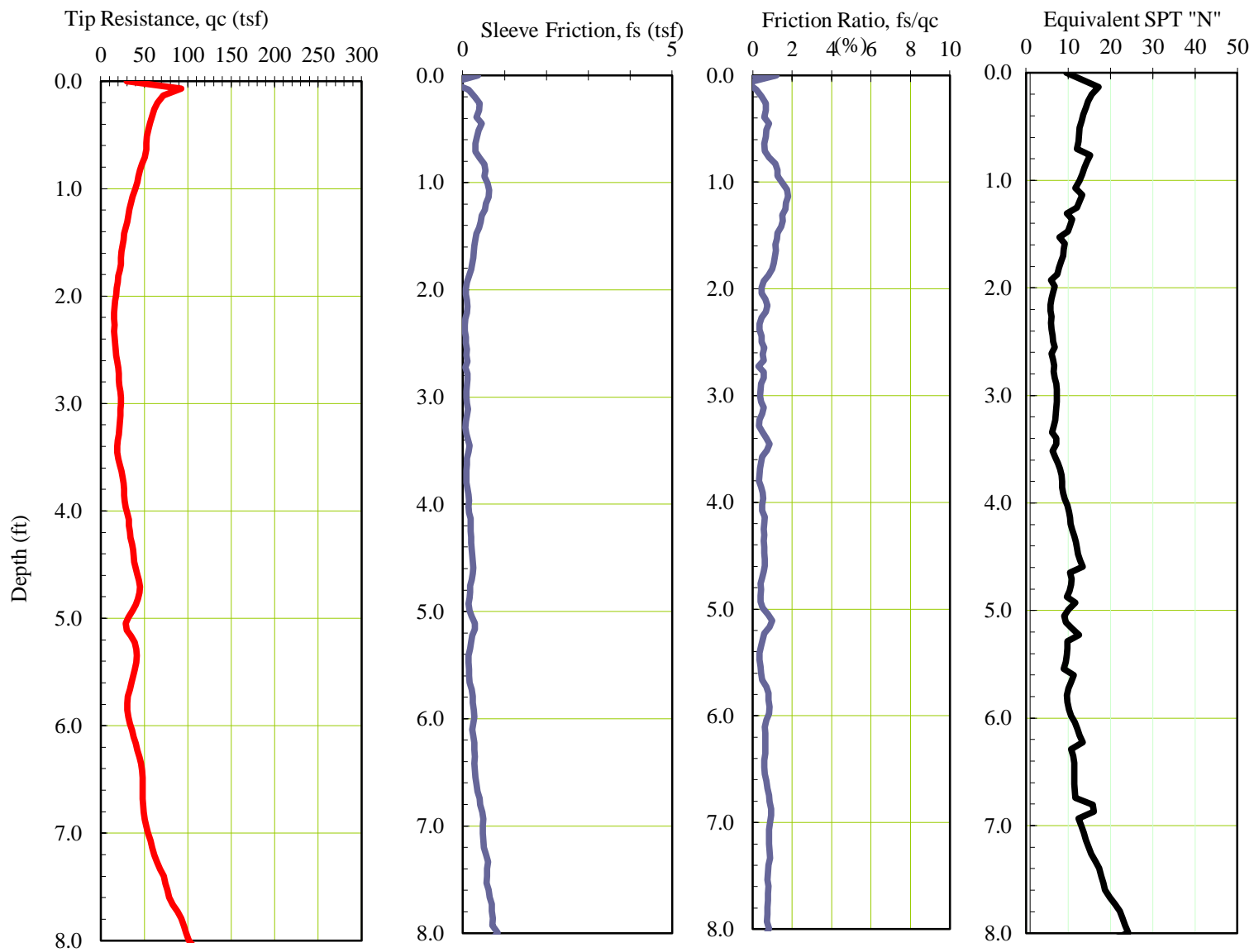
Figure 3.3 CPT results at first bentonite test location.

44
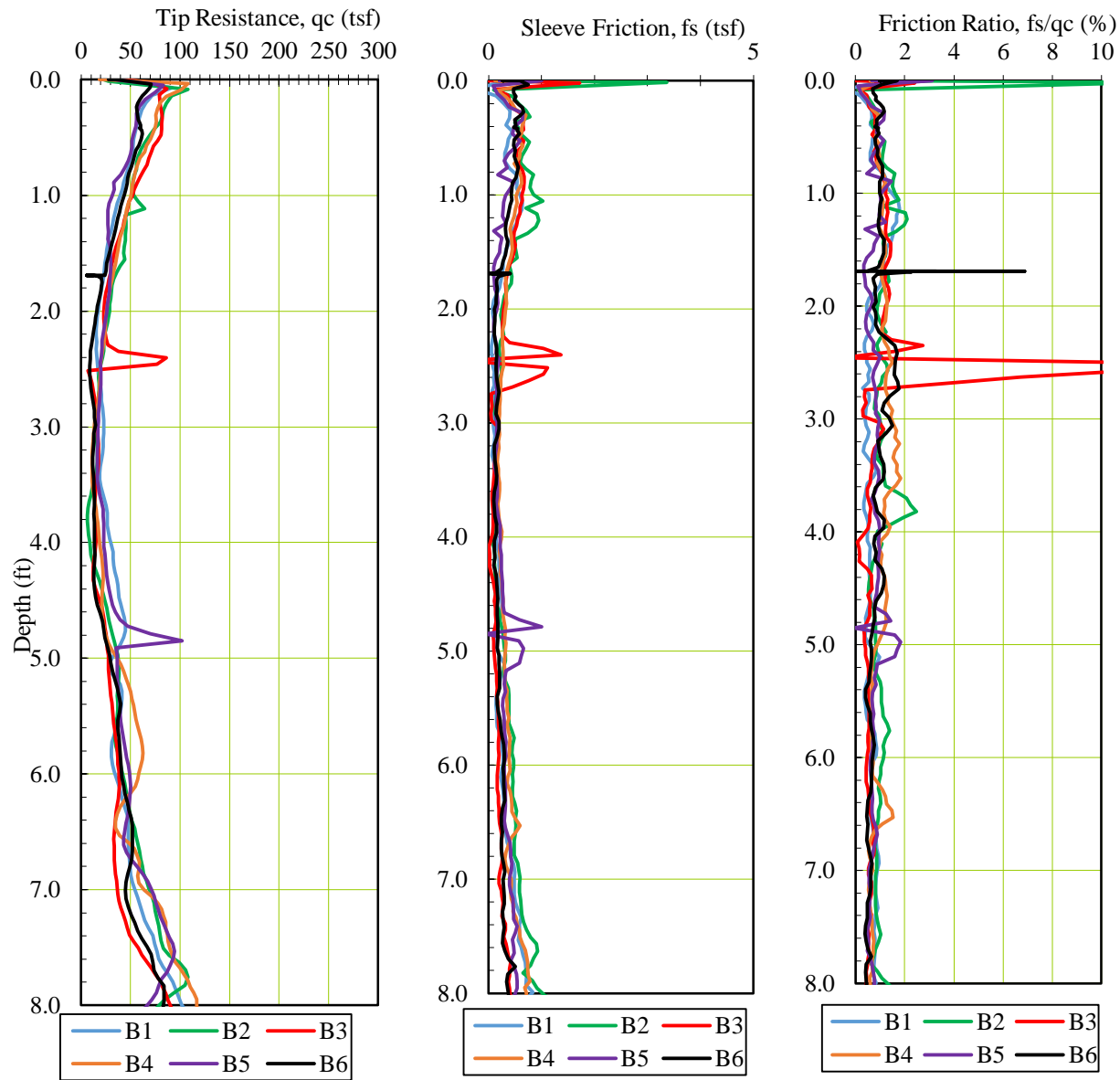
Figure 3.4 Combined plot of tip resistance, sleeve friction and friction ratio of six bentonite test locations.

3.1.3 Materials/Fabrication

Numerous fixtures were required for the excavation, concreting and shaft extraction processes. Some materials were commercially available but others were fabricated where necessary. These items are discussed below.

3.1.3.1 Excavation Materials

3.1.3.1.1 Hand Auger

The hand auger used for excavation had a 3.8in outer diameter, 8in long collection bucket with two "cutting teeth" along the diameter. The bucket was connected to a 4ft rod that allowed for the connection of the drilling handle or additional 4ft extension rods (Figure 3.5).

Figure 3.5 hand auger (left) and close-up of drilling bucket (right).

3.1.3.1.2 Surface Casing

The surface casing was used to stabilize the upper soils of the excavation prior to slurry introduction. The casing was fabricated out of steel pipe, having a 4in inner diameter and 4.5in outer diameter. The pipe was cut into 2ft sections and a steel ring (0.25in thick, 4.625in inner diameter and 7.625in outer diameter) was welded to the outside of the tubing, 1ft from each end. The steel ring was plasma cut out of ¼in steel and was installed to ensure the casing would rest on the surface soils surrounding the borehole. The pipe and ring, along with the assembled casing is shown in Figure 3.6.

46

Figure 3.6 casing tubing (left), casing ring (middle) & assembled casing (right).

3.1.3.1.3 *Slurry Mixing System*

The mixing system used for slurry preparation was comprised of a water holding tank, a centrifugal trash pump, Hootonanny™ eductor, aerator (polymer), air compressor (polymer) and a mixing / holding tank. The same system was used for all slurry products, but the aerator component was only used for polymer slurry.

The water tank had a capacity of 300 gallons while the mixing tank had a capacity of 175 gallons. Fluid entered the pump through a 2in hose coming from the holding tank and exited through a 1in hose connected to a non-clog eductor. Most polymer manufacturers call for the mix water to be pretreated to increase the pH to 9-11. In this case, a Hootonanny™ venturi disperser was used as there was prior experience with the eductor which provided a level of confidence in its performance. This method of introduction is preferred because it immediately injects the product into suspension or solution, resulting in a well-mixed stabilizing fluid. A continuous flow of water is introduced through to the Hootonanny™ and discharged at a 90° angle from the inflow. The fluid flow results in a vacuum which is capitalized upon via a port in-line with the discharge. Dry product is vacuumed in through the port and immediately introduced to the discharging fluid. Figure 3.7 shows the Hootonanny™ introducing fluid into the mixing tank.

The aerator was constructed out of 1in PVC pipes and had a 20in square base with an additional pipe across its centerline to increase agitation in the middle of the tank. The base was attached to standpipe and connected to an air hose fitting. Holes were drilled into the bottom of the aerator at 20° angles so that any bottom sediment would be agitated and placed back into suspension. Dead weight was added to aerator to ensure it would remain at the bottom of the tank during the mixing process. Compressed air was introduced to the system through the 5hp, gas powered air compressor. Figure 3.8 shows the mixing system re-agitating and mixing polymer.

Figure 3.7 Hootonanny™ discharging product into mixing tank.

Figure 3.8 Slurry mixing system; re-circulating (left), mixing (right).

3.1.3.2 Concreting Materials

3.1.3.2.1 Concrete Mixer

A 5hp gas powered concrete mixer was used to mix the mortar for the test shafts (Figure 3.9). The mixer was variable speed and had 14 possible tilt positions. There were two completely vertical orientations (90° and 270°) and 12 others (six on either side of vertical) varying between 45° above and below horizontal. The various orientations on either side of vertical proved to be extremely convenient for this project because it allowed for the entire mixing process to be performed on the transportation trailer. Once the mortar was mixed on the trailer side of the mixer, it could be emptied on the other side off the trailer and into the tremie hopper.

Figure 3.9 Gas-powered concrete mixer discharging to tremie hopper.

3.1.3.2.2 Slurry Catch Pan and Spill Ring

A catch pan was necessary to recover displaced slurry from the borehole during the concreting process. The catch pan was made out of a 3ft x 3ft section of 18 gauge sheet metal. A 4.5in hole was cut into the center of the sheet and the outer 6in on each side of the sheet was folded up to form a 2ft x 2ft x 6in pan. The corners of the pan were spot welded and sealed with silicone. Another 6in portion of sheet metal was rolled to form an open ended cylinder and was inserted into the 4.5in hole in the pan. It was then welded onto the bottom of the pan so that it protruded into pan to ensure captured fluid would not drain out of the center hole. A ring similar to the casing ring was also used with the catch pan to ensure no slurry would flow between the pan and the surface casing. Figure 3.10 shows the catch pan and overflow ring in use.

Figure 3.10 slurry catch pan and spill ring installed around casing.

3.1.3.2.3 Sheathed ¾in Steel All Thread

To provide a tension connection for testing and extraction, ¾in diameter steel all-thread rods were cast into the shafts during the concreting process. The rods measured 12ft in length and had a 1.5in diameter plate with a 0.8in hole in the center secured to its bottom 1.25in with two ¾" nuts (one above and one below the plate, Figure 3.12). PVC pipes, 1in diameter, 8ft long, were then placed onto the rods, secured with a top nut and the remaining 4ft of exposed steel all thread was protected to allow reuse. This approach sheathed the rod steel rod so that it would not be bonded to the concrete or contaminated during the concreting process. Figure 3.11 shows the sheathed rods.

The bottom plate shown in Figure 3.12 also ensured that the tensile force in the steel rod was transferred to the bottom of the shaft specimens and would apply a compressive force to the bottom of the concrete, decreasing the possibility of tensile failure in the concrete during shaft extraction. Subtle dimensional changes from Poisson effects would also not be encountered.

Figure 3.11 Sheathed ¾in all-thread steel bar.

Figure 3.12 Bottom plate secured with ¾in nuts.

3.1.3.2.4 Hopper and Tremie

Per the Standard Specifications for Road and Bridge Construction, concrete is only allowed to fall freely for 5ft, else it must be contained in pipes, troughs or chutes. Therefore a tremie and accompanying hopper were required to contain the concrete flow (FDOT 2018). The hopper served as the transport vessel for the fluid concrete (mortar) from the concrete mixer to the borehole and took the shape of an inverted square pyramid. It had a holding capacity of 1.5ft^3 and a 3in drain pipe on the smaller end of the pyramid. A 3in ball valve was attached to the end of the drain pipe and cam-lock fittings were also attached to the hopper and tremie, allowing for

immediate connection / disconnection of the two pieces. The hopper was also able to be suspended from hoist with a steel rod that spanned across the top of the hopper. After two series of test were performed, the brass ball valve was concreted shut, therefore it was replaced by a more serviceable plastic valve. Figure 3.13 shows the concrete hopper with both valve attachments.

Figure 3.13 Concrete hopper, brass valve (left) and plastic valve (right).

To allow for the entire anchor rod to be placed in the shaft prior to concreting, the tremie was 12ft long, 3in PVC pipe, long enough to hold the anchor bar within it (Figure 3.14). PVC knockout test caps were used as a temporary plug for the tremie. This ensured that no slurry would enter the tremie through the bottom upon insertion into the wet borehole. It is important to avoid slurry entering the tremie as the proper concreting procedure with hydrostatic stabilization is to have the concrete displace the slurry with no prior mixing of the two materials (FDOT, 2016).

The hopper and tremie originally had a 2in diameter outlet but these smaller dimensions proved problematic when a mock test was performed. The smaller tremie did not allow for rapid concrete flow through the two inch port and hence the concrete displacement of slurry was largely ineffective. This problem was also compounded by the use of an out-of-spec bentonite slurry (nearly 70s/quart) in the mock test. As a precaution, 3in diameter was used to increase concrete flow through the valve and improve the effectiveness of the slurry displacement. After the adjustment, full slurry displacement was witnessed in Figure 3.14 (bottom right).

Figure 3.14 Twelve foot long, 3in diameter tremie (left), poor slurry displacement with 2in tremie (top right), improved slurry displacement with 3in tremie (bottom right).

3.1.3.2.5 Structural Tripod, Shackle, Block and Tackle and Cathead

While performing the mock test, attempts were made to remove the tremie by hand but were unsuccessful as the tremie surface was too slick and kept slipping back into the borehole. Therefore, the overhead electric hoist at the outdoor research facility was used to extract the tremie from the borehole. (Figure 3.15).

Figure 3.15 Tremie extraction with electric hoist during mock test.

Since the electric hoist would be unavailable at the test site, a tripod was constructed to provide a field portable overhead hoist. The tripod was constructed from one 3in and two 2in diameter, 20ft long aluminum pipes. The 3in ID pipe (3.5in OD) was used as the main leg and the 2in pipes were the outer legs. Two 2.5in diameter, 7.5in long steel pipes were added to the end of the outer legs and bolted 1.5in from the end of the outer legs. The remaining 6in of added pipe was then crimped to increase the angle of movement of the outer legs. Holes of 1in diameter were drilled approximately 3in from the end of each leg and a $^{7}/_{8}$in threaded rod was used to connect the legs (Figure 3.16).

Figure 3.16 Main leg and modified outer legs of structural tripod.

A 2ft section was cut out of the main leg and replaced with a 3in OD, 2.5ft long section of solid aluminum rod (Figure 3.16). Using a lathe, a 2ft section (three inches from each end) of the rod had its diameter reduced from 3in to 2.5in. This modification was made so that a cathead could be mounted to the tripod and assist in any lifting that would occur. The cathead is a motorized spinning drum attachment around which a rope is looped to hoist objects as seen in Figure 3.17. This cathead had a 5hp rating and was gas powered.

Figure 3.17 Modified tripod leg (left) mounted cathead in operation (right).

A computer numeric controlled (CNC) plasma torch was used to cut a specialized shackle to hang from the tripod out of a ½in steel plate. The CAD drawing for the shackle is shown in Figure 3.18. Once the shape was cut by the plasma torch, it was heated by torch and shaped into the horseshoe portion of the shackle seen in Figure 3.18.

A block and tackle is a pulley system comprised of pulley-blocks and rope that is used as mechanical hoist. There were two pulley wheels per block, making the system capable of lifting four times the effort exerted on the free end of the rope. One block was attached to the shackle (standing block) and the other had a hook attach and was left free (travelling block). The standing block was suspended by two steel tabs going to a common shackle so that the load from each pulley wheel would be evenly transferred. Another steel tab was plasma cut and welded to the center of the standing block for the fixed end of the rope. Figure 3.19 shows the standing block and travelling block while Figure 3.20 shows the entire hoisting system.
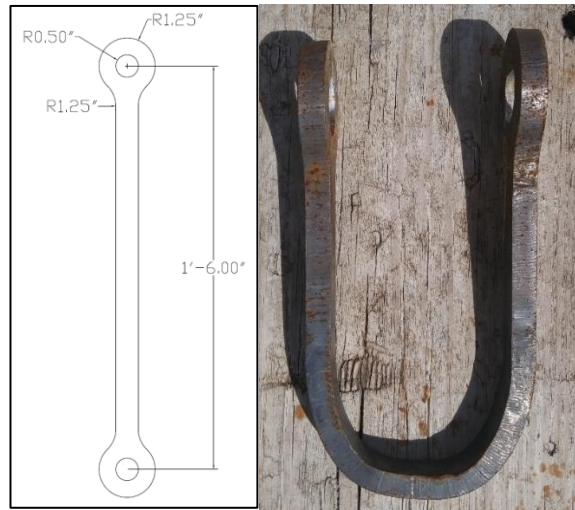
Figure 3.18 Shackle CAD drawing (left), final product (right).

Figure 3.19 Standing block (left), travelling block (middle), stored block and tackle (right).

Figure 3.20 Tripod and hoisting system.

3.1.3.3 Static Load Test, Shaft Extraction and Dissection Materials

3.1.3.3.1 *Hydraulic Pump and Jack*

Tensile load was applied to the embedded steel rod using two hydraulic pumps and a hollow-core jack. During the load tests, a hand pump was used to apply load in a slow, controlled manner whereas an electric pump was used to rapidly apply load during the extraction process. Both pumps sent fluid to a 30 ton, 6in stroke hollow-core hydraulic ram. Each of the hydraulic system components are displayed in Figure 3.21.

Figure 3.21 Electric hydraulic pump (left), hand hydraulic pump (middle), hydraulic ram (right).

3.1.3.3.2 *Load Frame and Reference Beam*

The load frame was responsible from transferring the reaction forces of those exerted on the steel rod to the ground. A previously built load frame, measuring 40in high and 30in wide was used to perform this task (Figure 3.22). The frame had two columns that were connected by a single beam at the top of the columns. Two I-beams were aligned vertically and welded together. Plate stiffeners were also welded at the meeting of the two beams to increase the stiffness of the columns. The beam connecting the columns had a hole passing through its center to allow for the steel rod to pass through. Small plates were also welded to the bottom of the columns to increase the column footprint and distribute the load over a larger surface area.

A previously fabricated reference frame was also used as the datum for displacement measurements (Figure 3.23). The reference beam was 8ft long and stood 1ft above the ground. It consisted of one piece of steel angle iron spanning between a triangular and a vertical support. Rigidity was added to the system through brackets between the horizontal beam and the supports.

Figure 3.22 Load frame.

Figure 3.23 Reference beam.

3.1.3.3.3 Load Testing Instrumentation

Forces exerted on the shaft were measured with a 10 ton compression load cell (Figure 3.24) while displacements were measured with a linear variable displacement transformer (LVDT) (Figure 3.25). The LVDT had a plunger extending from the shaft body that compresses in a linear fashion was capable of measuring displacements up to 4in. A bracket for mounting the

LVDT to the reference frame was made out of steel angles along with a small tab that would attach to the rod and compress the plunger. The LVDT, mounting frame and tab are shown in Figure 3.25.

Figure 3.24 Compression type load cell (10 ton).

Figure 3.25 Mounted LVDT, bracket and displacement tab.

3.1.3.3.4 Data Collection System

Test data was recorded with the same data collection system used for the CPT tests. This comprised of an Omega Model USB OMB-55 data acquisition device, field computer and a weather resistance enclosure (Figure 3.26). The CPT test setup was modified to account for the load cell and displacement gauge.

Figure 3.26 Data collection system.

3.1.4   Slurry Preparation

The total volume of slurry mixed for excavation was based on the volume of slurry needed for excavation during the mock test, 7.5 gallons per borehole equating to 45 total gallons for 6 boreholes. To account for losses, 65 gallons of bentonite slurry was mixed and 100 (later increased to 150) gallons of polymer slurry was mixed to perform the excavation.

3.1.4.1 Bentonite Slurry

Bentonite slurry was thoroughly mixed more than 24hrs prior to its use and stored in five gallon buckets. The bentonite powder was introduced to the pre-treated water using the Hootonanny™ eductor and was allowed to fully hydrate before being used (Figure 3.27). The Marsh funnel viscosity for the 65 gallons of bentonite slurry was 34sec/qt at the time of mixing and at the time of drilling it was 37sec/qt (Figure 3.28).

Figure 3.27 Slurry in the mixing tank.

Figure 3.28 Marsh funnel viscosity at time of drilling (37s/qt).

3.1.4.2 Polymer Slurry

The details of the preparation for each polymer slurry are explained below. The KB Enhanced SlurryPro System was mixed at the test site 30 minutes prior to excavation while the other polymer systems were mixed at least 12 hours prior to excavation.

3.1.4.2.1 KB International Enhanced SlurryPro Polymer System
This system was comprised of four individual products combined to create the stabilizing slurry. The base polymer of the system is the SlurryPro CDP, while EnhancIT100, EnhancIT200 and SlurryPro MPA are additives used to improve the performance of the base product (KB International, 2015(a)). SlurryPro CDP is a vinyl synthetic based, water soluble, anionic polyacrylamide (KB International, 2015(b)).

A manufacturer representative was present to assist with the mixing of the slurry. The representative explained that the CDP is capable of stabilizing without the additives but EnhanceIT100 helps to reduce fluid loss, EnhanceIT200 improves the slurry ability to suspend and the MPA is a finishing product that connects the polymer chains of the individual products. All of the products in the enhanced system are solid granular powders except the MPA, which is a liquid product. It should be noted that the KB system does not call for the pre-treatment of the mixing water (KB International, 2015(a)).

Per instruction of the company representative, the values displayed in Table 3.1 were used to mix 50 gallons of the polymer slurry. Each dry product was pre-weighed into containers while the liquid was placed into an 8oz spray bottle. After the 1oz of MPA was placed into the spray bottle, the remaining volume was filled with water and vigorously shaken for thorough mixing. The values in Table 3.1 were doubled to mix the 100 gallons of polymer slurry discussed above.

Table 3.1 KB International Enhanced SlurryPro CDP 50 gallon mixing proportions.

Product	Amount Added
SlurryPro CDP	0.441 lbs
EnhancIT 100	0.088 lbs
EnhancIT 200	0.044 lbs
MPA	5 ml

To correctly mix the slurry, the slurry products were introduced as 100 gallons of water were pumped from the storage tank to the mixing tank. The procedure called for all of the dry product to be added to the system in halves, half of each product, then the addition of the remaining half. Once all the dry product was added, the mixed slurry should then be sprayed with MPA. First the SlurryPro CDP was added, followed by EnhancIT100, then EnchanceIT200. SlurryPro CDP and EnhanceIT 200. EnhanceIT100 was sprinkled onto a flat aluminum plate while water flowed across the plate; the other three products used the eductor. After the first half of CDP was added, the aerator was activated to continuously agitate the product. When all the products was added to the mixing tank, the water supply was disconnected from the Hootonanny™ and placed directly into the mixing tank until the target volume was met. Once 100 gallons were in the mixing tank, the water supply was shut off and the slurry was allowed to mix with only the aerator for 25 minutes. After 25 minutes, the slurry was ready for use in the excavation. Figure 3.29 shows mixing of the Enhanced SlurryPro CDP polymer system while Figure 3.30 shows the slurry mixing after all the products had been added.

Figure 3.29 Hootonanny™ eductor (top left), vacuuming dry product with eductor (top right), Enhanceit100 introduction with spill plate (bottom left), spraying of MPA after all dry products were added (bottom right).

Figure 3.30 Continuous agitation of KB International Enhanced CDP polymer with aerator.

3.1.4.2.2 Matrix Bigfoot Polymer

Due to inclement weather and associated delays, the Matrix slurry was mixed one week prior to use in excavation and not immediately prior to excavation as originally intended.

The polymer slurry system consisted of three different water soluble, dry products. The main product is the Big-Foot polymer while Fortify is an additive to reduce slurry loss and M-Booster is the water pretreatment product. Big Foot is a synthetic anionic polyacrylamide whereas Fortify is a natural polysaccharide. A company representative was present to assist in the mixing of the stabilizing system. Table 3.2 documents the amounts of each product added to mix 150 gallons of the slurry stabilization system.

Table 3.2 Matrix Big-Foot polymer 150 gallon mixing proportions.

Product	Amount Added (lbs)
Big-Foot Polymer	1.75
Fortify Slurry Loss Additive	1.5
M-Booster pH Adjuster	1.25

M-Booster was first added to the water in the storage tank. The water tank was filled to 300 gallons and 2.5lbs of M-Booster was added to the tank. Using a centrifugal pump, water was re-circulated in the storage tank to allow the M-Booster to thoroughly mix the entire volume. After

10 minutes of re-circulation, the pH had increased from 8 to 10 and the hardness (measured as calcium carbonate) was120ppm. Since the pH was above 9, the water was deemed acceptable to mix the polymer system. It should also be noted that it is desirable, though not necessary, to have hardness levels less than 100ppm.

Next, water was pumped from the storage tank to the mixing tank and Fortify was introduced to through the Hootonanny™. Once all of the Fortify was added, the water supply was shut off and the Fortify was allowed to aerate for 5 minutes. At this point, approximately 75 gallons of water was in the mixing tank After the 5 minutes had expired, the water supply was started again and the Big-Foot polymer was added. When all 150 gallons of water was added to the mixing tank, the water supply was shut off once again and the system was allowed to aerate for 20 minutes. After aeration, the pH and hardness measurements were 9.5 and less than 100ppm, respectively. Immediately after mixing, the Marsh funnel viscosity was 115sec/qt which is above the recommended 50-55 sec/qt.

It was suspected by the company representative, based on prior experience that the foam generated by the Hootonanny™ during introduction resulted in the increase in slurry viscosity. However, after five days, the slurry was re-agitated for 15 minutes and the Marsh funnel viscosity was re-measured. This test yielded a viscosity of 136 sec/qt. It was at this point it was determined that the polymer slurry was too viscous and should therefore be diluted. Figures 3.31 and 3.32 show the mixing of the original batch of the Big-Foot polymer system.

Figure 3.31 Big-Foot product introduction through Hootonanny™ (left), aeration during mixing of Big-Foot polymer system (right).

Figure 3.32 Addition of Big-Foot slurry system to Marsh funnel (136sec/qt).

Dilution was achieved in 5 steps. First, 50 gallons of slurry was removed and replaced with 20 gallons of treated water. The replaced water did not equal the removed volume to reduce the overall volume as there was some concern of slurry spillage during transportation to the test site. In each dilution step after the first, 15 gallons of removed slurry was replaced with 15 gallons of treated. Viscosity was measured after each dilution. The final dilution resulted in a Marsh funnel viscosity of 73sec/qt. Table 3.3 shows the product concentration throughout the dilution process.

Table 3.3 Mix ratio and dilution schedule for Matrix Big Foot system.

Product Amount	Treated Water	Mix Ratio	Volume Removed	Weight Removed	Water Added	Total Slurry Exchanged w/ Water	Total Weight Removed	Marsh Viscosity
(lbs)	(gals)	(lb/gal)	(gals)	(lbs)	(gals)	(gals)	(lbs)	(sec/qt)
1.75	150	0.0117						115/136*
			50	0.583333	20	20	0.5833333	
1.17	120	0.0097						110
			15	0.145833	15	35	0.7291667	
1.02	120	0.0085						92
			15	0.127604	15	50	0.8567708	
0.89	120	0.0074						92
			15	0.111654	15	65	0.9684245	
0.78	120	0.0065						86
			15	0.097697	15	80	1.0661214	
0.68	120	0.0057						73

*5 days later

3.1.4.2.3 Cetco Shore Pac Polymer

Due to the viscosity issues experienced with the KB International and Matrix polymer systems, too thin and too thick, respectively, this stabilizing system was mixed one day prior to excavation.

For this system, only the base product, Shore Pac, was added to pH treated water. First, 2lbs of soda ash (pH adjuster) was added to the 300 gallon tank of water. Initial pH was 7, but after 5 minutes of re-circulation, the pH was approximately 10. Using the suction hose of the Hootonanny™, 1.05lbs of Shore Pac was introduced as the treated water was transferred to the mixing tank and continuously agitated with the aerator for 30 minutes. The resulting Marsh funnel viscosity was 74sec/qt. The following day, the Marsh funnel viscosity was 89sec/qt; therefore 30 gallons of slurry was removed and replaced with 30 gallons of treated water. This process was then again repeated to further reduce the viscosity. After dilution, the Marsh funnel viscosity of the system was reduced to 74sec/qt. Table 3.4 shows the product concentration throughout the dilution process. Figure 3.33 shows the agitation of the of the Cetco polymer system after the product had been introduced to the system.

Table 3.4 Mix ratio and dilution schedule for Cetco ShorePac.

Product Amount (lbs)	Treated Water (gals)	Mix Ratio (lb/gal)	Volume Removed (gals)	Weight Removed (lbs)	Water Added (gals)	Total Slurry Exchanged w/ Water (gals)	Total Weight Removed (lbs)	Marsh Viscosity (sec/qt)
1.05	150	0.0070						79 / 89*
			15	0.105	15	15	0.105	
0.95	150	0.0063						79
			15	0.095	15	30	0.200	
0.85	150	0.0057						74

*24hr value

Figure 3.33 Mixing of Cetco polymer stabilizing system.

3.1.5 Concrete Mix

The term concrete is used loosely here as the shafts were actually cast with mortar, meaning there was no coarse aggregate in the mix. The concrete mix was comprised of type I/II cement, water and commercially available sand. Since it was known that mortar has a unit weight of 135lbs/ft^3, an equation was derived to determine the quantities of each constituent in a 1ft^3 mix. A 0.5 water to cement (w/c) ratio was also used for the mortar mix. The 0.5 w/c ratio along with density/unit weight relationships were used to calculate the mix proportions. The calculated values were reduced so that 0.9ft^3 mortar would be mixed, resulting in a 28.5% waste for the 0.7ft^3 borehole. The values are shown below and the mix (0.9ft^3) can be seen in Table 3.5.

$$W_m = W_W + W_C + W_S$$

where,
W_m = unit weight of mortar
W_W = weight of water
$W_C = 2W_W$ = weight of cement
$W_{sand} = 135 - 3W_W$ = weight of sand
Hence,

$$135lbs = W_W + 2W_W + (135 - 3W_W)$$

Converting to Volume,

$$1ft^3 = \frac{W_W}{62.4lbs/ft^3} + \frac{2W_W}{(3.15)(62.4lbs/ft^3)} + \frac{135 - 3W_W}{(2.6)(62.4lbs/ft^3)}$$

$$62.4lbs = W_W + \frac{2W_W}{3.15} + \frac{135 - 3W_W}{2.6}$$

$$62.4lbs = W_W + \frac{2W_W}{3.15} + \frac{135}{2.6} - \frac{3W_W}{2.6}$$

$$10.477lbs = W_W(1 + 0.634 - 1.154)$$

Solving for W$_W$,

$$W_W = 21.778lbs$$
$$W_C = 43.556lbs$$
$$W_S = 69.7lbs$$

Table 3.5 mortar mix proportions for 0.9ft^3.

Description	Weight (lbs)
Cement	39.24
Sand	62.73
Water	19.62
Total	121.6

Before its use in production of test shafts, the concrete mix was tested during the mock test to ensure the slump would promote flow through the hopper and tremie. The mix proved to be extremely workable as the slump test yielded a slump of 10.5in. Essentially, once the slump cone was removed, the mortar mix fell into a puddle on the slump cone as seen in Figure 3.34. Though the mix was extremely fluid, this quality was desired for the mortar because of the small remaining volume once the tremie was placed in the borehole. This means that the mix needed to have liquid like properties but still have the necessary strength to sustain applied forces.

Figure 3.34 Filling the slump cone (left), measuring the slump of 10.5in (right).

Compressive tests on 3in x 6in test cylinders yielded compressive strengths of 2.9ksi. Thus, the test shafts were capable of withstanding 37.5 kips, far beyond the expected pullout strength of the shafts.

3.1.6 Transportation of Materials

All of the aforementioned materials were either loaded into a truck (smaller items) or onto a 24ft trailer (larger items) for transportation to the test site. The bentonite slurry that was mixed prior to excavation was placed in 5 gallon buckets and loaded onto the trailer. All of the materials required for the mortar mix were also pre-weighed, placed in sealed 5 gallon buckets and loaded onto the trailer for on-site mixing. The loaded trailer can be seen in Figure 3.35.

Figure 3.35 Loaded trailer for transportation to the test site

3.1.7   Shaft Construction and Load Testing

The field component of this study involved: borehole excavation, shaft concreting, load testing, shaft extraction and dissection. For each shaft, the procedure was similar, therefore each of the steps will be discussed for the bentonite shafts and only deviations, discrepancies and/or anomalies for that procedure for the other test series are identified.

3.1.8   Test Matrix

The testing included the casting of 24 shafts, 6 for each slurry product and with four products. Each product was denoted as a series. The slurry products tested were CETCO PureGold Gel (Bentonite), SlurryPro CDP (Polymer), Matrix Big-Foot (Polymer), and CETCO ShorePac. Images of these products are shown in Figures 3.36-3.39. Bentonite slurry was used as a baseline for the experiment, as it is the FDOT preferred drilling fluid for structural drilled shafts as identified in Chapter 2. Hence, the performance of the polymer shafts were compared to that of the bentonite shafts. As previously stated, the borehole slurry exposure times explored in the experiment were 0, 1, 2, 4, 8 and 24 hours after slurry introduction.

71

Figure 3.36 50lb bag of Cetco PureGold Gel (bentonite).

Figure 3.37 KB International Enhanced SlurryPro CDP products (polymer).

Figure 3.38 Matrix Big-Foot polymer products.
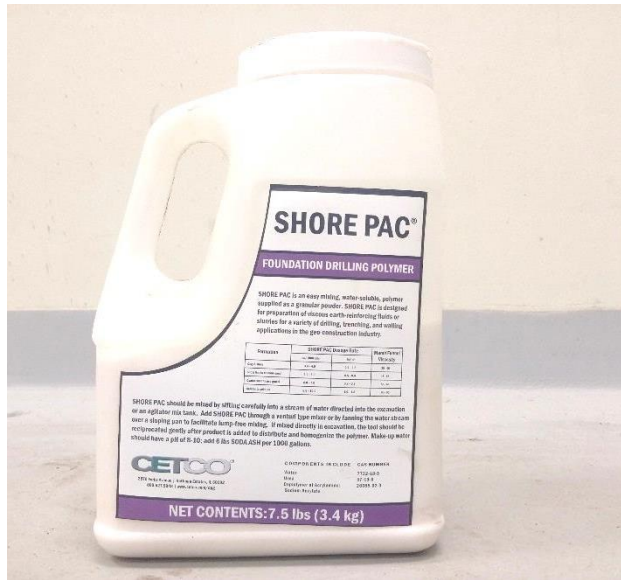
Figure 3.39 Cetco ShorePac polymer product.

A 20ft wide by 40ft long area within the GeoPark was identified as the test site for the $1/10^{th}$ scale shafts. Each test series was spaced 3ft on center while test shafts within each series were spaced 6ft on center. Figure 3.40 shows the layout of the test shafts with each slurry product and exposure time identified. One CPT was conducted at each location.
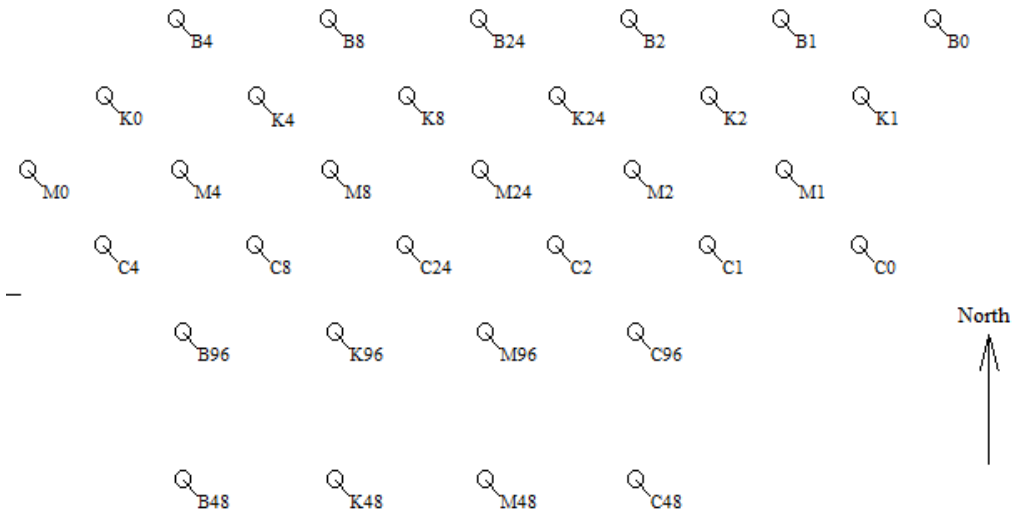
Figure 3.40 Layout of test shafts.

3.1.9 Cetco PureGold Bentonite Shafts

3.1.9.1 Borehole Excavation

Hand augers are a useful tool for near surface exploration but are typically limited to excavations above the water table. When submerged conditions are encountered (especially in sandy soil),

the contents of the auger bucket are simply washed out and cannot be removed from the hole. However with slurry products, both the contents can be removed and the sidewall stability can be maintained below the water table.

As previously discussed, 4in diameter 8ft long boreholes were drilled with the use of a hand auger. Prior to drilling, a bubble level was placed on the shaft of the hand auger to ensure that the boreholes and resulting shafts would be as close to vertical as possible (Figure 3.41). Once the first 1ft of borehole was drilled, the surface casing was installed as seen in Figure 3.41. Immediately after, the catch pan and overflow ring were placed over the casing and slurry was added to the borehole (Figure 3.42). The water table was found between 3 and 5ft throughout the timeframe of the field tests.

Figure 3.41 Levelling the hand auger (left), casing installation (right).

Figure 3.42 Slurry introduction into the borehole.

Excavated soils were inspected to ensure that they corresponded with the expected results from the CPT tests, i.e. mostly sandy soils (Figure 3.43). Any discrepancies in the excavated soil or obstacles encountered during excavation were noted in the field book with the approximate depth.

Figure 3.43 Excavated sandy soil.

During excavation, slurry was maintained at ground level but some decrease in slurry level was witnessed during the extraction of the tool. Once slurry level fell approximately 2ft below the ground surface, slurry was added to the borehole which was still well above the ground water table at depth 5-6ft. Slurry was poured directly into the borehole from the 5 gallon buckets. Once the 8ft depth was attained, the slurry level for each borehole was maintained at ground level. The Marsh funnel viscosity the bentonite fluid used in excavation was 39sec/qt within the state specified range of 30 to 40 sec/qt (Figure 3.44).

Figure 3.44. Marsh funnel viscosity field test.

Before any concreting commenced, all of the boreholes were excavated. Drilling began with the 4hr borehole and was followed in listed order by the 8hr, 24hr, 2hr, 1hr and finally the 0hr borehole. Excavation logs, noting the beginning and conclusion of drilling, were kept to ensure accuracy within the exposure times. The "exposure clock" used to identify each borehole began at the conclusion of drilling and went until the start of concreting. Once all of the boreholes were drilled, the concreting process began. All excavations took less than 20min, so the actual exposure time could be considered to be up to 20min more than that identified by each specimen name.

3.1.9.2 Borehole Concreting

Mixing of the mortar began once the 0hr borehole was drilled about 6ft. All mortar mixing was done in accordance with ASTM C305: *Standard Practice for Mechanical Mixing of Hydraulic Cement Pastes and Mortars of Plastic Consistency*. Once the mixing was completed, the mortar mix was emptied into the hopper (Figure 3.45). The hopper was placed near the end of the forks of a skid steer tractor for transportation to the borehole.

Figure 3.45 Mortar mix being transferred to the hopper.

While the mixing was being performed, the test plugs were taped to the bottom of the tremie and the steel rods with end plates were placed into the tremie (Figure 3.46). Once the mortar was in the hopper, the tremie was inserted into the hole and the hopper was then connected to the tremie via quick-connect cam locks. The travelling end of the block and tackle was then hooked to the hopper while the free end of the rope was loosely wrapped around the cathead.

Figure 3.46 Sheathed all-thread inserted into the tremie.

After the hopper was hoisted and connected to the tremie, the 3in valve was opened and the tremie was fully charged with the concrete. The entire hopper / tremie concreting system was then lifted slightly to ensure that the tremie plug was not resting on the bottom of the borehole (Figure 3.47). As the assembly was lifted, the concrete level inside the hopper was watched until it fell to a level below the hopper valve. At that point, the hopper was empty and it was disconnected from the tremie, set aside and the hoist was then connected to the tremie for extraction. As the tremie was raised very slowly, mortar flowed into the borehole, displaced the slurry and filled the volume once occupied by the tremie. Slurry was observed to flow out of the top of the casing (Figure 3.48). The volume of concrete slightly exceeded that required such that the concrete was seen just as the tremie was completely removed. As this time, the concreting process was concluded. Once concreting was completed, the overflow ring, catch pan, and temporary casing were removed (Figure 3.49). Figure 3.50 shows the finished shafts.

Figure 3.47 Hopper connected to the tremie (left), confirmation of mortar flow into tremie (right).

Figure 3.48 Mortar expelling slurry (left), fully concrete shaft (right).

Figure 3.49 Removal of temporary surface casing.

Figure 3.50 Concreted bentonite shafts.

3.1.9.3 Pullout Static Load Tests, Shaft Extraction and Dissection

The shaft extraction process was briefly mentioned in previous sections but will be discussed in greater detail here. Load testing was achieved by exerting tensile forces on the embedded all thread. Both the load applied to the rod and resulting displacements were measured. The tensile force was transferred directly to the base of the shaft by way of the debonded bar whereby a compressive force was applied to the circular plate fastened to the bottom of the rod. A 10 ton load cell and 4in LVDT were used to measure the load and displacement, respectively while the measurements were recorded with the data collection system mentioned in Section 3.2.2.3. After testing was completed, the shafts were fully extracted and sectioned for filter cake measurement.

Shaft extraction was achieved with the use of the hydraulic pumps, hydraulic ram and load frame, whose responsibility was to control the force in the system, apply load to the rod and transfer load to the ground, respectively. Once the sheathing was removed from the all thread, the load frame was placed over the test shaft and the embedded all thread was exposed through the hole in the center of the load frame. The hollow core hydraulic ram was then placed on the load frame with the embedded rod passing through its center. The 10 ton load cell was then placed on top of the ram with a 6in x 6in x ¼in steel plate with a 1in hole in the center on top of it. A ¾in nut was then used to fasten the assembly together and transfer any applied forces from the ram to the all thread. Hence, the loads registered by the load cell came as a result of being sandwiched in compression between the hydraulic ram and the steel plate.

Displacement of the shafts were measured with the use of the 4in LVDT, reference beam and plunger stop tab. The reference beam was effectively a datum for the displacement measurements as the LVDT was fastened to the reference beam with the plunger fully extended so that the plunger moved upward and closer to the beam as it compressed. Compression of the plunger came as a result of the plunger stop tab which was fastened to the exposed all thread, i.e. as the shaft displaced, so did the stop tab. The testing apparatus can be seen in Figure 3.51.

Figure 3.51 Pullout static load testing apparatus.

Load testing was performed in accordance with the Quick Load Test Method of ASTM D3689-90: *Standard Test Method for Individual Piles Under Static Axial Tensile Load*. Load increments of $1/10^{th}$ the expected load of 5000lbs were used (500lbs). Each load increment was held for two minutes before the next load increment was applied. At the end of the two minute period, the load and displacement measurements were recorded manually as a back-up in a field notebook to accompany the automated data collection system. Testing continued until a stable load could no

longer be held. Once the shaft had displaced 4in, displacement measurements were no longer monitored. Continuous load was applied to shaft until the side shear / pullout force registered 1000lbs or less. When this point was reached, the shaft was attached to the overhead, tripod hoist and fully extracted with the cathead. Figure 3.52 shows the testing of the shaft while Figures 3.53 and 3.54 show various stages of shaft extraction.

Figure 3.52 Static load test of shaft.

Figure 3.53 Shaft extraction; breaking ground surface, 2ft, 4ft, and 6ft extracted (left to right).

Figure 3.54 Fully extracted shaft.

During the load test, the hand operated hydraulic pump was used to apply load to the shafts (Figure 3.55). The hand pump allowed for improved control of the loading rate and maintaining the target load of each load increment. After the load test had concluded, an electric hydraulic pump was used to quickly apply hydraulic power to the ram in 6in strokes. When the full stroke was achieved, the ram was retracted, the nut on the all thread rod was moved down 6in to make contact with the load cell and the ram was again stroked to full length. In all, most shafts required between 4 and 6 full stroke cycles before the load was low enough for extraction using the tripod hoist.

Figure 3.55 Operation of hand pump during static load test.

After extraction, the shafts were placed on the trailer, the true length of each shaft was measured, the embedded rod was then removed (slid out of 1in PVC pipe), and the shafts were cut into quarters using a concrete saw (Figure 3.56). Once the cross section was exposed, each quarter was labelled with its shaft number and corresponding location along the length of the shaft. The cross section was broken into "clock quadrants" and filter cake thickness measurements were taken at each quadrant boundary with a caliper (12:00, 3:00, 6:00 and 9:00 positions, Figure 3.57). Once all the shafts were extracted, the filter cake was cleaned off and the diameter was measured at third points of each shaft quarter (Figure 3.58). Figure 3.59 clearly shows the hardened filter cake witnessed during cleaning of the shafts for true diameter measurements.

Figure 3.56 Cutting of shafts at quarter points.

Figure 3.57 Measurement of bentonite filter cake thickness.

Figure 3.58 Filter cake removal of shaft quarters.

Figure 3.59 Hardened filter cake on bentonite shaft quarters.

3.1.10 KB International Enhanced SlurryPro CDP Polymer Shafts

The testing procedure for the KB International polymer shafts was the same as that used for the bentonite shafts. All of the same materials were used in production of the shafts except for the type of slurry used. The preparation of the slurry used for this series of tests was previously discussed in Section 3.1.4.2.

3.1.10.1 Borehole Excavation

During excavation, it was found that the originally estimated 100 gallons were insufficient to complete the excavation due to greater than expected fluid loss. The original 100 gallons were based on an estimate that each borehole would require 15 gallons of slurry but in actuality, each borehole required on average 20 gallons of slurry. The Marsh funnel viscosity of the original batch was 47.12sec/qt while the second batch viscosity was 54.1sec/qt. Both of these values are below the manufacturer's recommended viscosities of 65-100sec/qt for silt and fine to medium sand (KB International, 2015(a)).

Slurry supply was exhausted after the 1hr borehole was drilled. Therefore, the 0hr borehole was postponed and drilled after the 4hr borehole was concreted. This allowed for the mixing of additional slurry without jeopardizing the intended exposure time of 0hr. Only the 0hr polymer shaft was excavated using the second batch of slurry while all others were excavated with the original batch of slurry. The second batch of slurry was also used to maintain the slurry level of all excavated boreholes at or above ground level within the temporary casing. The slurry used from both batches was gravity fed into 5 gallon buckets for deposition into the boreholes during excavation (Figure 3.60). Other excavation images can be seen in Figures 3.61 and 3.62. Notice how the excavated soil seen in Figure 3.62 has formed individual masses of partially polymer-saturated sand. This was noticed during excavation where the polymer encapsulated large lumps of soil roughly the size of the auger diameter within the lumps the soil was observed to be dry or free of any polymer material.

Figure 3.60 Gravity feed of KB International Enhanced CDP polymer into 5 gallon bucket.

Figure 3.61 Introduction of KB International Enhanced CDP polymer into borehole.

Figure 3.62 Excavated soils using KB International Enhanced CDP polymer.

It should also be noted that a large root was encountered during the excavation of the 8hr borehole within this test series. The root was encountered 5ft below the surface and took approximately 5 minutes to drill through. A portion of the root can be seen in Figure 3.63.

Figure 3.63 Portion of root encountered during excavation.

Figure 3.40 shows that the 0hr shaft for this test series is 7ft to the east of the 4hr shaft instead of 6ft to the west of the 1hr shaft as seen in the other test series. The decision to move the shaft from the intended location (6ft east of the 4hr shaft) was made during the excavation when a clayey sand layer was encountered in the bottom foot of the 1hr shaft (on west end of test area). As previously mentioned, the shafts were only targeting sandy soils therefore the 0hr shaft was moved to other end of the line shafts where only sand had been encountered. Figure 3.64, below shows the excavated clay from the 1hr borehole.

Figure 3.64 Clayey-sand encountered during excavation of KB5-1hr borehole.

3.1.10.2 Borehole Concreting

Concreting of the KB shafts was performed using the same procedure as that used for the bentonite shafts. No issues were encountered during the concreting process except for the concreting of the 24hr shaft where the hopper ball valve had cemented by the next day in the open position. Therefore, the mortar for the shaft was transported to the borehole using 5 gallon buckets. The tremie was placed in the borehole and the empty hopper was then connected to it. The mortar was then poured into the hopper and flowed directly into the tremie. Once all of the mortar had been placed, the tremie was lifted slightly and concrete flow was witnessed through volume loss in the hopper. Slurry displacement was also witnessed as reassurance of concreting of the shaft and confirmed that the concrete did not exit the tremie prior to lifting the assembly off the bottom of the excavation.

3.1.10.3 Pullout Static Load Tests, Shaft Extraction and Dissection

Pullout tests performed on the KB shafts occurred in the same manner as the bentonite shafts. First, the testing apparatus was placed on the exposed steel rod and load was applied 500lb increments as previously described. The resulting displacements were then recorded and the test was terminated once the shafts had displaced 4in.

Similarly, the extraction process followed that of the bentonite extraction process. As expected, no slurry based filter cake was witnessed on the extracted shafts but rather a layer of semi-saturated soil adhered to the outside of the shaft (Figures 3.65 and 3.66).

During the extraction of the 8hr shaft, a large anomaly in the shaft perimeter was found. It is believed that the anomaly came as a result of the root encountered during excavation. This anomaly is also believed to have increased capacity as a slight bulge activated more surrounding soil and required almost 4ft of extraction before the capacity fell below the 1000lb tripod hoist capacity. This displacement is double the expected displacement as other shafts in the series only required displacements of 2ft to reduce the side shear to 1000lbs. The anomaly can be seen in Figures 3.67 and 3.68.

Figure 3.65 Bottom 2ft of extracted KB International Enhanced CDP shaft.

Figure 3.66 "Soil Cake" of saturated soil removed from extracted KB International Enhanced CDP shaft.

Figure 3.67 Anomaly encountered on KB2-8hr shaft.

The 2hr and 24hr shafts had polymer slurry clinging from bottom upon extraction which is assumed to have been trapped below the tremie plug which almost fully covered the bottom of the excavation (Figure 3.69). This was not considered problematic given that portion of the shaft would not have contributed to the side shear. After extraction, the shafts were once again dissected into quarters and the "soil cake" of each quarter was recorded (Figure 3.70). Inspection of the cross section also revealed moisture on the outer quarter of an inch of the shaft perimeter as seen in Figures 3.71.

Figure 3.68 Close up of anomaly encountered on KB2-8hr shaft.

Figure 3.69. Slurry hanging from KB2-8hr shaft (left), drop of liquid on KB3-24hr shaft (right).

Figure 3.70 Moisture laden mortar at the base of the shaft.
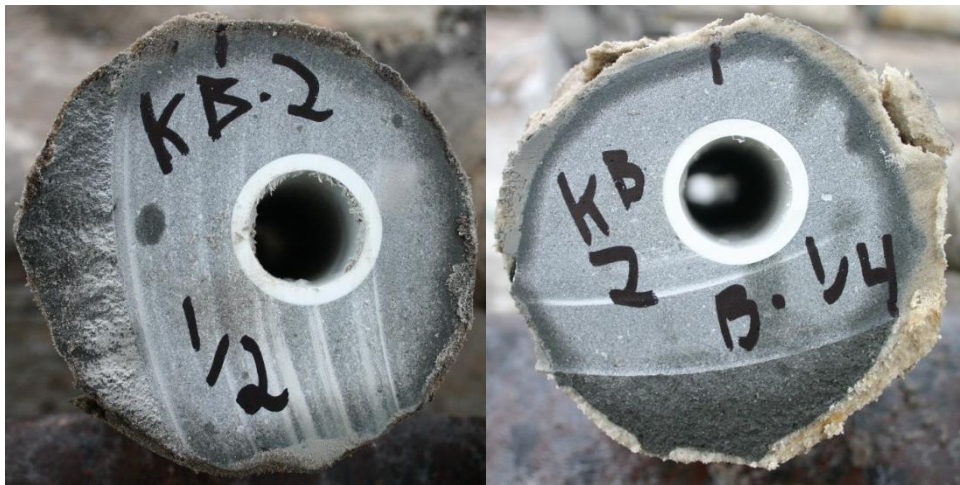
Figure 3.71 Close up of dissected KB2-8hr shaft sections.

Cleaning of the extracted shafts revealed that the upper 3ft of shaft had an excellent bond to the soil. Soil on the surface of the concrete in this area was very difficult to remove and the two materials were practically indistinguishable from each other. The soil on the surface in other regions of shafts was not as difficult to remove and after spraying for a while, the concrete surface was revealed. Figures 3.72 and 3.73 shows the difference in the two shaft regions after cleaning.

Figure 3.72 Soil bonded to concrete surface in upper 3ft of KB Polymer shafts.

Figure 3.73 Removal of soil in lower portion of KB polymer shafts.

3.1.11 Matrix Bigfoot Polymer

The testing procedure for the shafts using Matrix Bigfoot polymer was again the same as that mentioned in the previous sections. All of the same equipment was used; the slurry type was different which was discussed in Section 3.1.4.2. Any variation from the previously discussed testing procedure is discussed herein.

3.1.11.1 Borehole Excavation

The methods discussed in the previous sections were also used to excavate the boreholes for the Matrix shafts. The 120 gallons of slurry prepared to perform the excavation for these shafts was slightly low as the 4hr and 8hr borehole saw slurry levels fall 2ft below the ground surface prior to concreting. This was not the case in the 24hr borehole due to uncontaminated, reclaimed slurry being re-used to maintain the borehole. In hindsight, 150 gallons of slurry should have been prepared.

Figure 3.74 shows the emptying of the auger after a grab had been completed. Take notice of the polymer chains hanging from the auger. These strands that represent the behavior of polymer slurry were noticed continuously throughout the excavation process and show that the Matrix slurry was performing effectively. Soil excavated under Matrix polymer slurry can be seen in Figure 3.75. Once again, the excavated material took the form of stabilized masses of saturated sand. Recall, this characteristic of the excavated materials was also observed during the excavation of the KBI polymer shafts. As mentioned in Section 3.1.4.2, the viscosity of the Matrix slurry was 73 sec/qt after dilution and during excavation was 70sec/qt (Figure 3.76).

During the excavation of shaft M4-1h, a root was encountered in the upper 1ft of the borehole. This root took about 5 minutes to drill through. Clayey sands were encountered in the lower portion of the shafts. Most shafts had approximately 0.5ft of clayey sand near the toe but during the excavation of the 1hr shaft, clay was encountered near depths of 6.5-8ft. This layer was in a similar location to that of the clay layer encountered during the excavation of the KBI shafts. Similarly to what was done in that instance, the 0hr shaft was moved 6ft to the east of the 4hr shaft. The CPT test identified this layer as a clayey sand but as a precaution the 0hr shaft location was moved. Throughout the test series, inspection of excavated material showed that clay layer became shallower from east to west. Figure 3.77 shows the soil encountered and labelled in the field as clay. Note how the material was able to be rolled which is a typical characteristic of clayey soils (Figure 3.78).

Figure 3.74 Matrix Bigfoot polymer chains hanging from auger during emptying.

Figure 3.75 Soil excavated with Matrix Bigfoot polymer.

Figure 3.76 Matrix Bigfoot polymer field Marsh funnel test (70sec/qt).

Figure 3.77 Clayey soils encountered at bottom of Matrix polymer shafts.

Figure 3.78 Excavated material rolled to confirm clay-like properties.

3.1.11.2 Borehole Concreting

There were no problems encountered during the concreting of the Matrix shafts. For this series the new ball valve was placed on the hopper, therefore the concreting method described in Section 3.1.9.2 was used. Slurry displacement, concrete flow and concreted shaft can be seen in Figure 3.79.

Figure 3.79 Matrix polymer slurry displacement (left), concrete overflow (middle), concreted shaft (right).

3.1.11.3 Pullout Static Load Test, Shaft Extraction and Dissection

Load testing of the Matrix shafts used the procedure previously described. Tensile load increments of 500lbs were applied to each shaft and held for two minutes before additional load was applied. Load-displacement data for each test was recorded for the 4in of stroke allowed by the LVDT. After this point, only applied load was monitored so that it could be determined when the shaft could be extracted with the use of the structural tripod. The target load range for this ranged between 800-1200lbs.

Upon extraction of shaft M1-4h, a 1in thick protrusion was found. It can only be assumed that this came as a result of mortar flowing into the cavity once occupied by the root mentioned in Section 3.1.10.1. The mortar protrusion is shown in Figure 3.80.
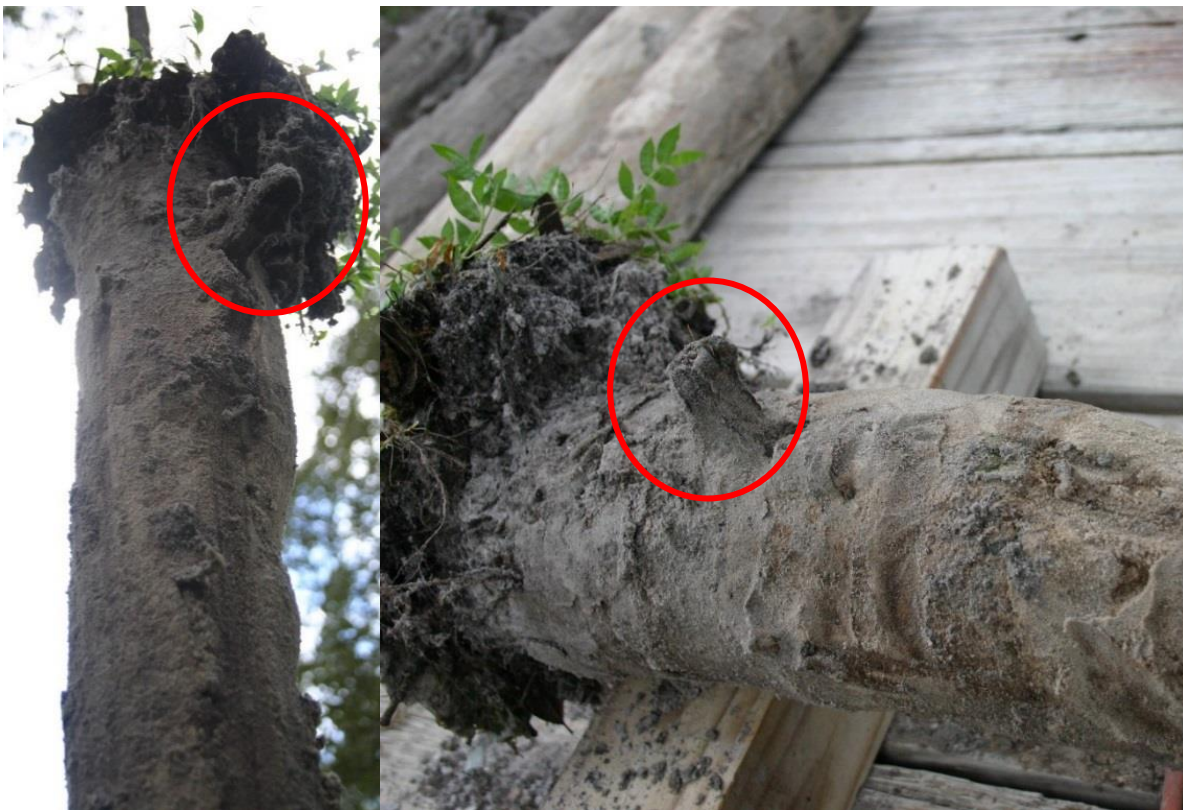
Figure 3.80 Concrete protrusion found on shaft M4-1h.

Once again, a saturated layer of soil was found on the perimeter of extracted shafts. After dissection, the thickness of this "soil cake" of saturated soil was measured. Dissection also revealed a similar ring of moist mortar on the outer quarter of an inch of the shaft perimeter. Figure 3.81 displays the exposed cross section of the Matrix shafts where the ring of moisture can be seen.

Figure 3.81 saturated soil on shaft perimeter (left), ring of moisture in cross section of shaft (right).

Cleaning of the Matrix shafts once again revealed the two different properties of saturated soil adhered to the outer shaft perimeter. From 0-3ft, the saturated material was very difficult to remove from the concrete surface by spraying with the high pressure water hose. The concrete and this layer was virtually indistinguishable from each other. Whereas, from 3-8ft, the concrete surface of the shaft was easily exposed by spraying the saturated soil with the hose. This soil characteristic was also witnessed on the outside of the KB shafts. Figure 3.82 shows the difference in spraying both surfaces with the high pressure water hose.

Figure 3.82 Exposed concrete surface (left) next to soil laden surface (right) for matrix polymer shafts.

3.1.12 Cetco ShorePac

The testing procedure for Cetco ShorePac polymer shafts was the same as that used for all other shafts except that the shaft lengths were reduced to 7ft. All of the same materials were used in production, except for the slurry type. Slurry preparation for this test series was described in Section 3.1.4.2.

3.1.12.1 Borehole Excavation

As previously mentioned, boreholes in this test series were reduced to 7ft long. This reduction came as a result of difficulties excavating through a stiff root near a depth of 7ft which was anticipated to artificially inflate pullout strengths. Efforts were also made to avoid the higher clay layer in excavated material at this depth. Figure 3.83 displays a portion of the root that was able to be removed by the auger and the clayey soils near depths of 7ft.

Other than the reduced shaft lengths, there were no other deviations from the previously discussed procedures. Slurry levels were maintained near the ground level by adding slurry to the borehole after two grabs of the auger (Figure 3.84). Once boreholes were completed, they were continuously monitored to ensure the slurry level remained near ground level. Approximately 160 gallons of slurry were used to complete the boreholes, 135 gallons of fresh slurry and 25 gallons of uncontaminated, reclaimed slurry. The measured Marsh funnel viscosity during excavation was 70sec/qt (Figure 3.85).

Figure 3.83 Excavation difficulties resulting in reduced shaft length; portion of root (left), clayey-sand soil (right).

Figure 3.84 Emptying of auger bucket and simultaneous slurry addition to borehole.

Figure 3.85 Marsh funnel viscosity (70 s/qt).

Similar to the Matrix slurry, the polymer chains formed by the Cetco product were also visible to the naked eye during bucket emptying (Figure 3.84). Once again, the majority of the removed masses were conglomerated masses of material as seen in Figure 3.86.

Figure 3.86 Soils excavated with Cetco ShorePac polymer.

3.1.12.2 Borehole Concreting

For this phase, the skid steer tractor used to transport the mortar filled hopper from the trailer to the excavation was out for repair. Therefore, mortar was transferred from the mixer to the borehole using 5 gallon buckets. The buckets were filled halfway and carried over to the hopper, which was suspended from the tripod hoist (Figure 3.87). Once the hopper was filled with mortar, the rest of the concreting procedure was completed in a similar manner to the aforementioned procedure in the previous sections (Figure 3.88).

Figure 3.87 Bucket of mortar transferred to hopper.

Figure 3.88 Concreting of Cetco polymer shaft; slurry displacement (left), concrete overflow (middle), completed shaft (right).

3.1.12.3 Pullout Static Load Test, Shaft Extraction and Dissection

The method discussed in previous sections was used to perform the static load tests on the shafts of the Cetco series. Again, 500 pound load increments were applied to the test shafts and the corresponding displacements were measured. After failure, load increments were no longer used but instead load was applied continuously until a displacement of 4in was achieved. At this point, the LVDT was removed and the shafts were systematically pulled out and extracted once the capacity was reduced to 1000lbs.

Exhumation of the shafts revealed no anomalies such as the root protrusions experienced in the previous series of tests. A layer of soil was also witnessed on the outside of the shafts though the material was not as saturated as that witnessed in the other polymers tests (Figure 3.89). The thickness of this "soil cake" was once again measured by shaft dissection. Dissection revealed the 1in ring of moisture which was also witnessed within the other polymer shafts (Figure 3.90).

The "soil cake" was once again easily removed from the concrete surface by spraying with a hose (Figure 3.91). The soil in the upper 3ft of shaft, was very difficult to remove with the high pressure water hose. Multiple passes and some hand scrubbing was necessary to remove the material in this portion of the shaft whereas soil was easily removed in by the hose in the bottom 4ft of shaft.

Figure 3.89 Layer of soil on perimeter of cetco polymer shafts.

Figure 3.90 Dissected cross section of Cetco polymer shaft.

Figure 3.91 Removal of soil cake on Cetco polymer shafts.

3.2 Results of Test Program

The above sections discussed the materials, slurry products and mixing procedures along with the construction methods used to construct, test and exhume $1/10^{th}$ scale drilled shafts for the purpose of exploring slurry effects on side shear resistance. Through this process, data regarding shaft performance was obtained and the difference in "filter cake" or "soil cake" due to different slurry exposure was revealed. While the bentonite shafts produced a traditional slurry based "filter cake," the polymer shafts produced a "soil cake" which was essentially a layer of soil on the perimeter of the shafts. In the upcoming sections, the data obtained from CPT and load testing, along with "filter cake" data is presented and discussed.

3.2.1 CPT Analysis

Cone penetration tests revealed that the subsurface of the test site consisted of mostly sands and silts. Some areas with clayey sand were identified but substantial clay layers were only encountered in the lower 2ft of the polymer shafts on the west end of the test area. As a result, the 0h shafts for two series (KB and Matrix) were moved to the east of the 4h shafts during excavation. The results of the CPT tests were also confirmed by inspection of excavated material. Figures 3.92-3.95 show tip resistance, sleeve resistance and friction ratio plots for each series of tests. Each figure shows the results for all shafts within the test series. For the most part, the plots are similar but some variation can be seen in the bottom 2ft within the tip resistance plots.

Due to the discrepancies, side shear resistance, f_s, was calculated based on tip resistances, q_c, using the following equations, where σ_{vo} is the total overburden pressure (Gunaratne, 2014; Alsamman, 1995):

$$f_s = 0.015q_c \ for \ q_c \leq 50tsf \ \text{(Sand/Silty Sand)}$$
$$f_s = 0.012q_c + 0.7 \leq 1.0 \ for \ q_c > 50tsf \ \text{(Sand/Silty Sand)}$$
$$f_s = 0.023(q_c - \sigma_{vo}) \leq 0.9 \ \text{(Clay)}$$

These calculations were performed for every depth interval of recorded CPT data and the total side shear resistance was determined. By using the trapezoidal rule, the total area under the f_s curve (generated from q_c) and total side shear resistance, was found for each shaft. Total area calculations used the as-built length of each shaft to ensure only soils contributing to side shear were considered. The calculated f_s represents the theoretical compressive shear resistance of the in situ strata but evidence has shown that uplift resistance ranges between 0.66 and 0.74 of compression resistance (O'Neill, 2001; Fellenius, 2001; Mayne, 2001). These variations come as a result of decreased overburden pressures and hence horizontal soil pressures when applying uplift forces to the surrounding soils. Although minimal, some studies cite that horizontal soil pressures can also be affected by Poisson effects, i.e. increase of shaft diameter in compression, decrease of shaft diameter in tension (O'Neill, 2001; Mayne, 2001). For this study, the overall range of observed variation (uplift vs compression) was applied using values of 0.66 and 0.74 when calculating the theoretical uplift capacity range of each shaft (Tables 3.6-3.9).

Tables 3.6-3.9 show that even though the curves were similar and the soils were identified as mostly sands/silty sands, soil strengths differed for each shaft location. The variations witnessed are mostly due to the inconsistencies in the bottom 2ft of the tip resistance plots as noted in Figures 3.92-3.95. These variations are especially pronounced within the polymer test shafts where capacity differences of approximately 2.6, 2.4 and 2kips are predicted for the KB, Matrix and Cetco polymer shaft locations respectively. The bentonite shaft locations only had a difference of 1.2kips. This is important in that the measured pull out capacity may need to consider the local soil strength to ensure comparisons based on time exposure are meaningful.

Table 3.6 Minimum and maximum theoretical uplift resistance for bentonite shafts.

Shaft Label	Shaft Length (ft.)	Minimum Uplift Resistance (kips)	Maximum Uplift Resistance (kips)
B6-0h	7.50	4.289	4.808
B5-1h	7.96	4.544	5.095
B4-2h	7.50	5.038	5.649
B1-4h	7.79	5.176	5.803
B2-8h	8.04	5.579	6.256
B3-24h	8.00	4.868	5.458

Table 3.7 Minimum and maximum theoretical uplift resistance for KB polymer shafts.

Shaft Label	Shaft Length (ft.)	Minimum Uplift Resistance (kips)	Maximum Uplift Resistance (kips)
KB6-0h	8.042	4.699	5.268
KB5-1h	7.833	5.478	6.142
KB4-2h	7.125	2.979	3.340
KB1-4h	7.875	4.112	4.610
KB2-8h	7.833	2.871	3.220
KB3-24h	7.75	3.739	4.192

Table 3.8 Minimum and maximum theoretical uplift resistance for Matrix polymer shafts.

Shaft Label	Shaft Length (ft.)	Minimum Uplift Resistance (kips)	Maximum Uplift Resistance (kips)
M6-0h	8.125	5.671	6.358
M5-1h	8.240	5.125	5.746
M4-2h	8.208	6.060	6.795
M1-4h	7.958	4.338	4.863
M2-8h	8.167	4.722	5.295
M3-24h	8.104	6.681	7.491

Table 3.9 Minimum and maximum theoretical uplift resistance for Cetco polymer shafts.

Shaft Label	Shaft Length (ft.)	Minimum Uplift Resistance (kips)	Maximum Uplift Resistance (kips)
C6-0h	7.208	4.555	5.108
C5-1h	6.667	3.810	4.272
C4-2h	6.896	2.742	3.075
C1-4h	6.938	3.159	3.542
C2-8h	7.188	3.150	3.532
C3-24h	6.854	3.071	3.444
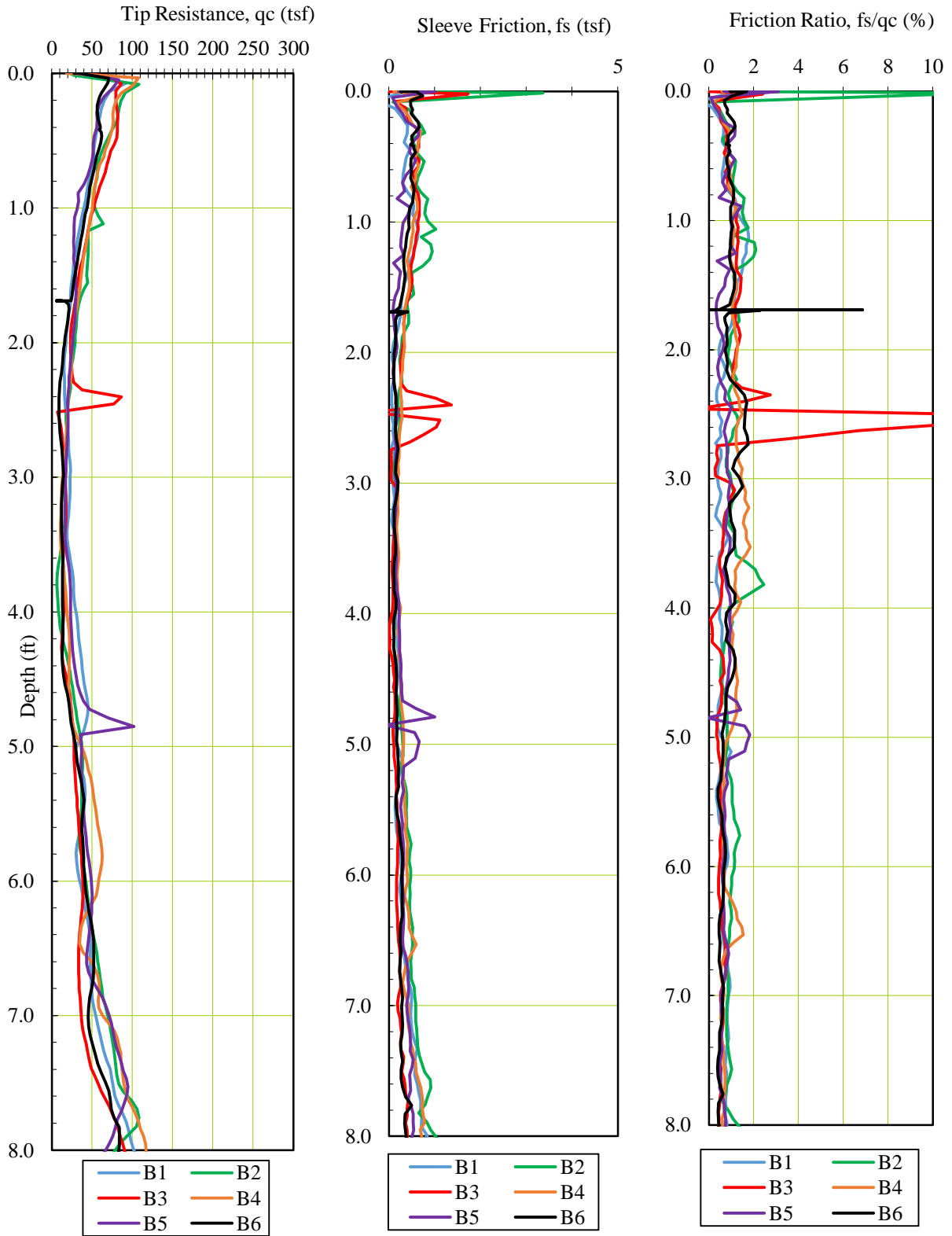
Figure 3.92 Tip resistance, sleeve resistance and friction ratio for Cetco PureGold Bentonite Gel shafts.
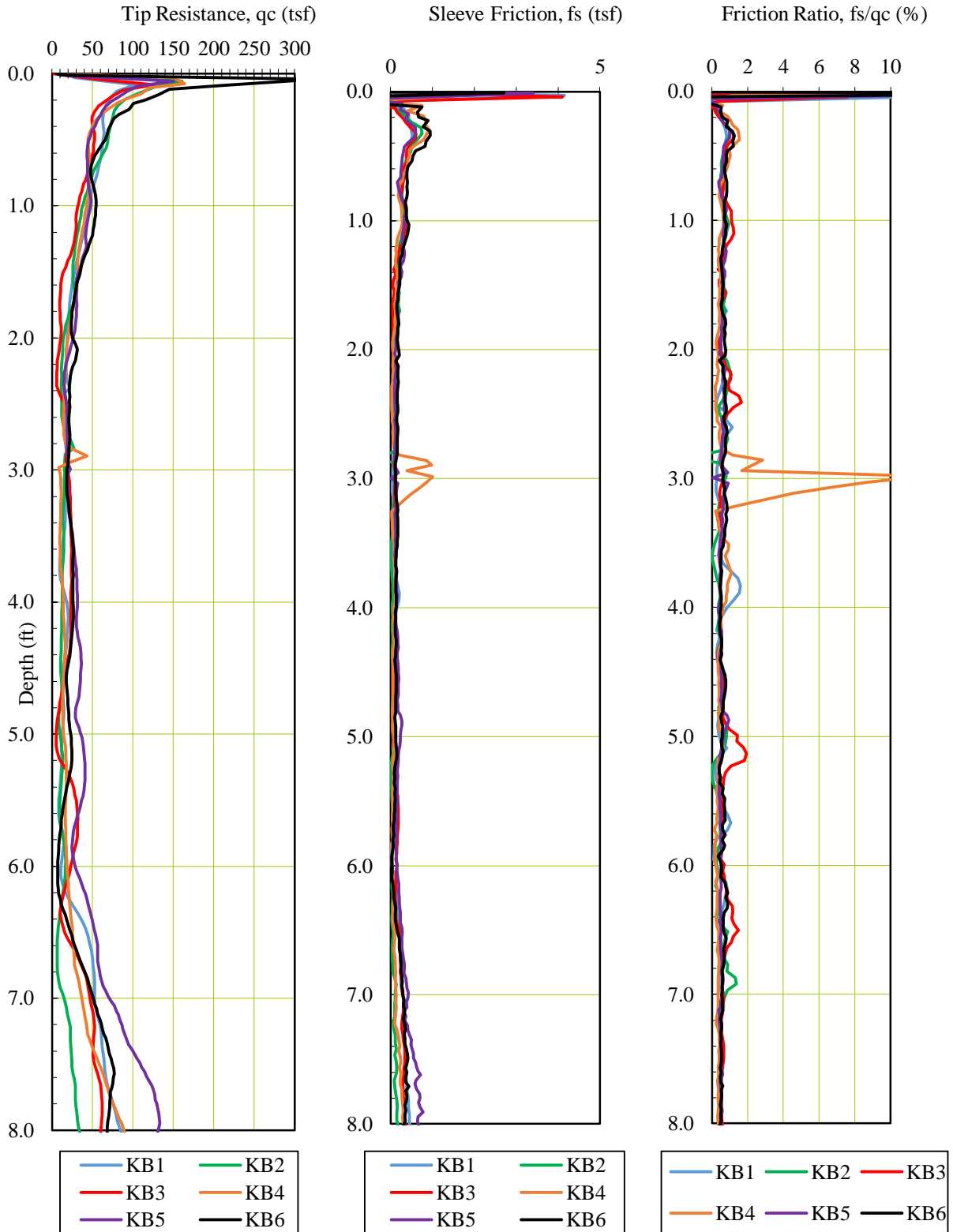
Figure 3.93 Tip resistance, sleeve resistance and friction ratio results for KB International Enhanced CDP polymer shafts.
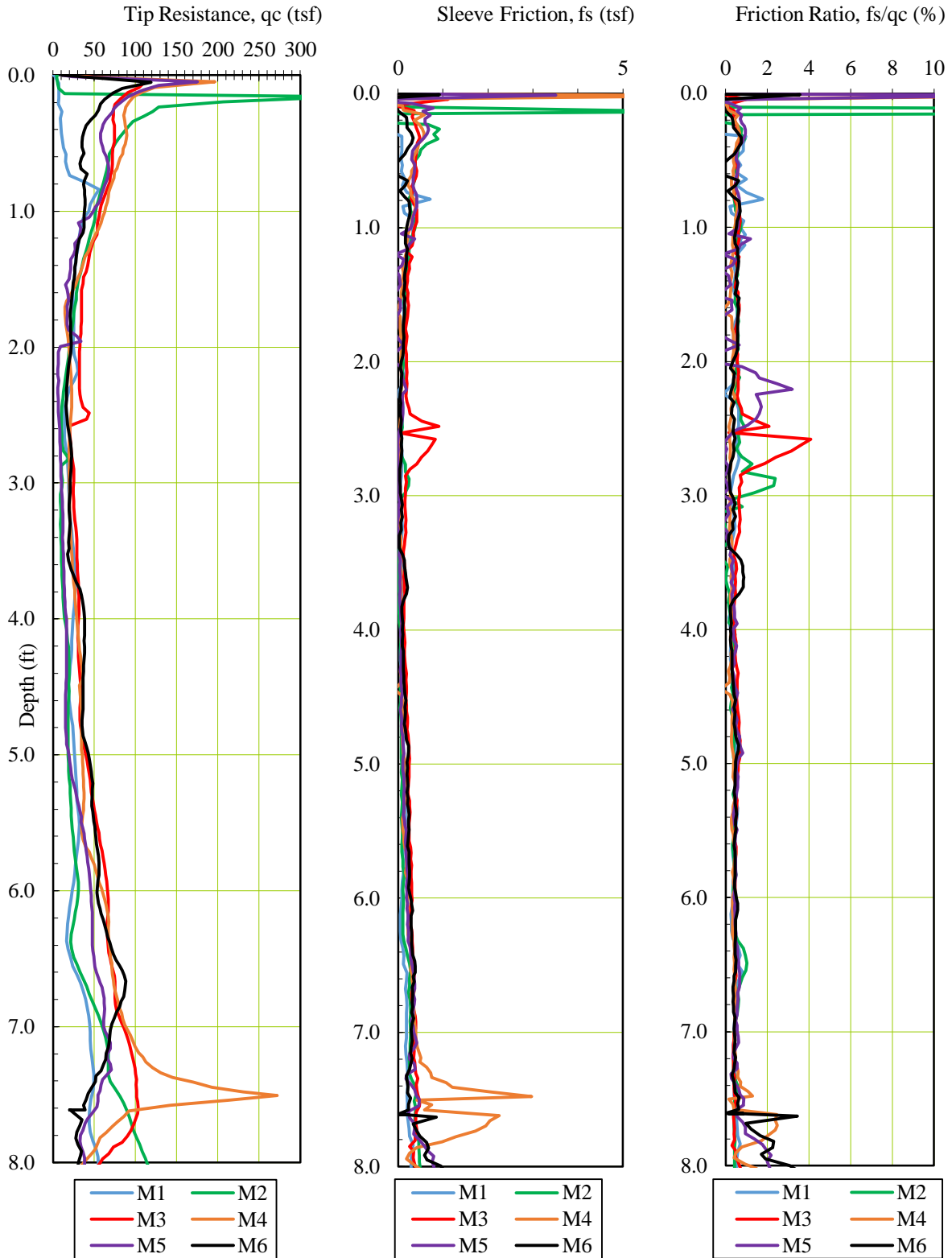
Figure 3.94 Tip resistance, sleeve resistance and friction ratio results for Matrix Bigfoot polymer shafts.
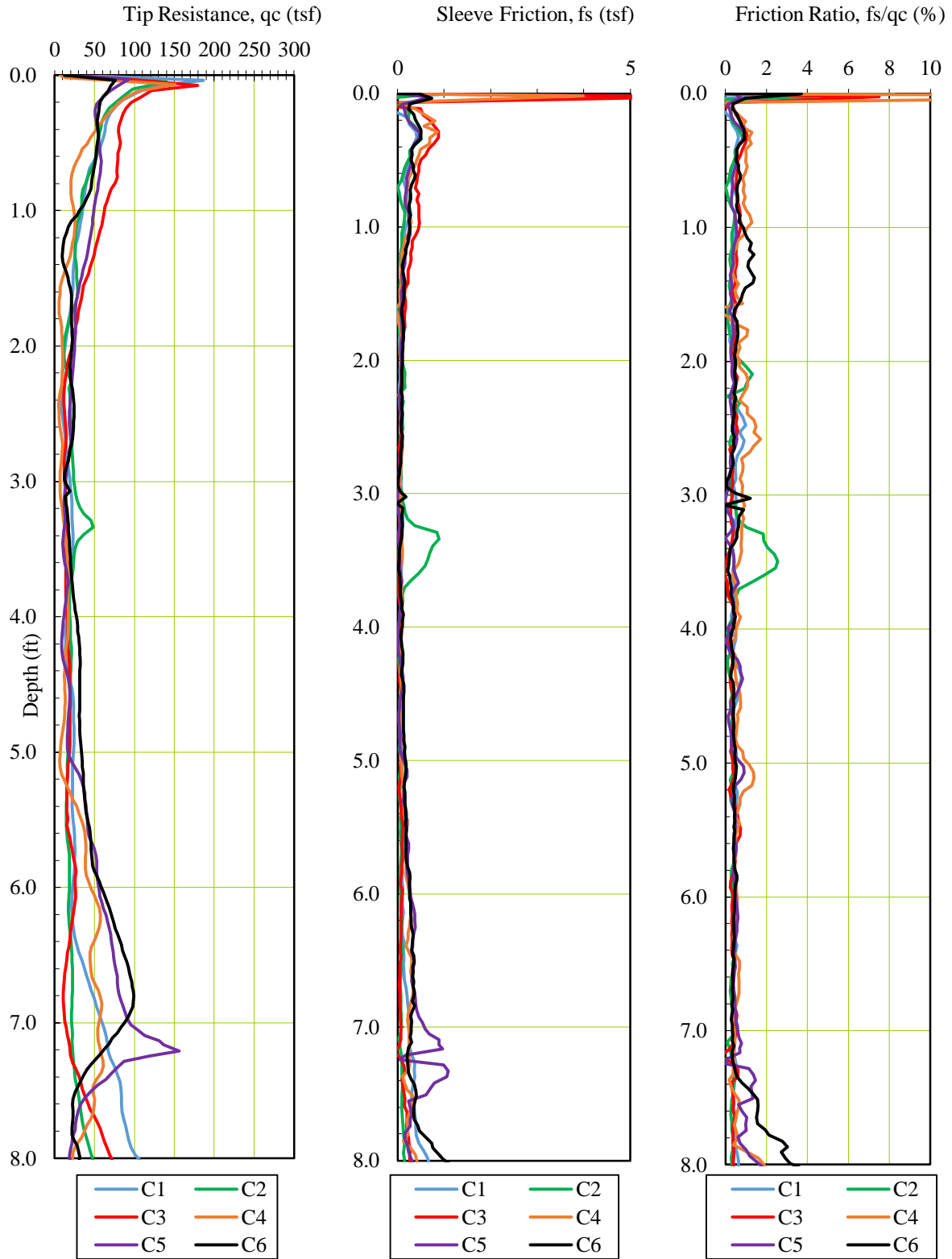
Figure 3.95 Tip resistance, sleeve resistance and friction ratio results for Cetco ShorePac polymer shafts.

3.2.2　Uplift Static Load Tests

Figure 3.96 shows the raw data recorded from the static load tests. Notice, each load step is clearly defined by constant load while displacement continuously increases throughout the test. This data was used to generate load vs displacement curves for each test shaft.
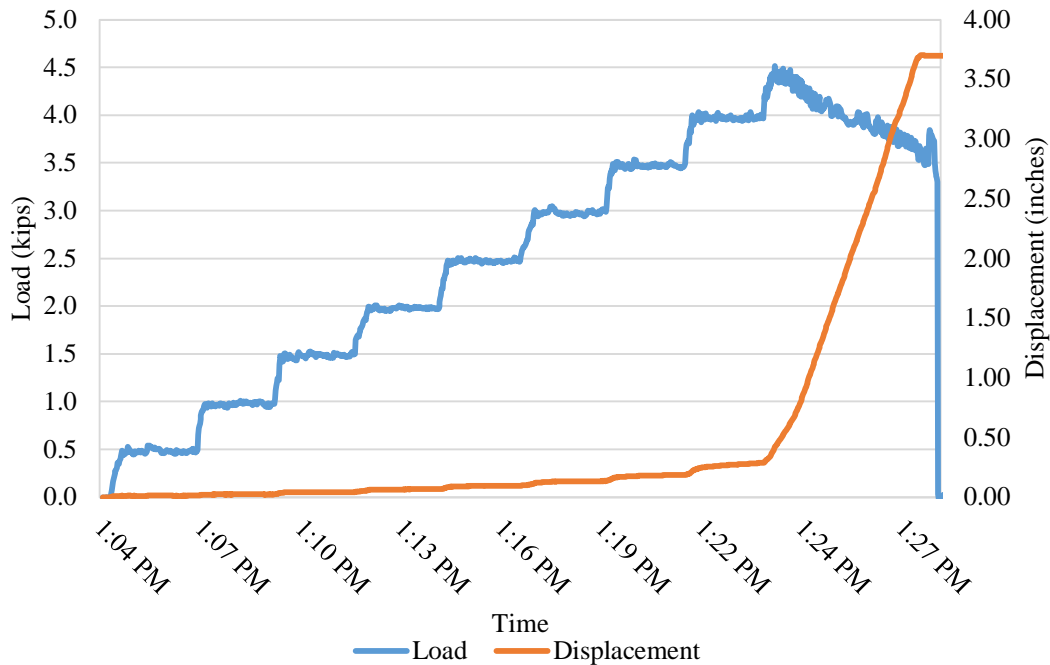
Figure 3.96 Raw load and displacement vs time curves (specimen C3-24h).

Comparison of side-by-side pile or shaft load tests has always been complicated by the possibility of variable soil strength profiles for otherwise identical shafts. To combat the effects of variations in shaft performance there are numerous correction philosophies that might be adopted; the simplest is to account for physical / dimensional disparities (e.g. changes in length or diameter). Where corrections for changes in length are immediately justifiable, variations in diameter can be a side effect of the slurry efficiency. For this section only length corrections were considered; a more in depth review of confounding effects are presented in greater detail in the upcoming sections.

A correction factor was computed for all shafts to account for additional or loss of capacity due to the as-built length of the shaft. Since the target shaft length was 8ft, the target length was divided by the actual length to obtain the correction factor. Therefore, shafts shorter than 8ft had a correction factor greater than 1 while those longer than 8ft had a correction factor less than 1. Shaft lengths, the applied correction factors and ultimate load prior to pull out can be found in the Tables 3.10-3.13.

3.2.2.1 Bentonite Test Results

The results of the static load tests performed for the four series of tests are shown in Figures 3.97-3.100. These show the load versus displacement response for each shaft grouped by test series. Even though both the load and displacement data was collected continuously up to four inches of extraction (in most cases), these graphs only show the first inch of displacement thereby focusing on the initial stiffness. The shaft naming convention denotes the slurry type, order shaft was drilled and exposure time (e.g. B4-2h used Bentonite slurry, was fourth to be drilled and had an exposure time of 2hrs). Recall concreting was not performed in the same order.

Table 3.10 Shaft length, uncorrected and corrected load for Cetco PureGold Gel bentonite slurry shafts.

Shaft Label	Shaft Length (ft.)	Uncorrected Load (kips)	Correction Factor	Length Corrected Load (kips)
B6-0h	7.5	5.063	1.067	5.4
B5-1h	7.958	4.835	1.005	4.86
B4-2h	7.5	5.484	1.067	5.85
B1-4h	7.792	4.032	1.027	4.14
B2-8h	8.042	3.729	0.995	3.71
B3-24h	8	3.580	1	3.58
B7-48h	7	2.906	1.143	3.32
B8-96h	7	2.492	1.143	2.85

The results show that after two hours of exposure to bentonite slurry, there was a loss in capacity. Figure 3.97 further emphasizes this observation as there was a 2.27kip difference between the maximum (2h shaft) and minimum (24h shaft) measured loads. Notice, the curves of 0, 1 and 2 hour shafts are very similar as are the curves for the 8 and 24 hour shafts. On the other hand, the capacity of the 4 hour shaft falls almost exactly in the middle of these upper and lower boundary curves. This suggest that little to no reduction effects occur within the first 2 hours of bentonite exposure while capacity reductions begin to occur after 2 hours of exposure. Only moderate reductions appear to have occurred after 8hrs of open excavation exposure.
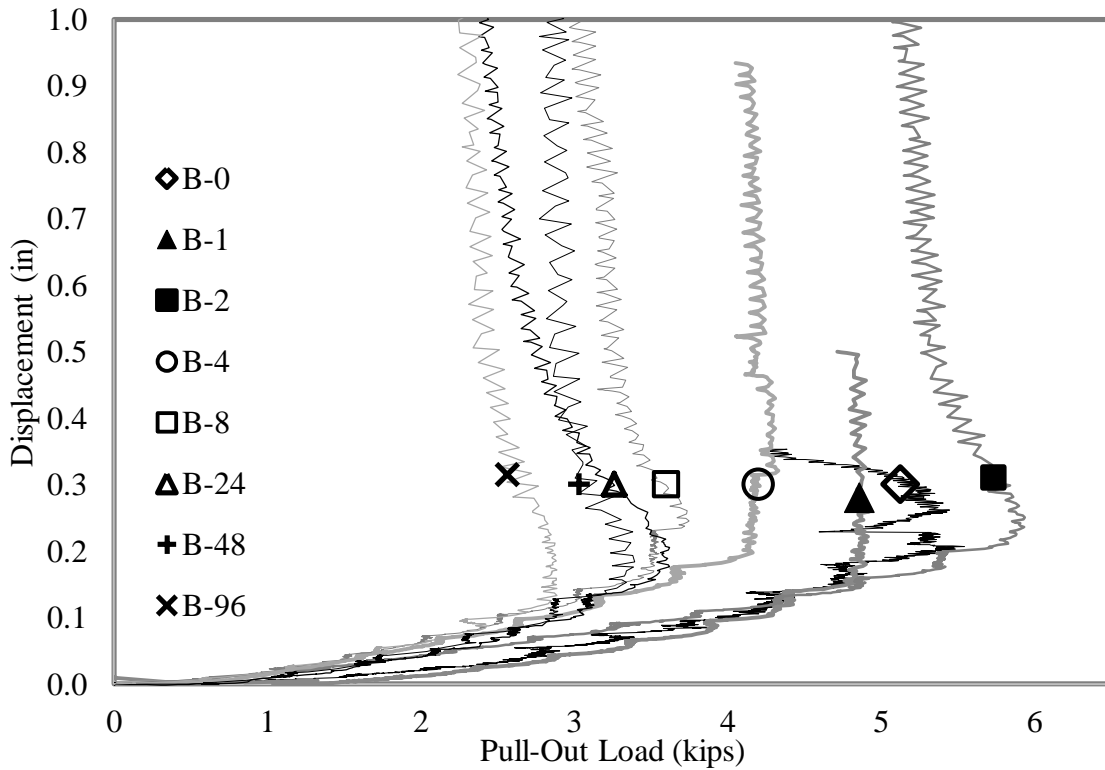
Figure 3.97 Load vs. displacement curves for Cetco PureGold Gel bentonite shafts.

3.2.2.2 KB Polymer Test Results

The results from the second series of tests involving the shafts cast with the KB International polymer slurry are presented in the same format as the pure bentonite in both tabular and graphical formats. Table 3.10 and Figure 3.98 show the results of the tests.

Table 3.10 Shaft length, uncorrected and corrected load for KB International Enhanced CDP polymer slurry shafts.

Shaft Label	Shaft Length (ft.)	Uncorrected Load (kips)	Correction Factor	Length Corrected Load (kips)
KB6-0h	8.042	4.06	0.995	3.979
KB5-1h	7.833	4.54	1.021	4.698
KB4-2h	7.125	4.10	1.123	4.379
KB1-4h	7.875	4.63	1.016	4.571
KB2-8h	7.8333	5.16	1.021	4.704
KB3-24h	7.75	4.12	1.032	4.129
KB7-48h	7	4.08	1.143	4.660
KB8-96h	7	4.19	1.143	4.783

117

Much less capacity variation was observed with the KB International Enhanced CDP Polymer when compared to bentonite. A difference of only 725lbs between maximum (8h shaft) and minimum (0h shaft) was observed. Therefore, the time dependent exposure of the KB International Enhanced CDP Polymer had very little effect on shaft performance. It should be noted, however, the KBI polymer shafts had a lower capacity than the bentonite shafts for short exposure times, but when compared to the 24hr bentonite shaft, all shafts performed better. Recall, 24hr bentonite exposure has been traditionally accepted as a reasonable construction practice. In fact, state specifications use 36hr bentonite exposure as the threshold for unacceptable construction practice.
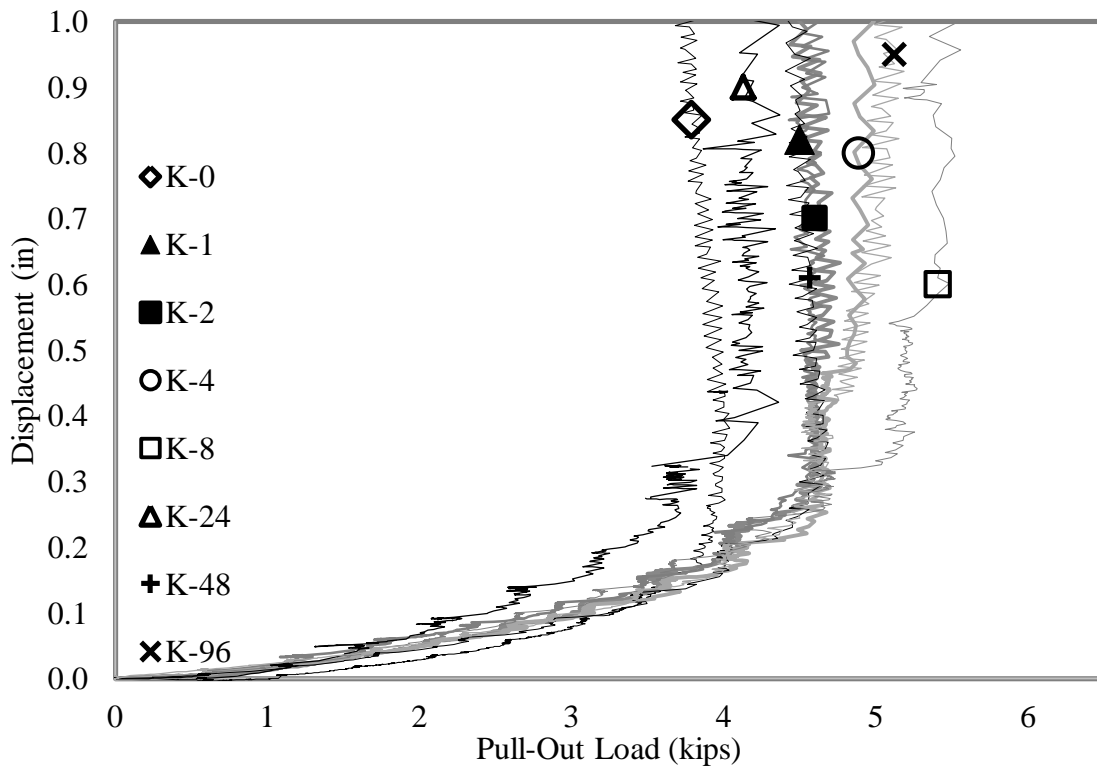
Figure 3.98 Load vs displacement curves for KB International Enhanced CDP polymer.

3.2.2.3   Matrix Polymer Test Results

The results from the third series of tests involving the shafts cast with the Matrix brand polymer slurry are also presented in the same format as the pure bentonite in both tabular and graphical formats. Table 3.11 and Figure 3.99 show the results of the tests.

Table 3.11 Shaft length, uncorrected and corrected load for Matrix Big-Foot polymer slurry shafts.

Shaft Label	Shaft Length (ft.)	Uncorrected Load (kips)	Correction Factor	Length Corrected Load (kips)
M6-0h	8.125	5.03	0.985	4.95
M5-1h	8.240	5.09	0.971	4.94
M4-2h	8.208	5.58	0.975	5.44
M1-4h	7.958	5.22	1.005	5.25
M2-8h	8.167	5.24	0.980	5.13
M3-24h	8.104	5.07	0.987	5.00
M7-48h	7	3.95	1.143	4.52
M8-96h	7	4.85	1.143	5.54

Again, very little variation was witnessed with the results of the static load tests performed on the Matrix polymer shafts. Measured loads differed by only 750lbs and only a 14% difference in capacity was witnessed between the maximum (M2-4h) and minimum (M6-0h) pullout strengths.
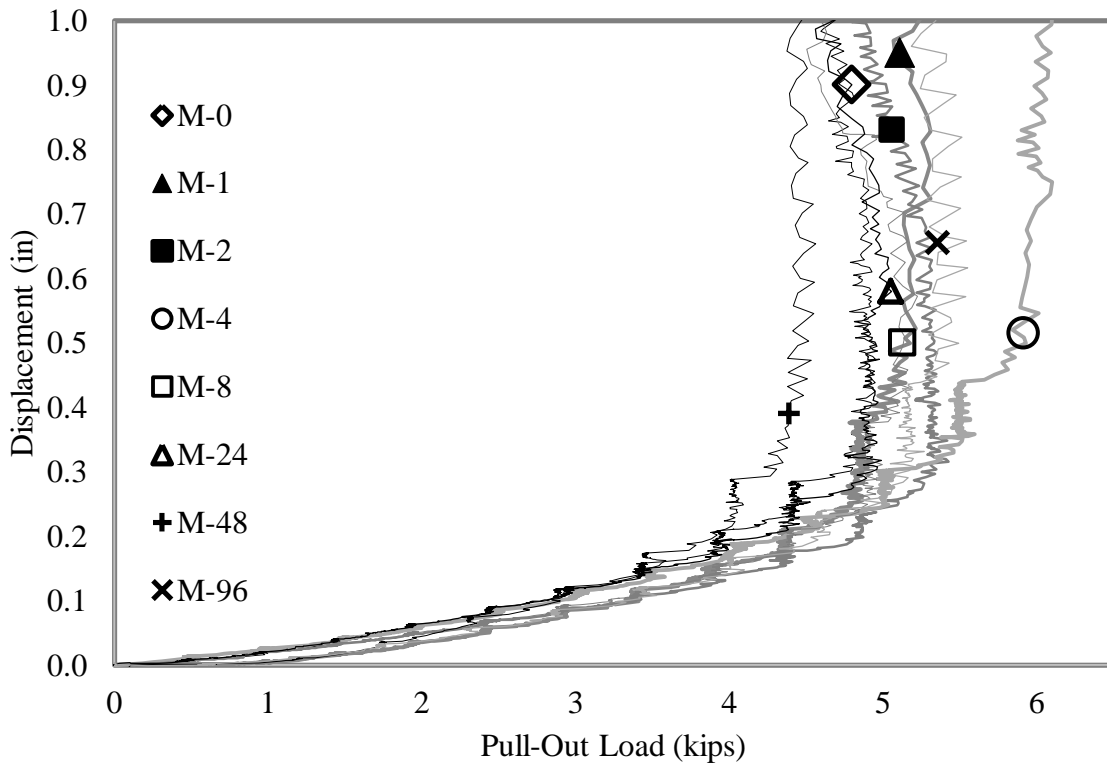
Figure 3.99 Load vs displacement curves for Matrix Big-Foot polymer shafts.

3.2.2.4 Cetco Polymer Test Results

The results from the fourth series of tests involving the shafts cast with the Cetco ShorePac polymer slurry are again presented in the same format as the pure bentonite in both tabular and graphical formats. Table 3.12 and Figure 3.100 show the results of the tests.

Table 3.12 Shaft Loads, Uncorrected and Corrected Load for Cetco polymer slurry shafts.

Shaft Label	Shaft Length (ft.)	Uncorrected Load (kips)	Correction Factor	Length Corrected Load (kips)
C6-0h	7.208	4.51	1.110	5.00
C5-1h	6.667	3.99	1.200	4.79
C4-2h	6.896	4.07	1.160	4.72
C1-4h	6.938	4.39	1.153	5.06
C2-8h	7.188	4.28	1.113	4.76
C3-24h	6.854	4.52	1.167	5.27
C7-48h	7	4.04	1.143	4.62
C8-96h	7	5.14	1.143	5.87
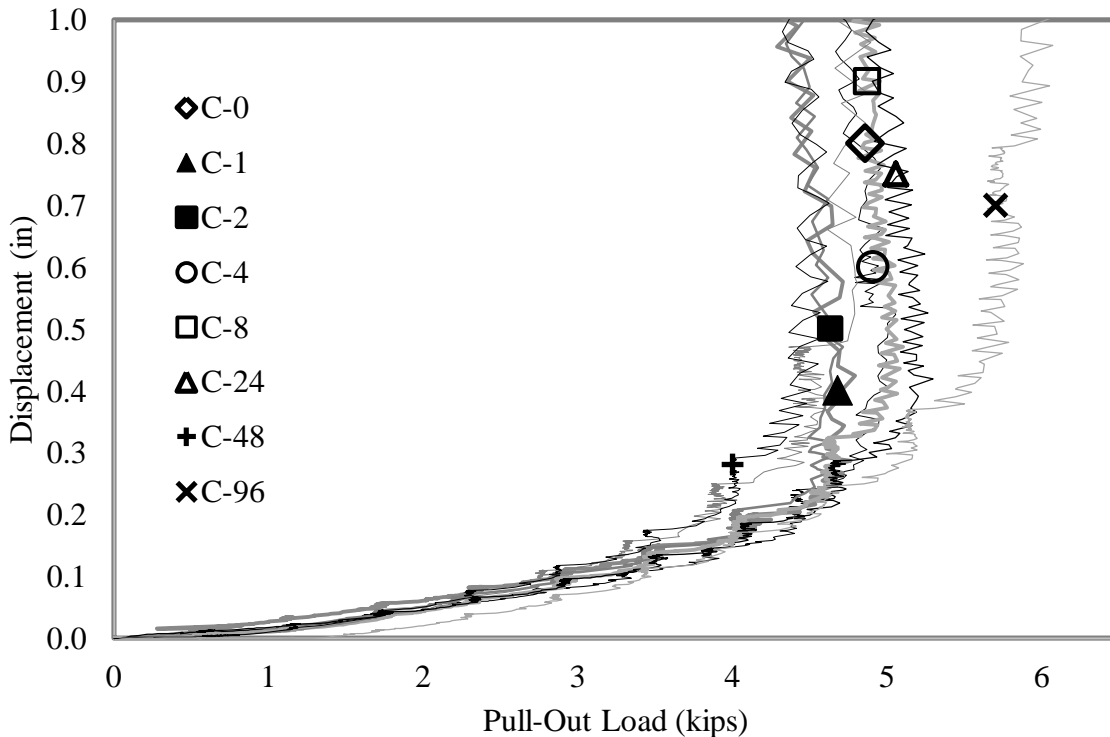
Figure 3.100 Load vs displacement curves for Cetco polymer shafts.

Very little variation was witnessed within the Cetco Polymer shaft results. Length corrected loads only differed by 550lbs resulting in a difference in capacity of just 10% between C3-24h

(maximum) and C4-2h (minimum). Note the maximum capacity in this series was obtained from the 24 hour shaft. The subtle variations in test results suggest that the Cetco polymer slurry (like the other polymer products) was insensitive to open-hole exposure time.

3.2.3 Filter Cake Measurements

The physical dimensions taken from each test shaft included: length, average filter / soil caked to the sides of the shaft, the average shaft diameter after washing, and the computed average shaft diameter when extracted from the ground (i.e. washed diameter plus filter / soil cake). Tables 3.13-3.16 show the average measured filter cake thicknesses, along with the measured shaft diameter after cleaning. Percent difference between the shaft diameter before washing and the actual concrete diameter (after washing) are also shown in the tables. Differences in diameter up to 10% were observed with the bentonite shafts while the maximum in polymer shafts was 8%. The effective diameter defines the actual shear plane where side shear was developed, while the actual diameter is more meaningful to structural properties. The average effective diameters for the four series, were 4.14, 4.08, 4.10, and 4.07in for the bentonite, KB, Matrix and Cetco shafts, respectively. The average concrete diameters were 3.85, 3.89, 3.84 and 3.87in, again respectively.

Table 3.13 Filter cake measurements for bentonite slurry shafts.

Shaft Label	Average Filter Cake Thickness (in)	Diameter After Cake Removal (in)	Diameter Before Cake Removal (in)	Percent Difference (%)
B6-0h	0.139	3.936	4.213	-7%
B5-1h	0.146	3.894	4.186	-7%
B4-2h	0.099	3.954	4.152	-5%
B1-4h	0.130	3.869	4.129	-6%
B2-8h	0.166	3.803	4.134	-8%
B3-24h	0.203	3.648	4.054	-10%

Table 3.14 Soil cake measurements for KB polymer slurry shafts.

Shaft Label	Average Filter Cake Thickness (in)	Diameter After Cake Removal (in)	Diameter Before Cake Removal (in)	Percent Difference (%)
KB6-0h	0.084	3.895	4.062	-4%
KB5-1h	0.083	3.834	4.001	-4%
KB4-2h	0.07	3.827	3.966	-4%
KB1-4h	0.077	3.862	4.016	-4%
KB2-8h	0.137	3.97	4.244	-6%
KB3-24h	0.123	3.936	4.182	-6%

Table 3.15 Soil cake measurements for Matrix Big-Foot polymer slurry shafts

Shaft Label	Average Filter Cake Thickness (in)	Diameter After Cake Removal (in)	Diameter Before Cake Removal (in)	Percent Difference (%)
M6-0h	0.165	3.801	4.130	-8%
M5-1h	0.112	3.849	4.073	-6%
M4-2h	0.135	3.776	4.046	-7%
M1-4h	0.149	3.934	4.233	-7%
M2-8h	0.129	3.779	4.037	-6%
M3-24h	0.096	3.885	4.077	-5%

Table 3.16 Soil cake measurements for Cetco polymer slurry shafts.

Shaft Label	Average Filter Cake Thickness (in)	Diameter After Cake Removal (in)	Diameter Before Cake Removal (in)	Percent Difference (%)
C6-0h	0.059	3.869	3.988	-3%
C5-1h	0.100	3.805	4.005	-5%
C4-2h	0.113	3.859	4.085	-6%
C1-4h	0.076	3.873	4.025	-4%
C2-8h	0.154	3.950	4.258	-7%
C3-24h	0.082	3.874	4.038	-4%

3.3 Analysis of Test Results

Based on the results in Figures 3.97-3.100, slurry exposure had minimal effect on side shear resistance within the polymer shafts. Bentonite on the other hand saw some degradation of capacity with increased exposure times (Figure 3.97).

Tables 3.13-3.16 show that similar cakes and dimensional reductions were observed for both the bentonite and polymer shafts even though the capacity reduction within bentonite shafts were consistently larger. However, based on the observation of caked material on the perimeter of exhumed shafts described in Section 3.1, the increase in filter cake thickness reduces the effective shaft diameter within the bentonite shafts whereas the soil cake increases the effective shaft diameter of the polymer shafts. Hence, it is likely that increased filter cake thicknesses within bentonite shafts would result in a shear interface located within the filter cake, i.e. the shear resistance is limited by the strength of the filter cake. This would not be the case with the polymer shafts due to the formation of the soil cake which results in the shear interface being located within the surrounding soil. Therefore, the shear resistance of the polymer shafts would come as a direct result of grain interlock within the subgrade. These concepts are further discussed in this section in order to establish a tangible relationship between increased exposure time of drilling slurries and side shear resistance of drilled shafts. In short, while the shaft

diameter was slightly different between slurry types, it was the composition of the soil cake/filter cake largely responsible for side shear capacity differences.

3.3.1 Static Load Tests

As seen in Figure 3.97, clear variations of shaft capacity were witnessed with the shafts constructed under bentonite slurry. Far less fluctuation was witnessed within the shafts stabilized with polymer slurry. This suggests that bentonite slurry exposure time has a considerable effect on the performance of drilled shafts while polymer slurries do not have the same effect. Figure 3.101 shows a clear deterioration in bentonite shaft capacity with increased exposure time whereas there was very little variation with increased exposure time among the polymer shafts.

It should be noted that the shaft capacities presented throughout this project, serve as a direct measure of the strength of the failure (shear) interface which may or may not have been modified due to continuous exposure to drilling slurries. Using the values presented in Table 3.10 for 0 and 96hrs, 5.41 and 2.49kips, respectively, Figure 3.101 shows a 54% reduction in capacity with the bentonite shafts. Inspection of Figure 3.101 also shows that all polymer series exhibited very little change in capacity with exposure time.
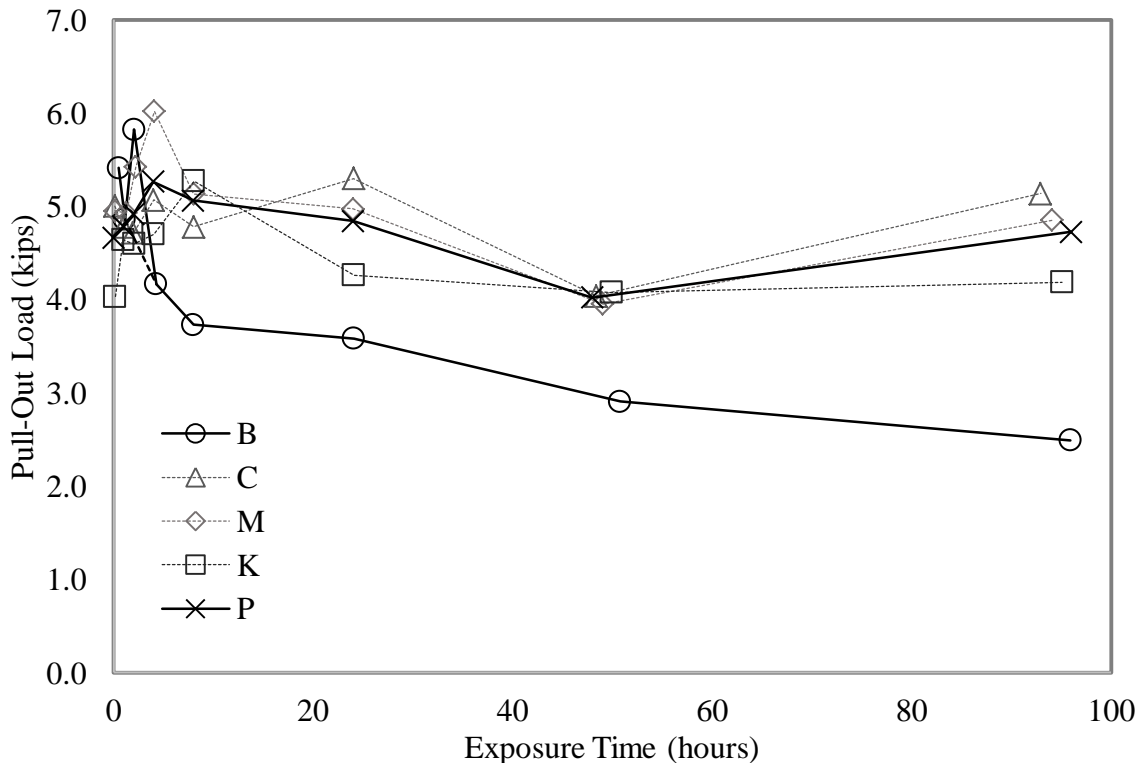
Figure 3.101 Length corrected load vs exposure time for each test series.

Based on the length correct capacities shown in Figure 3.101, the polymer shafts outperformed the bentonite shafts even though the capacities of the bentonite shafts exceeded that of the

polymer shafts for the first 2 hours of exposure. However as excavation, cage placement, and concreting (normal shaft construction) usually far exceeds the 2 hour window in which the bentonite shafts outperformed the polymer shafts, it would be virtually impossible to capitalize on this capacity due to construction time constraints. Further analysis is presented in Chapter 5 which discusses the local soil strength and the bias associated with considerations between the measured load versus the anticipated design capacity from the local soil strength profile.

3.3.2   Filter / Soil Cake Thickness

The term "filter cake" as used in this report refers to the layer of bentonite clay that builds/deposits on the side of the excavation walls. For polymer shafts the term "soil cake" is used to denote the thickness of polymer laden soil that adhered to the side of the shaft upon excavation. In general, the filter cake is truly a different material from the surrounding soil whereas the soil cake is the same native soil type that surrounded the shaft. Figure 3.102 shows the relationship between exposure time and filter cake (or soil cake) thickness for each test series. As expected, a general trend of filter cake thickness increasing with exposure time for the bentonite shafts was witnessed though there was an initial decline in cake thickness. No appreciable relationship was found between exposure time and for the polymer shafts as the soil cake thickness varied with increased exposure time for each test series.
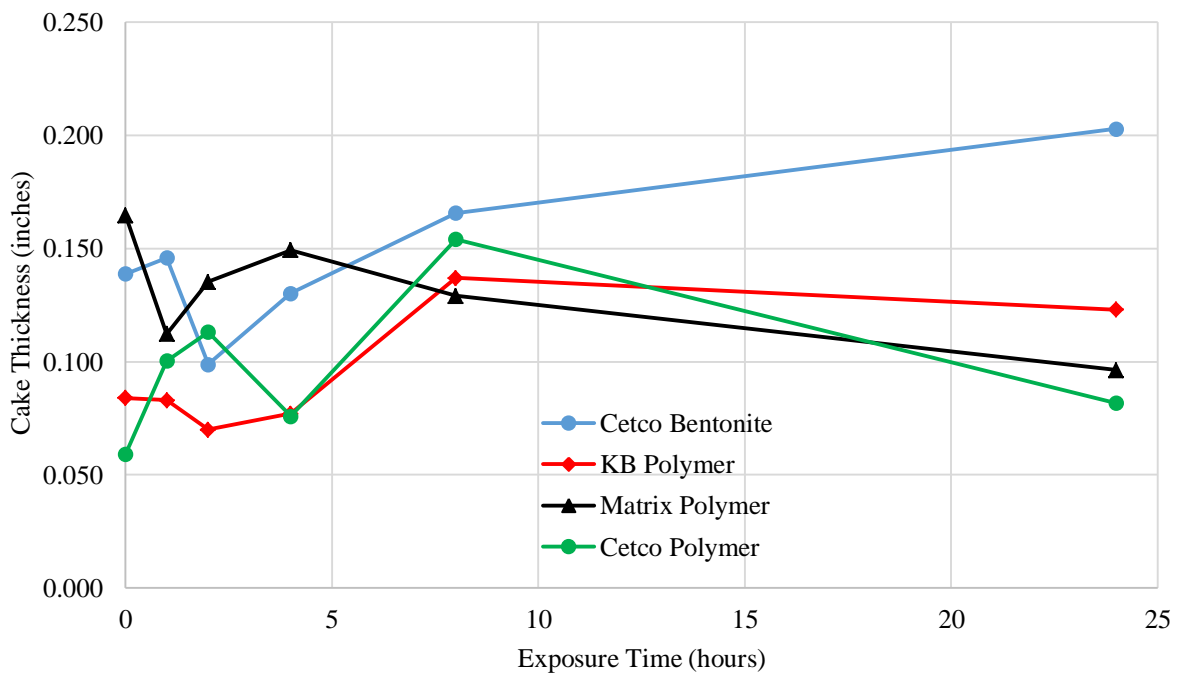
Figure 3.102 Filter cake / soil cake thickness vs. exposure time for all shafts

Since, filter cake thickness generally increases with time for bentonite (Majano, 1992), it was expected that capacity would also decrease with filter cake thickness. Similar results were

witnessed with the test results obtained experiments performed as seen in Figure 3.103. Therefore, it can be concluded that time dependent capacity reductions in bentonite shafts come directly as a result of increase of filter cake thickness with time. No analogous statement can be said about polymer slurry as no time dependency was noted relative to soil cake thickness. In fact, the absence of appreciable capacity reduction generally concludes similarly. The subtle variations in capacity for polymer shafts (increases or decreases) are thought to be only caused by similarly subtle variations in the soil strength profiles.
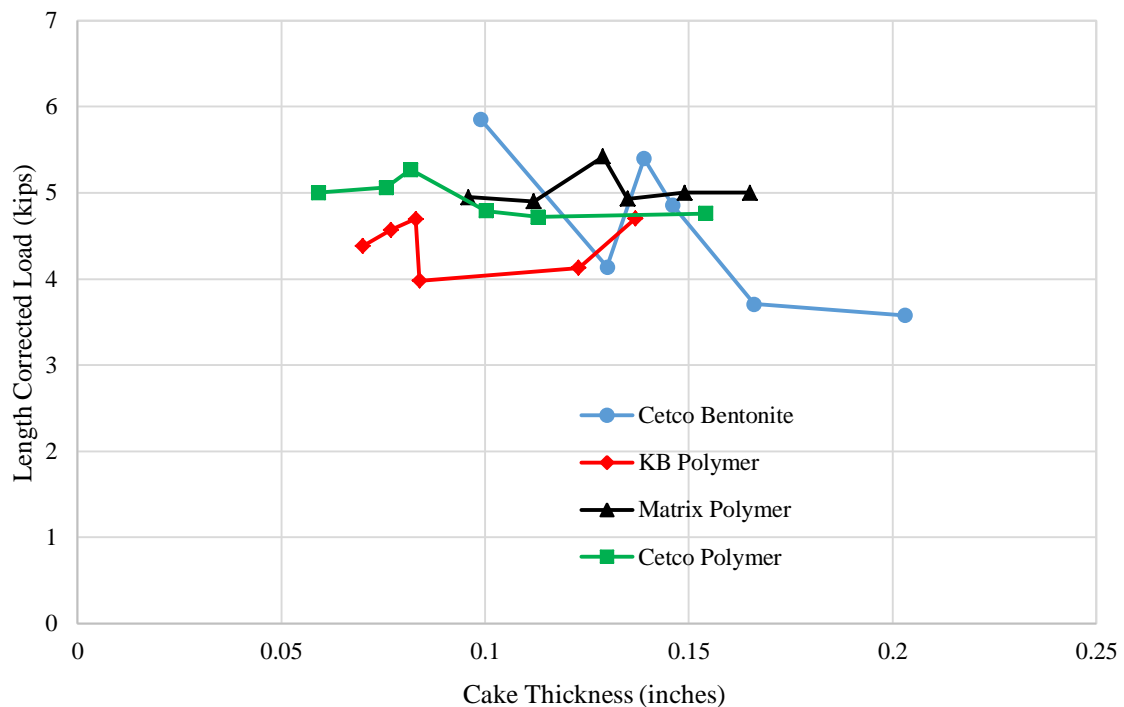
Figure 3.103 Pullout capacity vs cake thickness.

Measurements of the filter cake thickness and the washed/true concrete diameter gave rise to a concept of the effective diameter of a shaft. Based on the values in Tables 3.10-3.13, it was seen that the as-built diameter (after cake removal) and effective diameter (with cake attached) of the bentonite shafts reduced with increased exposure time. This reduction did not occur in polymer shafts but rather some increases in shaft diameter were noted with increased polymer exposure. This relationship is explored in Figures 3.104 and 3.105 where it can be seen that both the as-built and effective diameters decreased slightly with exposure time. Combining the effects of diameter reduction and reduced shear strength of the failure interface due to filter cake formation (as cited by Ata and O'Neill, 2002), it is only logical that bentonite shafts would exhibit reduced shear resistance capacities at increased exposure time as witnessed in Figures 3.106 and 3.107. Although in full size shafts dimensional reductions would have proportionally less effect. Polymer test specimens on the other hand, did not exhibit such a relationship due to the absence of a substantial diameter reduction or weakened failure interface. Therefore, little diameter-based capacity variations were witnessed with the polymer specimens (Figure 3.106 and 3.107).
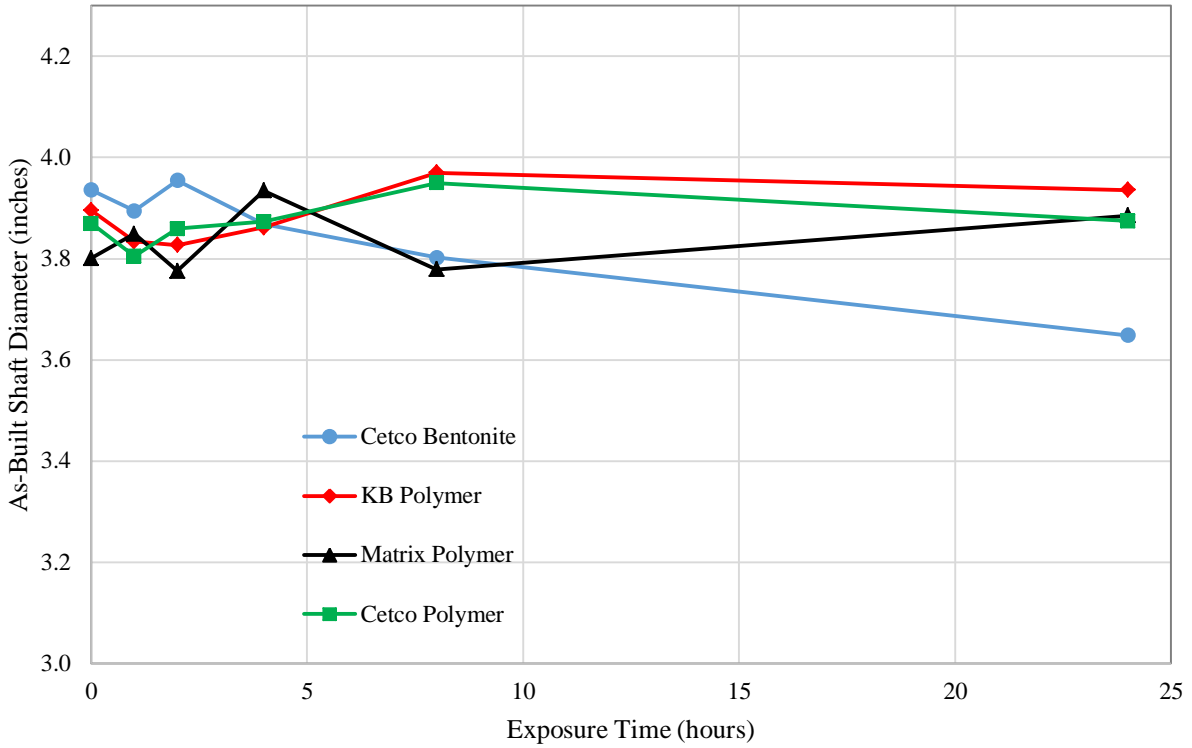
Figure 3.104 As-built shaft diameter vs exposure time for all shafts.
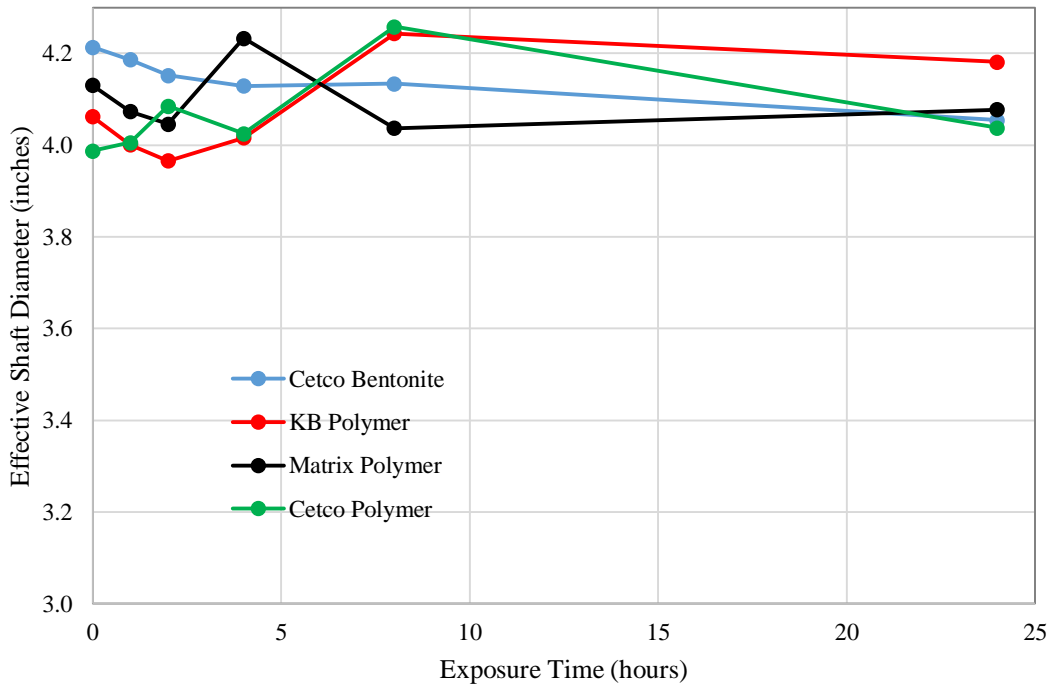
Figure 3.105 Effective shaft diameter vs exposure time for all shafts.
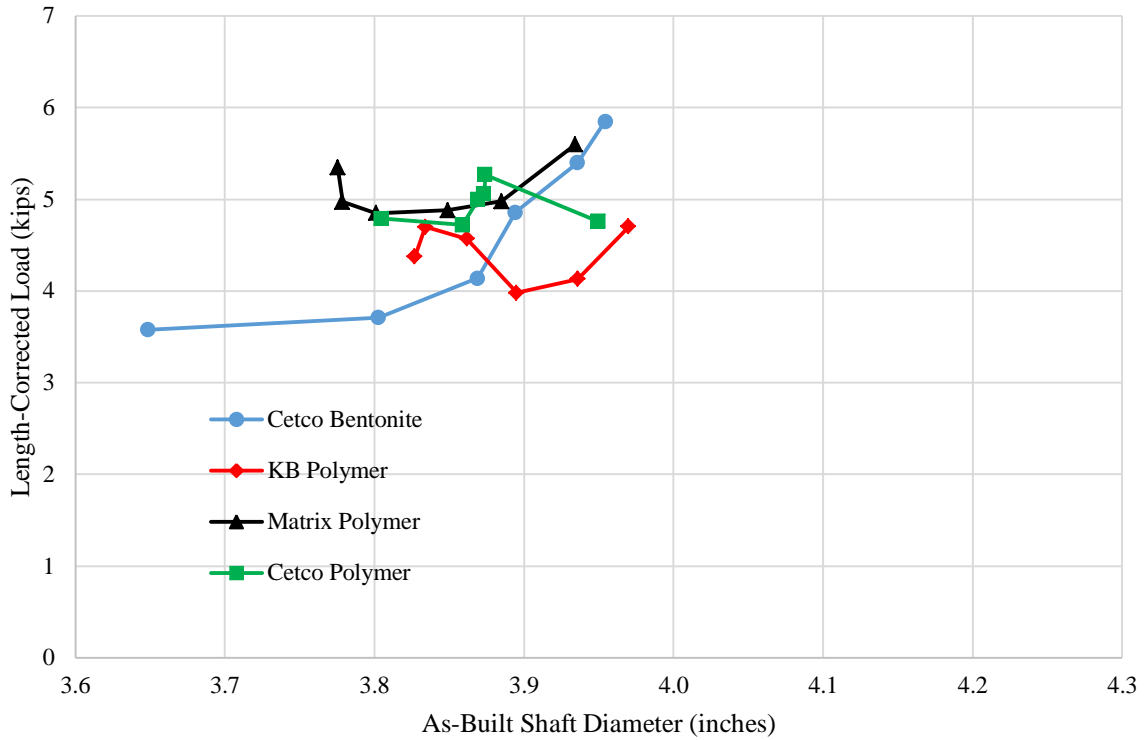
Figure 3.106 Length-corrected load vs as-built shaft diameter for all test shafts.
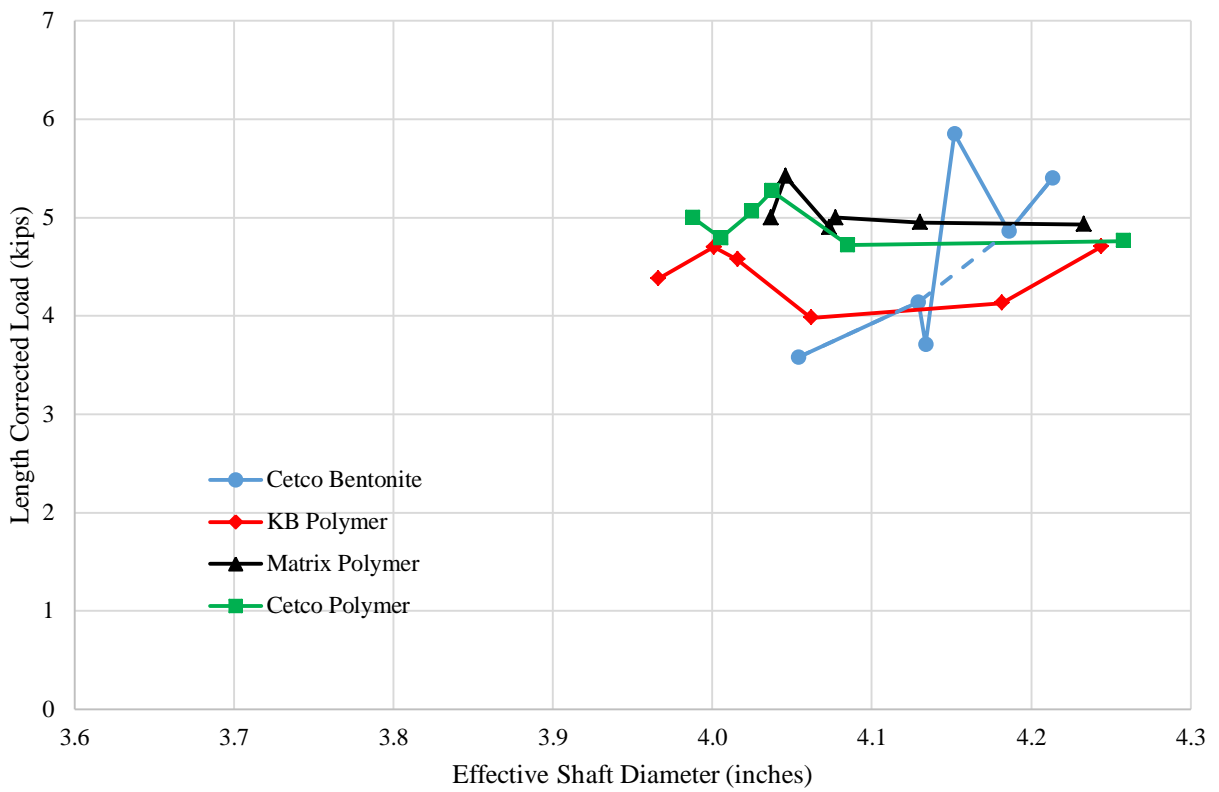
Figure 3.107 Length corrected load vs effective shaft diameter for all test shafts.

127

3.3.3 Side Shear Resistance

Since the failure interface was defined by the effective diameter, this diameter was used to calculate the shear stress along this interface for each test shaft. This was done by dividing the ultimate length-corrected load by the surface area of the shaft (surface area using effective shaft diameter). By using the effective diameter rather than the as-built diameter, artificial inflation of shear stresses associated with reduced shaft diameters due to filter cake build-up (bentonite shafts) was avoided. Tables 3.17 - 3.20 shows the length corrected ultimate loads, effective shaft diameters and corresponding shear stresses for each shaft.

Figure 3.108 shows the side shear resistance generated along the shear interface plotted against exposure time and effective shaft diameter. Nearly a 30% reduction in side shear resistance was observed between 0 and 24 hours for the bentonite shafts. All of the polymer shafts on the other hand exhibited side shear resistances either equal to or above the respective 0 hour shaft. While some decrease with exposure time was observed in the bentonite shafts after 8hrs, the soil strength in those areas coincidentally was also progressively weaker (Sect. 3.3.4). Nevertheless, after 8 hours of exposure there was very little difference in capacity (Figure 3.108).

Table 3.17 Interface shear stresses of bentonite shafts.

Shaft Label	Effective Shaft Diameter (in)	Length Corrected Load (kips)	Side Shear Resistance (ksf)
B6-0h	4.213	5.41	0.612
B5-1h	4.186	4.86	0.554
B4-2h	4.152	5.85	0.673
B1-4h	4.129	4.14	0.479
B2-8h	4.134	3.71	0.429
B3-24h	4.054	3.58	0.422
B7-48h	4	2.54	0.347
B8-96h	4	2.18	0.297

Table 3.18 Interface shear stresses of KB Polymer shafts.

Shaft Label	Effective Shaft Diameter (in)	Length Corrected Load (kips)	Side Shear Resistance (ksf)
KB6-0h	4.062	3.979	0.468
KB5-1h	4.001	4.698	0.561
KB4-2h	3.966	4.379	0.527
KB1-4h	4.016	4.571	0.543
KB2-8h	4.244	4.704	0.529
KB3-24h	4.182	4.129	0.471
KB7-48h	4	3.568	0.487
KB8-96h	4	3.662	0.500

Table 3.19 Interface shear stresses of Matrix polymer shafts.

Shaft Label	Effective Shaft Diameter (in)	Length Corrected Load (kips)	Side Shear Resistance (ksf)
M6-0h	4.130	4.95	0.572
M5-1h	4.073	4.90	0.574
M4-2h	4.046	5.42	0.640
M1-4h	4.233	4.93	0.556
M2-8h	4.037	5.00	0.591
M3-24h	4.077	5.00	0.585
M7-48h	4	3.46	0.472
M8-96h	4	4.24	0.579

Table 3.20 Interface shear stresses of Cetco polymer shafts.

Shaft Label	Effective Shaft Diameter (in)	Length Corrected Load (kips)	Side Shear Resistance (ksf)
C6-0h	3.988	5.00	0.599
C5-1h	4.005	4.79	0.571
C4-2h	4.085	4.72	0.552
C1-4h	4.025	5.06	0.600
C2-8h	4.258	4.76	0.534
C3-24h	4.038	5.27	0.623
C7-48h	4	3.53	0.482
C8-96h	4	4.49	0.613
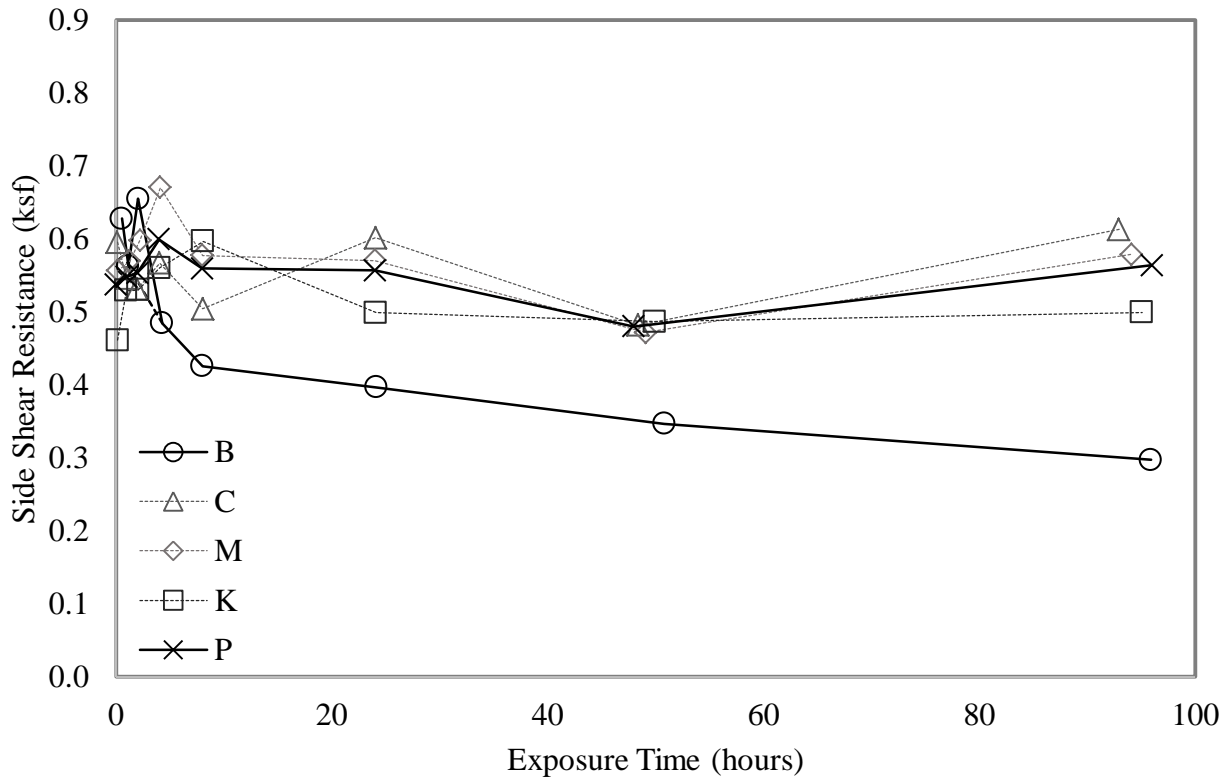
Figure 3.108 Side shear resistance vs exposure time for all shafts.

As seen in Figure 3.109, the effective shaft diameter and side shear generated along the interface decreased proportional to effective shaft diameter for the bentonite shafts. These reductions in effective shaft diameter were very subtle as the difference between the largest and smallest shaft less than ¼ of an inch. Note Figure 3.109 shows the minor reduction in effective diameter resulted in nearly a 30% decrease in side shear resistance. It is unlikely that the subtle change in diameter resulted in such a large reduction in side shear resistance, but rather, the reduction should be attributed to the degradation of the shear interface associated with the clay filter cake formation.

Polymer shafts saw sporadic changes in effective shaft diameter with increased exposure time. Interestingly, a general decreasing trend in shaft resistance was witnessed with an increase in shaft diameter. This reduction was likely due to a poorly established soil cake at these diameters. Recall, soil cake formation is due to polymer slurry infiltration into the surrounding soil and the three-dimensional lattice (by which polymers work) inducing cohesive behavior in the soils exposed. Hence, the thickness of the soil cake is dependent upon the distance away from the borehole, the slurry infiltrated the surrounding soil. Since slurry infiltration slows radially with increased distance from the borehole, it can be expected that slight decreases in capacity would be expected as radial distance from the borehole increases. On that note, it is important to recognize that the side shear resistance in the polymer specimens will only reduce to the shear capacity of the in situ strata. Therefore, the reductions witnessed within the polymer specimens were not caused by slurry type used.

130
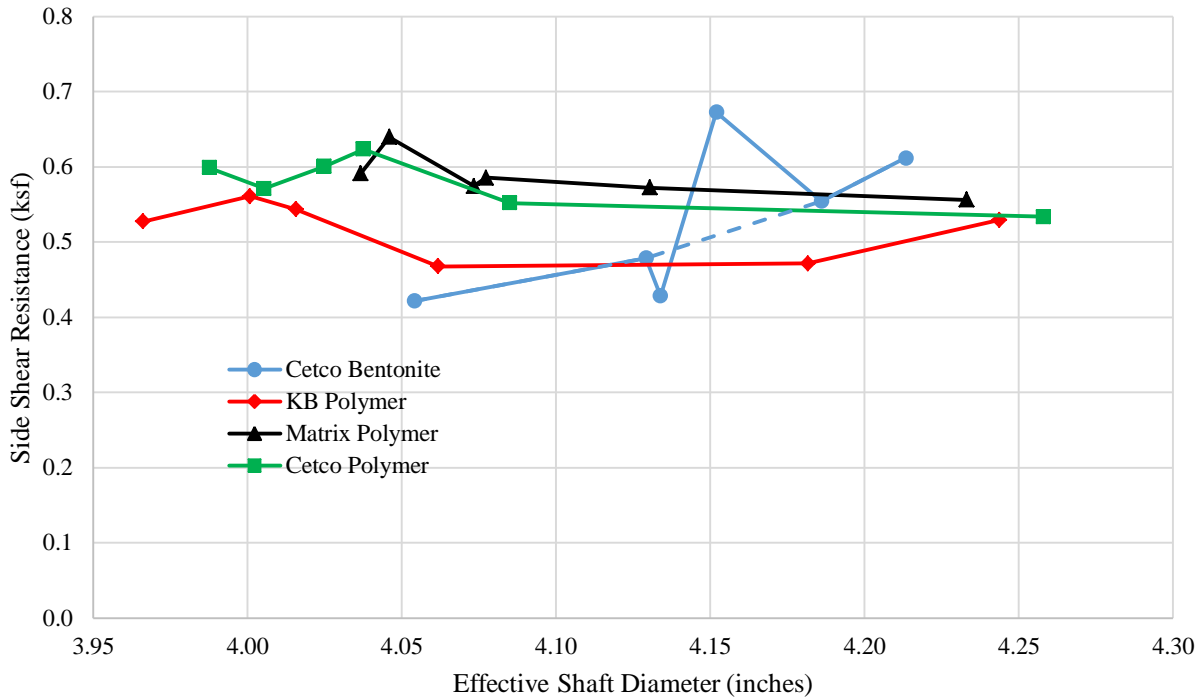
Figure 3.109 Side shear resistance vs effective shaft diameter for all test shafts.

3.3.4   Soil Strength Consideration

Tables 3.6-3.9 provided the theoretical minimum and maximum uplift resistances of each test shaft based on the CPT data. These values were averaged to obtain a reasonable idea of the capacity of the in situ soils for 4in diameter test shafts. The average values resulted in differences ranging between 2 and 3 kips for the test performed at the polymer test locations while a difference of 1.5 kips was computed for the bentonite test locations. Based on the values presented in Tables 3.21-3.24, the specimens which were stabilized under Cetco ShorePac a stabilizing fluid were cast in the weakest soils while those stabilized under Matrix Big-Foot polymer slurry were cast into the strongest soils. Due to these differences, soil strength corrections were calculated to normalize strengths to the 24hr bentonite shaft since it is the closest value to the 36h limit before overreaming is required according to FDOT standards (2018).

This correction factor was calculated by dividing the capacity of the 24hr bentonite shaft by the capacity of each test shaft. Therefore, a correction factor greater than 1 is computed where the capacity of a given soil profile was less than the 24hr bentonite soil profile and vice versa. The correction factor for each shaft was then multiplied by the corresponding average shear resistance. By applying this correction factor, the loads obtained during the static load testing were scaled to the soil strength and length of the 24hr bentonite shaft. Some consider this type of correct to be a true comparison of side-by-side tests while others are prone to look only at the uncorrected load as one soil exploration is not 100% representative of soil strengths. Regardless, Figure 3.110 shows the CPT corrected load versus exposure plot.

131

Table 3.21 Soil strength corrections for bentonite test series.

Shaft Label	Uncorrected Soil Resistance (kips)	Uncorrected Load (kips)	Soil Strength Correction Factor	Soil Strength Corrected Test Load (kips)
B6-0h	4.548	5.063	1.128	5.71
B5-1h	4.820	4.835	1.075	5.20
B4-2h	5.343	5.484	0.973	5.34
B1-4h	5.490	4.032	0.941	3.79
B2-8h	5.918	3.729	0.886	3.30
B3-24h	5.163	3.580	1.000	3.58
B7-48h	4.502	2.906	1.270	3.69
B8-96h	4.103	2.492	1.393	3.47

Table 3.22 Soil strength corrections for KB polymer test series.

Shaft Label	Uncorrected Soil Resistance (kips)	Uncorrected Load (kips)	Soil Strength Correction Factor	Soil Strength Corrected Test Load (kips)
KB6-0h	4.983	4.06	1.035	4.20
KB5-1h	5.810	4.54	0.904	4.11
KB4-2h	3.159	4.10	1.538	6.30
KB1-4h	4.361	4.63	1.180	5.46
KB2-8h	3.045	5.16	1.601	8.26
KB3-24h	3.965	4.12	1.283	5.28
KB7-48h	4.849	4.08	1.179	4.81
KB8-96h	4.862	4.19	1.176	4.93

Table 3.23. Soil Strength Corrections for Matrix Polymer Test Series.

Shaft Label	Uncorrected Soil Resistance (kips)	Uncorrected Test Load (kips)	Soil Strength Correction Factor	Soil Corrected Strength Test Load (kips)
M6-0h	6.014	5.03	0.878	4.41
M5-1h	5.435	5.09	1.045	5.32
M4-2h	6.427	5.58	0.818	4.57
M1-4h	4.600	5.22	1.220	6.37
M2-8h	5.009	5.24	1.054	5.52
M3-24h	7.086	5.07	0.748	3.79
M7-48h	4.151	3.95	1.377	5.44
M8-96h	4.198	4.85	1.362	6.61

Table 3.24. Soil Strength Corrections for Cetco Polymer Test Series.

Shaft Label	Uncorrected Soil Resistance (kips)	Uncorrected Load (kips)	Soil Strength Correction Factor	Soil Strength Corrected Test Load (kips)
C6-0h	4.832	4.51	1.072	4.84
C5-1h	4.041	3.99	1.256	5
C4-2h	2.909	4.07	1.679	6.84
C1-4h	3.351	4.39	1.473	6.46
C2-8h	3.341	4.28	1.477	6.3
C3-24h	3.257	4.52	1.506	6.8
C7-48h	4.023	4.04	1.422	5.74
C8-96h	4.365	5.14	1.871	9.62
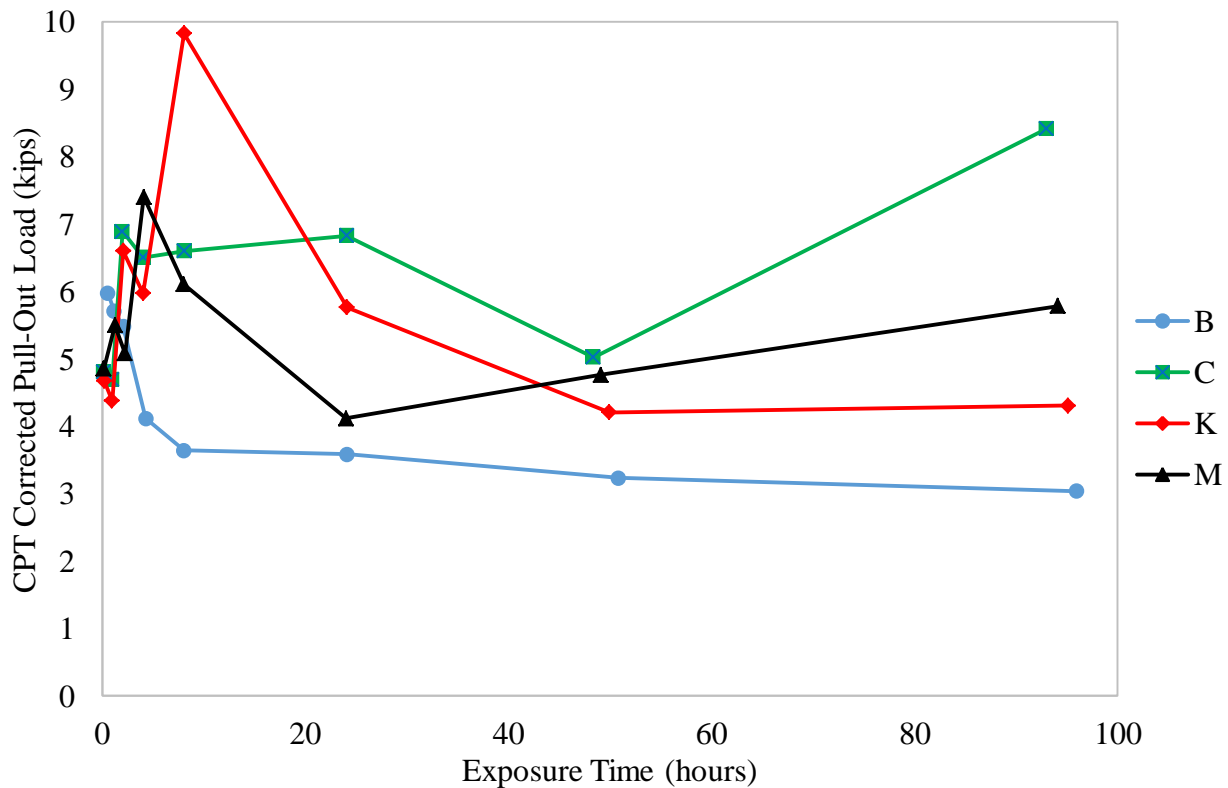
Figure 3.110. Soil strength corrected load vs. exposure time.

As shown in Figure 3.110, only the bentonite test series exhibits a soil strength load versus exposure curve similar to the length corrected curves. Even after correcting the pullout capacity by normalizing to the 24hr area under the CPT tip stress curve, the bentonite 0 and 96hr ultimate pullout loads of 6.89 and 3.04kips, respectively, almost identical reduction in capacity was noted (56%) when compared to simple length corrected methods (54%). Capacity increases on the

order of 1-1.5 kips were computed for the KB and Cetco polymer series while the Matrix series exhibited an erratic trend once the soil strength corrections were applied. Though all of the polymer shafts continued to outperform the bentonite shafts after 4 hours of exposure, the absence of a similar trend to the collected data indicates that it is unreasonable to consider soil strength differences as the only factor to the side shear resistances obtained in these experiments. This stance is further emphasized by the fact that the polymer shafts all exhibited very similar side shear resistances while bentonite shafts experienced the expected decrease in capacity due to filter cake formation with increased exposure time. Therefore, the absence of the formation of filter cake with polymer slurries results in favorable side shear resistances with increased exposure time.

3.3.5 Further Comparisons

All of the polymer shafts exhibited similar shear resistances while the bentonite shafts experienced reduced shear resistance with increased exposure time. After 8 hours of exposure, the capacity reduction in the bentonite series began to stabilize. With that in mind, it can be suggested that after 8 hours of exposure, the capacity of bentonite shafts approach an asymptotic shear resistance. This asymptote is likely defined by the shear strength of the filter cake formed by the bentonite slurry of which the rate of formation was shown to similarly decrease after 8hrs.

Recall, FDOT currently allows for bentonite slurry to be exposed to the walls of an open excavation for 36 hours before overreaming of the walls is required (12 hours for bottom 5ft). Given virtually all degradation occurred within 8hrs, it is reasonable to assume that no further degradation would occur beyond 24 or 36hrs. No such reduction was witnessed with the shafts stabilized under polymer slurry and in all cases the side shear resistance exceeded the 24 hour bentonite by 12% to 50% as seen in Figure 3.111.

Closer inspection of Figure 3.111 shows that even if the 8h exposure time of bentonite slurry was considered as the comparative standard, all of the polymer shafts except KB6-0h would still produce larger side shear resistances. Similar results were witnessed by Majano (1992) and Brown (2002) where it was found that the resistance of the polymer shafts greatly exceeded that of the bentonite shafts (Figure 3.112). In the legend of Figure 3.112, the first letter represent the author name (M-Majano, B-Brown), the second letter represents the type of slurry used (B-bentonite, L-liquid polymer, D-dry polymer) and the numbers represent that slurry viscosity. The results displayed in Figure 3.112 are also presented for comparison. Generally, polymer shafts outperformed the bentonite shafts by at least 20%.
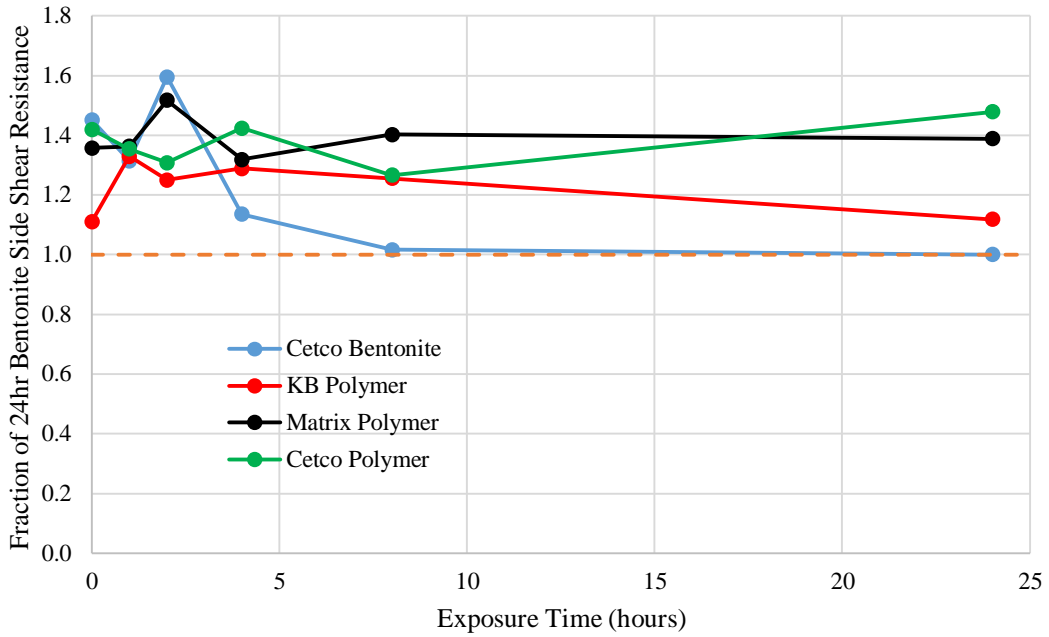
Figure 3.111 Side shear resistance vs exposure time expressed as fraction of 24hr bentonite side shear resistance.
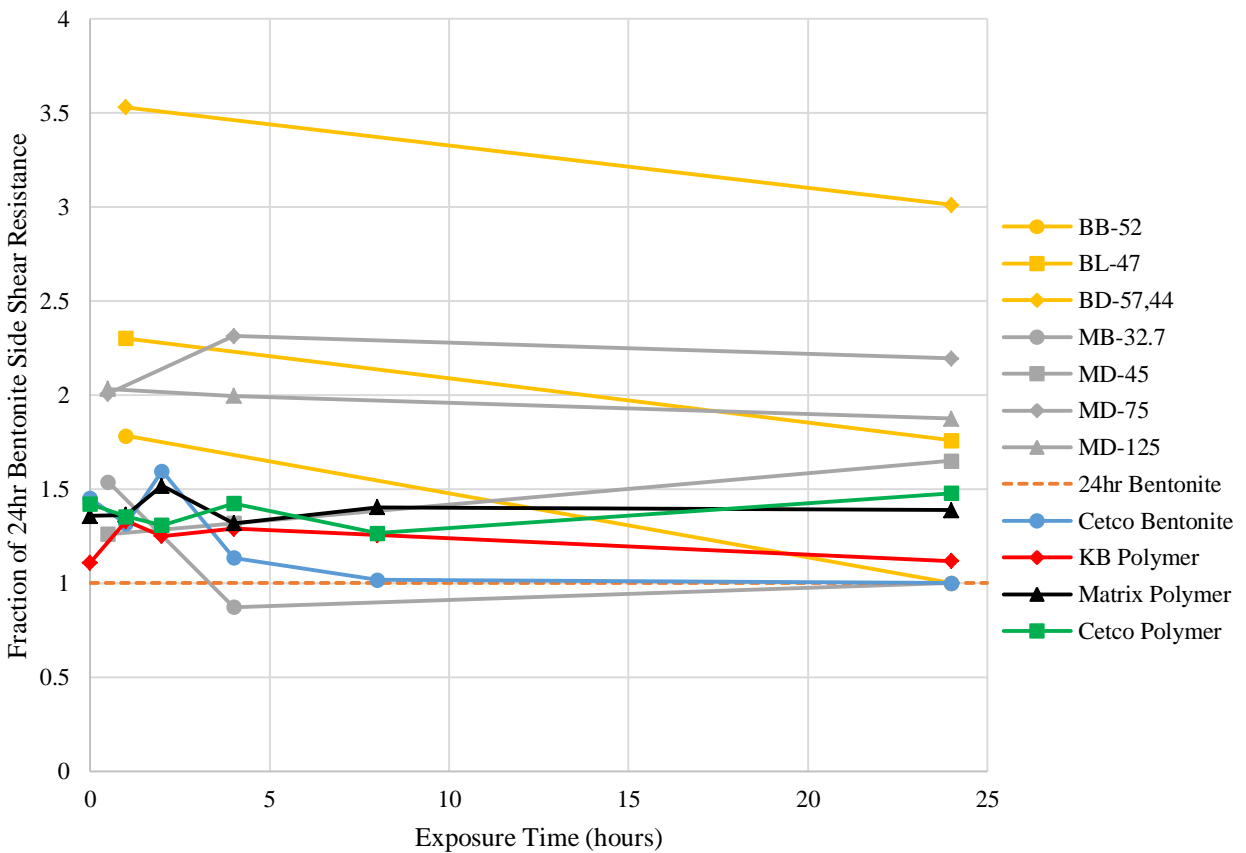
Figure 3.112 Fraction of 24hr bentonite vs exposure time from literature review and test data.

135

3.4 Chapter Summary

Thirty two 1/10th scale shafts were constructed in field conditions to assess the effects of slurry type and open-hole exposure times. While all shaft concrete was tremie placed, the full effect of a rebar cage was not included as only a single, centralized anchor bar was cast into the specimens. Pullout tests were performed on each shaft and compared to the 24hr bentonite shaft as a point of reference. Comparisons were performed on the basis of length corrected load and the local soil strengths. Both methods of comparison showed substantial reductions in side shear resistance for bentonite stabilized excavations from the time of slurry introduction onward (54 to 55% after 96hrs). The forensic reviews indicated that these reductions were due to increases in filter cake thicknesses with increased with exposure time. Not only did this weaken the shear interface to a strength controlled by the filter cake but it also results in a decrease in effective shaft diameter and hence a smaller area to transfer shear (less significant for full size shafts).

Shafts constructed with polymer slurry, on the other hand, showed no substantial reductions in capacity regardless of the polymer product tested. As this includes shafts constructed with exposure times from 0 to 96hrs, this also indicates that there is no apparent consequence to increased exposure time when polymer slurries are used. The results showed that rather than forming a filter cake, polymer slurries stabilized an effective area around the shaft which resulted in a soil cake made of insitu soil around the perimeter of exhumed shaft. This essentially increases the effective shaft diameter due to the solidified bond between the concrete shaft and the surrounding soil created by polymer slurry infiltration. A roughened, sandpaper like texture was more apparent above the water table, but in all, resulted in a soil to soil shearing interface around the polymer shafts rather than a bentonite, clay / clay interface.

Chapter Four: Full Scale Field Testing

This chapter discusses the full scale testing performed to verify laboratory testing targeting the effect of drilling fluid exposure time, primarily polymer systems, on the side shear resistance of drilled shafts. To achieve this goal, full scale shafts (24in diameter, 15ft long) were constructed using slurry stabilization with both polymer and mineral slurry with varied slurry exposure times ranging from 4 hours to 48 hours. The results of the tests performed are presented including analysis of the CPT soundings and the static load tests.

4.1 Preparations for Field Pullout Testing

Full-scale pullout testing was performed on five shafts, where both mineral and polymer slurry were tested at varied viscosities and exposure times. Table 4.1 shows the testing matrix for the full-scale program. In general, the Shaft ID designation is made up of the slurry type (B or P for bentonite or polymer), the duration of slurry exposure (48 or 0hrs), and the target Marsh funnel viscosity in seconds.

Table 4.1 Full-scale testing matrix

Shaft ID	Slurry Type	Exposure Time (hr)	Target Viscosity (sec/qt)
B48-40	Bentonite	48	40
P48-60	Polymer	48	60
B0-40	Bentonite	0	40
P0-60	Polymer	0	60
P0-100	Polymer	0	>100

The overall field testing program involved: (1) CPT testing of the test site to confirm consistency or show where variations existed; (2) slurry preparation; (3) construction of the test shafts; (4) pullout testing and extraction; and (5) detailed measuring of the constructed shaft dimensions.

4.1.1   CPT Testing

The location of the test site was confirmed to be in the south yard of a local Association of Drilled Shaft Contractors (ADSC) member, R.W. Harris, Inc., in Clearwater, Florida. Figure 4.1 shows a satellite/map view of the site. This firm has been supportive with several drilled shaft research projects with the University of South Florida, where many aspects of quality assurance and construction methods have been assessed. Past projects dealt with post grouting shaft tips, thermal integrity profiling, viability of voided shafts, rapid hydration of mineral slurries, remote monitoring of foundations, effects of polymer slurry, and defining the upper viscosity limit of bentonite slurry (Mullins et al., 2014, 2012, 2010, 2009a, 2009b, and 2007).

In cooperation with R.W. Harris personnel, an area of the storage yard was selected which provided access to five separate shaft locations that would logistically enable convenient access

for both drilling and concreting. Shafts were cast over a three day period according to the intended exposure times for each slurry (Table 4.1). Spatial layout consisted of four shafts in a 20ft CTC square with a fifth shaft in the center. The shaft layout locations are shown in Figure 4.2.

Figure 4.1 Test site location in Clearwater, Florida at 122nd Ave N and 44th St N (Google Maps, 2017).

Cone penetration tests (CPT) were conducted at each of the proposed shaft locations using a miniature CPT device (Figure 4.3) to document variations in the soil strength and/or soil types. These types of variations, although usually minimal at close spacing, can affect shaft capacity and can in turn lead to confusing results if not quantified.
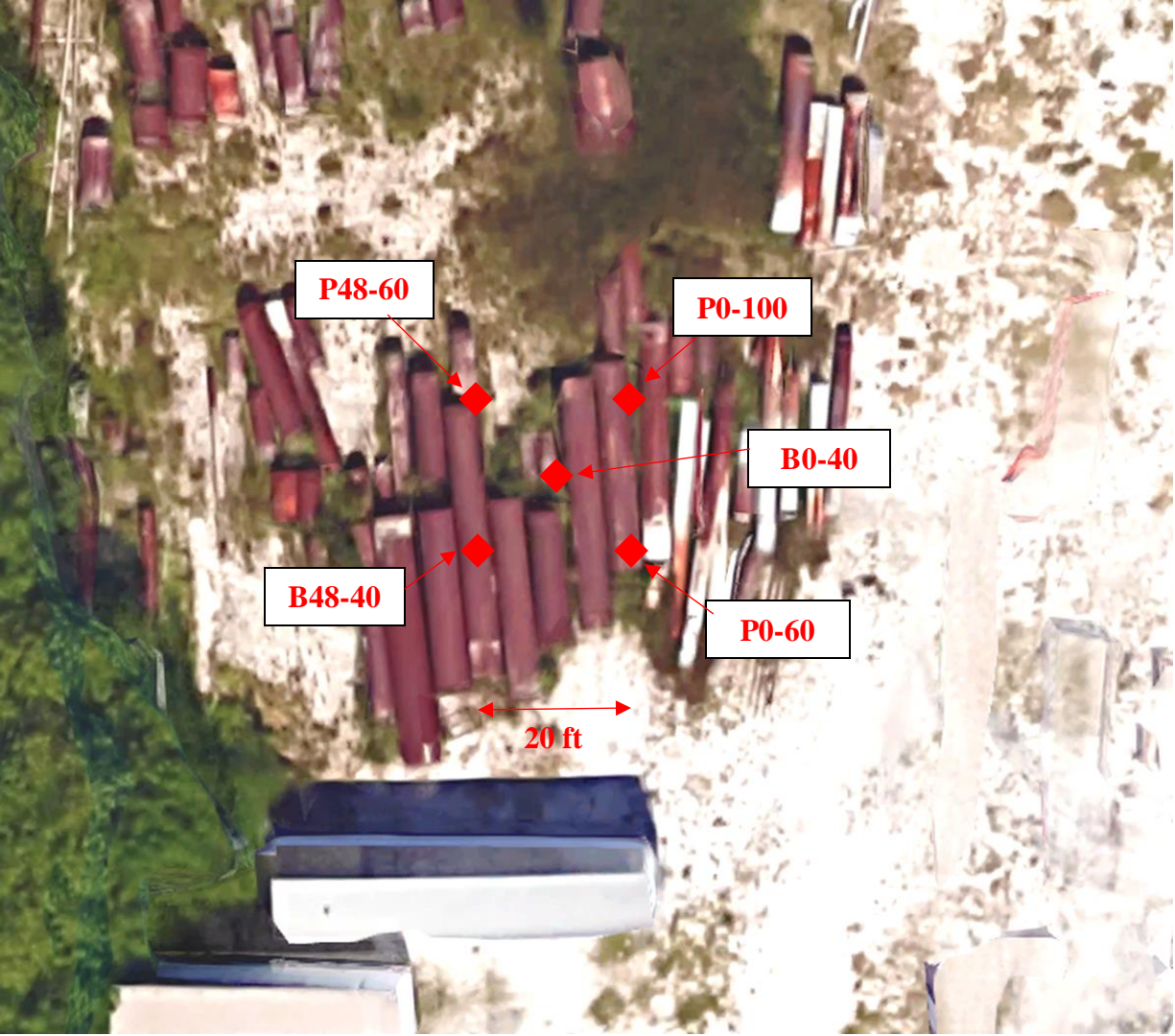
Figure 4.2 Shaft layout and location of CPT soundings (Google Maps, 2017).

Figure 4.3 Cone penetration testing at Clearwater test site.

A 3 ft layer of compacted limestone base was removed with a 4 inch diameter gas-powered auger prior to each sounding and replaced with local soils containing no rock. Each of the five soundings showed a layer of silty sand down to 12-15ft, followed by clay to silty.

Although there is general agreement among the soundings, it is apparent that soil strength layering is not exactly the same which can be quantified by the average tip stress, q_c. This provides a mechanism to predict capacity variations between locations. Some methods of computing the side shear capacity of drilled shafts use only tip stress values and others use direct measurements of sleeve friction corrected for the difference in the coefficient of friction from a steel / soil interface to a cast-in-place concrete / soil interface. Over the same depth interval the average tip stress is essentially the cumulative area under the tip stress curve divided by the interval length. However, graphically it more clearly shows the differences in cumulative load carrying capacity. Figure 4.5 provides an indication of variations in likely shaft capacity using the cumulative area under the tip stress curve for each of the CPT soundings. Therein, the predicted shaft capacity is proportional to the cumulative area under the tip stress curve.
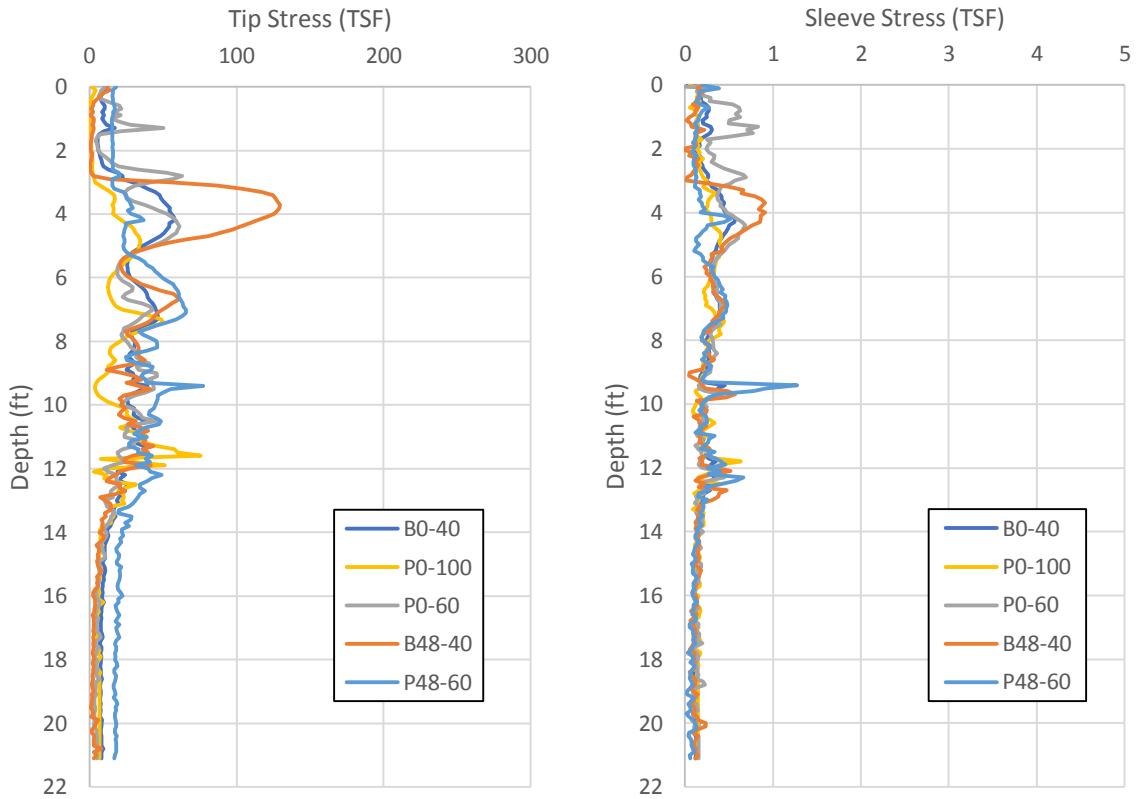
Figure 4.4 CPT tip stress (left) and sleeve friction (right) for each of the CPT soundings.
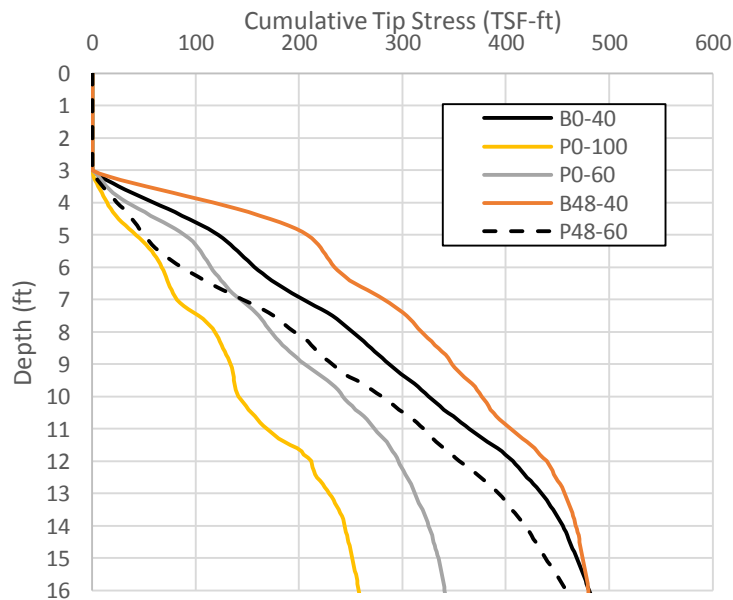
Figure 4.5 Cumulative area under the tip stress curve as a function of depth.

Location P0-100 (NE corner) showed the lowest cumulative tip stress and a general trend of weaker soils to the east and increasing strength to the west was noted. Table 4.2 shows each of the CPT locations sorted from highest to lowest potential capacity.

140

Table 4.2 Capacity potential sorted for each phase (highest to lowest)

Sounding	Location	Cumulative q_c at 15ft (TSF-ft)
B48-40	SW	474.3
B0-40	Center	468.4
P48-60	NW	438.4
P0-60	SE	334.7
P0-100	NE	251.4

4.1.2 Anchor Bars

The test program outlined for this study required that shafts be constructed with full-length debonded anchor bars, which would, in effect, load the shaft concrete in compression by applying a tension load to the anchor bar secured at the toe of the shaft. The soil therefore resists by pulling down on the shaft as the shaft is pulled upward. Upward loading typically results in lesser side shear resistance than downward loading due to the potential reduction in net effective stresses around the shaft. However, as all shafts were constructed and tested in the same manner, this serves as a convenient means to compare the shaft capacities and the effect of the slurry used at the time of shaft construction.

Anchor Bar Assemblies. The anchorage bars were 1in nominal diameter Williams Form 150 ksi fully threaded bars with a minimum ultimate strength of 128 kips. The bars were debonded from the shaft to prevent concrete cracking and Poisson necking effects that might affect side shear capacity. Debonding was achieved using 1-½ in ID SCH 40 steel pipe which was cut to length and also used as access tubes for thermal integrity testing after construction. Although integrity testing was not within the scope of the project, data was collected in case a shaft could not be extracted and the as-built shape could then be estimated without measurements.

An anchorage was provided at the toe of each shaft using a 16 in diameter circular plate made of ¾ in steel through which the anchor rods where inserted and threaded into the assembly. A Williams Form nut was welded to the underside of the anchor plate, and a steel pipe coupler was welded to the top of the plate (Figure 4.6). Further, to provide access within the 1.5 inch access pipe, the assembly was designed for bar removal (unthreading) from the anchor plate after concreting. This required that the plate be chamfered on the upper surface to direct the 1in diameter bar from within the 1.5in access tube into the center of the hole in the plate; a chamber below the anchor nut was also required to prevent soil and water intrusion into the access tube and to maintain clean access to the nut. Shear studs were added to each plate to facilitate removal and installation of the threaded anchor bar (so thermal profiling could be performed in the vacant access tubes). Figure 4.6 shows the completed anchor bar assemblies.

Figure 4.6 One quarter inch chamfer (top left), coupler and nut welded (top right), shear studs to prevent rotation during rod installation (bottom left), and completed anchor bar and base plate assembly (bottom right).

4.1.3 Slurry Mixing

For shafts constructed with mineral slurry (B48-40 and B0-40), *CETCO Puregold Gel* bentonite powder (no additives) was used to represent a standard 90 barrel yield mineral slurry (3780 gal / 2000lbs of bentonite), while *Matrix Big Foot* was used as the selected product for the polymer constructed shafts (P48-60, P0-60, & P0-100) (Figure 4.7). Recall, small scale field testing showed no appreciable difference in the polymer products.

Both the mineral and polymer materials where prepared and stored in dedicated slurry tanks. The pH of the supply water was adjusted using 6 lb of soda ash in 1000 gal of water to change it from pH 7 to 9.

Bentonite Slurry. Mineral slurry was prepared using the multi-eductor mixing system developed in an earlier FDOT project for the rapid hydration of mineral slurries shown in Figure 4.8. While the manufacturer recommended mix ratio for pure bentonite was 0.55 lb/gal to produce a 40 sec/qt viscosity, only 0.5 lb/gal was needed. As found by the previous study, virtually no material went unmixed and settled to the bottom of the tank thereby reducing the overall quantity needed. Figure 4.9 shows the bentonite slurry being recirculated.

Figure 4.7 Slurry products used: CETCO Puregold Gel bentonite (left); Matrix Big Foot polymer (right).

Figure 4.8 Multi-eductor mixing system used to prepare slurry.

Figure 4.9 Bentonite slurry ready for use immediately after mixing.

Polymer Slurry. The polymer slurry prepared per manufacturer recommendations with a representative on-site. The mix water was pretreated as note earlier but with the manufacturer provided pH adjusting additive, M-Booster. Recommended order of mixing and proportions of the slurry products and/or additives are given in Table 4.3. Figure 4.10 shows the products in the shipping containers and Figure 4.11 shows the products being introduced via a non-clog eductor. Polymer slurry for the first day of drilling targeted a 60 sec/qt Marsh funnel viscosity. This tank of approximately 1000 gal was used for both of the lower viscosity polymer shafts (i.e. 0 and 48hr exposures). For the higher viscosity polymer slurry specimen, a fresh tank of slurry was prepared on the third day for specimen P0-100.

Table 4.3 Dry polymer product/additives, order of mixing and dosages.

Order	Product	Suggested Mixing Amount	Type of Product	Purpose
1	M-BOOSTER®	6 lbs./1,000 gals mix water	Dry pH adjuster	Optimizes BIG FOOT® polymer performance and yield
2	FORTIFY™	4-6 lbs./1,000 gals	dry cellulosic polymer	Filtration control / slurry Booster
3	BIG-FOOT®	0.5-1.0 lbs./100 gals	PHPA dry polymer (high molecular weight)	Polymer slurry to fortify the excavation
4	GRID-LOCK™	Add 10-20 lbs. (1-2 pails) straight into excavation slurry	Water swell-able solid crystalline polymer	Controls loss of slurry into sidewalls
5 (not used)	NEUTRALIZER®	15-lbs/6,000 gallons high viscosity slurry	Dry reducing compound	Slurry breaker for disposal

Figure 4.10 Polymer slurry and additives.

Figure 4.11 Mixing of polymer slurry.

4.2 Shaft Construction

Shaft excavation was performed on two days. On day 1 both the 48hr exposure shafts were excavated (B48-40 and P48-60). For the next 48hrs, slurry levels were maintained within the 3ft surface casing which required periodic site visits to ensure proper levels. Some additional polymer slurry was required although only modest level adjustment was required. No additional bentonite slurry was needed.

On the third day after 48hrs had elapsed, three more shafts were excavated: P0-60, P0-100, and B0-40. So in effect, the structure of the testing addressed slurry exposure for both mineral and polymer slurry (B0-40 vs B48-40 and P0-60 vs P48-60) as well as the effect of polymer slurry viscosity without the mixed effects of time (P0-60 vs P0-100). Figures 4.12 – 4.15 show the three day shaft excavation equipment and process.

Figure 4.12 Excavation tools – auger (left), surface casing (center), and clean-out bucket (right).

Figure 4.13 Auger extraction (left) and slurry replacement (right) during construction of Shaft B48-40.

Figure 4.14 Auger extraction (left), slurry replacement (center), and polymer strings during auger spin off (right) of Shaft P0-100.
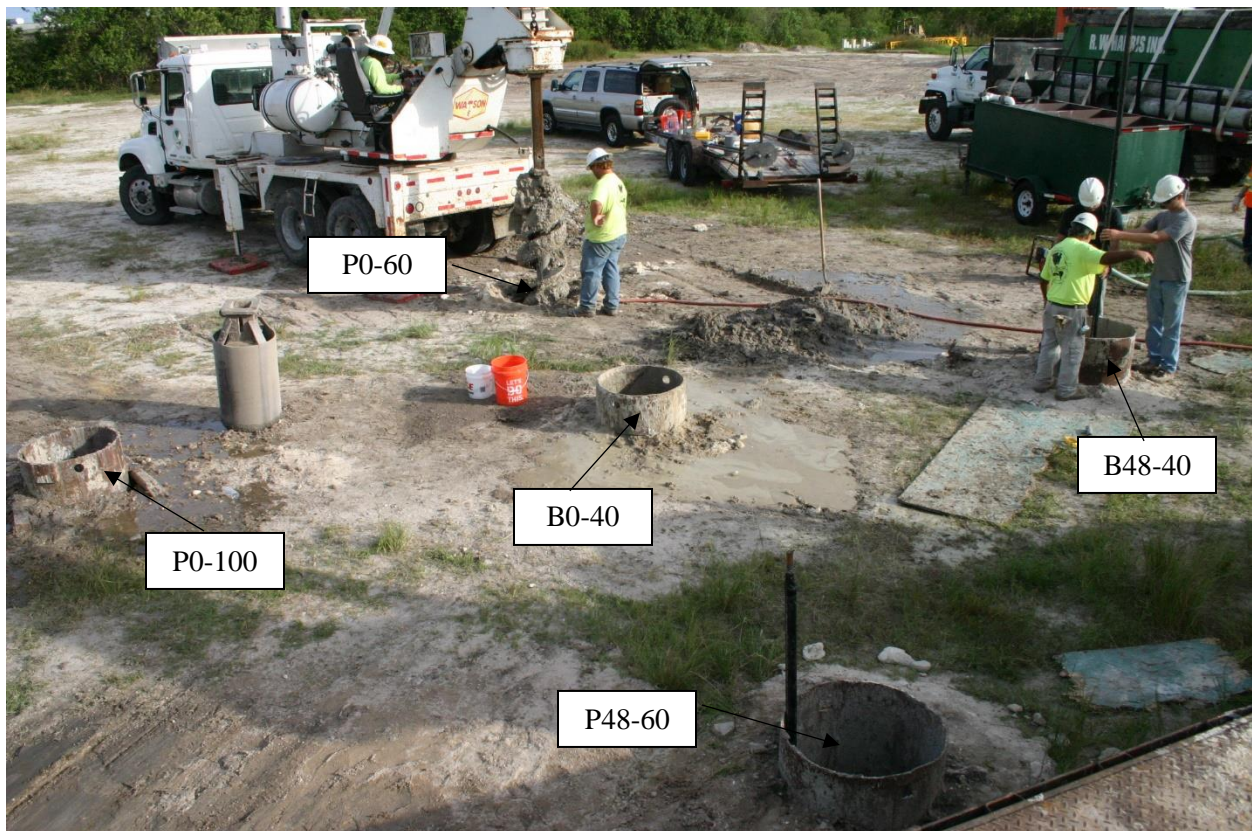
Figure 4.15 Shaft locations on final day of drilling.

148

Prior to pullout bar placement and concreting, the slurry was tested in each excavation was tested via automated downhole testing methods. Four of the five shaft results are presented in Figures 4.16 – 4.19.
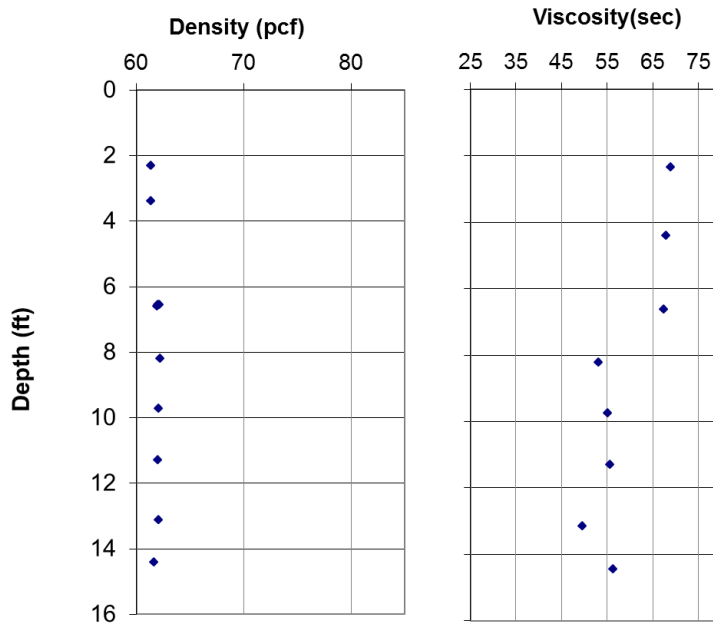
Figure 4.16 Slurry properties prior to concreting (Shaft P48-60).
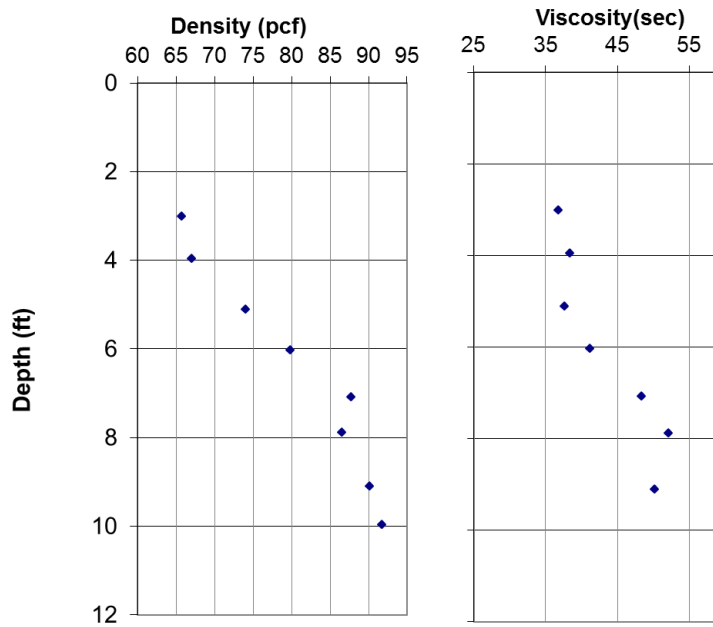
Figure 4.17 Slurry properties prior to concreting (Shaft B48-40).
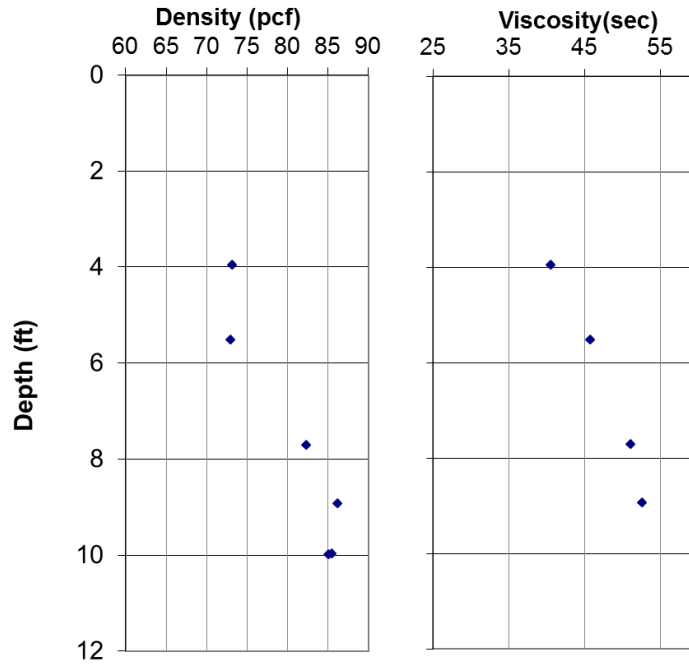
Figure 4.18 Slurry properties prior to concreting (Shaft B0-40).
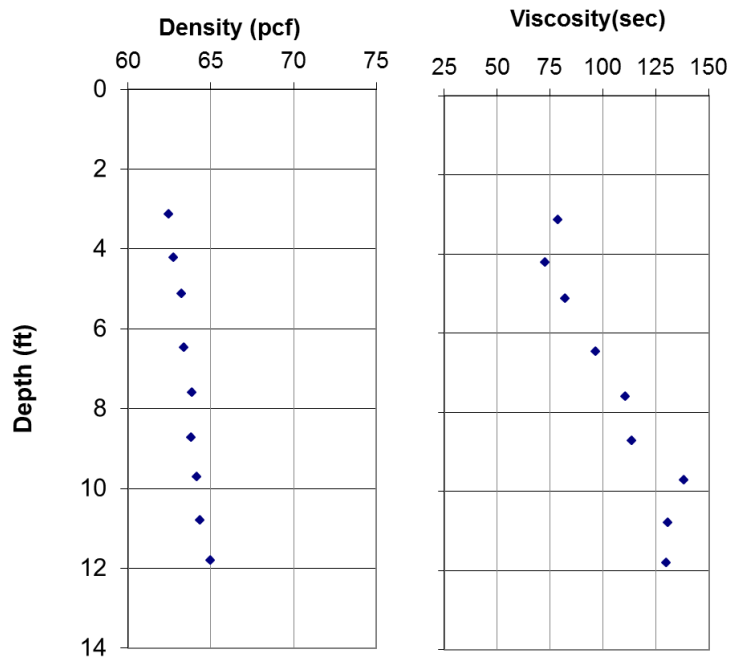
Figure 4.19 Slurry properties prior to concreting (Shaft P0-100).

The final steps in constructing the test shafts involved installing the anchor rod / plate assemblies, tremie placing the concrete with a small diameter (6in) rigid pump line, removal of the casing and cleaning / removal of the excess concrete at the shaft surface. Figures 4.20 – 4.23 show the steps in concreting the shafts.

Figure 4.20 Anchor rod installation.

Figure 4.21 Tremie placed aside suspended anchor bar (top left), slurry displacing during concreting (top right), concrete overflow (bottom left), and casing removal (bottom right).

Figure 4.22 Concreting of final shaft.

Figure 4.23 All shafts completed and site back-bladed clean (short casing not embedded).

4.3 Post Construction Testing

Evaluation of the constructed shafts included: thermal integrity testing, pull out static load tests, exhumation of the shafts and detailed as-built dimension measurements.

4.3.1 Thermal Integrity Profiling

Thermal integrity profiling commenced after the site was cleaned using a thermal probe and an automated reel system (Figure 4.24). Profiles were taken from each shaft on 3 hour intervals starting 4hrs after concreting until peak temperature was observed (16hrs). Raw data is shown in Figure 4.25; interpreted results are presented in the next chapter.

Figure 4.24 Thermal probe testing using automated reel system starting immediately after casting.
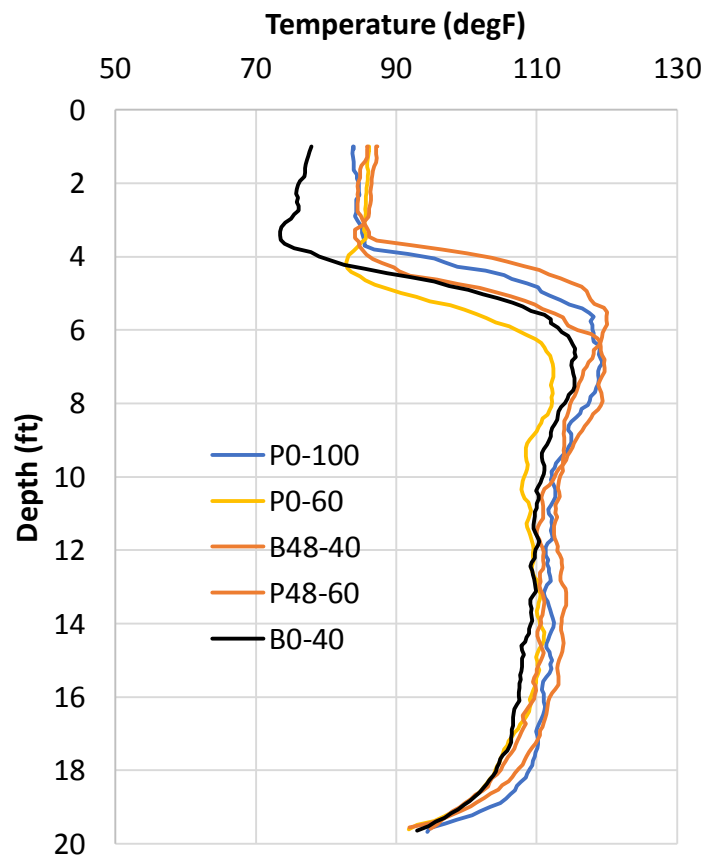
Figure 4.25 Raw thermal integrity profiles of all shafts 16hrs after casting.

4.3.2 Load Testing and Exhumation

Using a self-erecting load frame designed for static pull out testing and shaft extraction, each of the five shafts was tested using a quick test protocol in general accordance with ASTM D1143. The estimated capacity of 100kips was divided into 10 loading steps of 10kips each (i.e. 10k, 20k, 30k, etc.) and each load step was held for 2 minutes. This approach is valid for sandy soils, but is not recommended for clayey soils. The intent for any load test program is to hold a given load for enough time such that the rate of creep decreases to a stable level of or near 0.01in/hr. Shafts in clayey soils, for instance, will not reach a stable displacement rate in times less than an hour (or longer) for loads anywhere near full capacity. However, for the sandy silty soils at this test site, the 2 minute holds have been found to be sufficient. Figure 4.26 shows the erection process of the load frame.

The base of the four legs were confined by four ½ in prestressing strands around the perimeter. A hollow core 60 ton hydraulic jack and load cell were placed on the load frame cross beam above an open steel box which provided access to the anchor bar and a nut below the jack and load cell. This nut was maintained at the bottom of the opening in the box via high lift where a researcher would constantly track the upward anchor rod movement during testing and would spin the nut downward. This allowed all elastic distortion of the frame and soil reaction to be locked-in when the jack reached full stroke and required resetting. This also expedited extraction by optimizing the full 6in stroke of the jack after each reset. Figure 4.27 shows a test in progress where the load frame was founded on crane mats, a 30ft reference frame spanned between the load frame legs, the displacement transducer set up, and the final stages of the test where the 4in displacement transducer was near full stroke. All but one test was run to an upward displacement of approximately 4in.

The design of the load frame provides 14ft of clearance between the reaction beam and the ground surface. After the shaft was pulled to 4in uplift and full capacity had been demonstrated, the loading procedure transitioned to an extraction process. This is a relative fast procedure where the jack is extended (upward) to the fullest extent of the stroke and where the locking nut in the open steel box is secured in the lowest position. The jack direction is then reversed and retracted and the nuts on top of the load cell and jack chase the lowering jack piston to the lowest position. The jack is then activated to go upward again and the locking nut again is moved down simultaneously. This process is repeated until the load registered by the load cell is within the crane capacity for the given crane reach / location. In past studies, the process was repeated until the load cell-registered weight was at the minimum (self weight of the shaft $\approx 8000 - 11000$ lbs) and which could be lifted by a boom truck (20 ton). For this study, a larger capacity crane (70 ton) was used which reduced the extraction time by allowing higher loads when the load frame was removed. Figure 4.28 shows the stages in shaft extraction; Figure 4.29 shows the load vs time trace that was used in conjunction with the crane operator to decide when the load frame could be removed. Each of the vertical lines showing drop in load coincide with resetting the load frame by locking the bottom nut and moving the upper nut down to the retracted jack position. At 30 kips the crane could extract a shaft from any of the five positions.
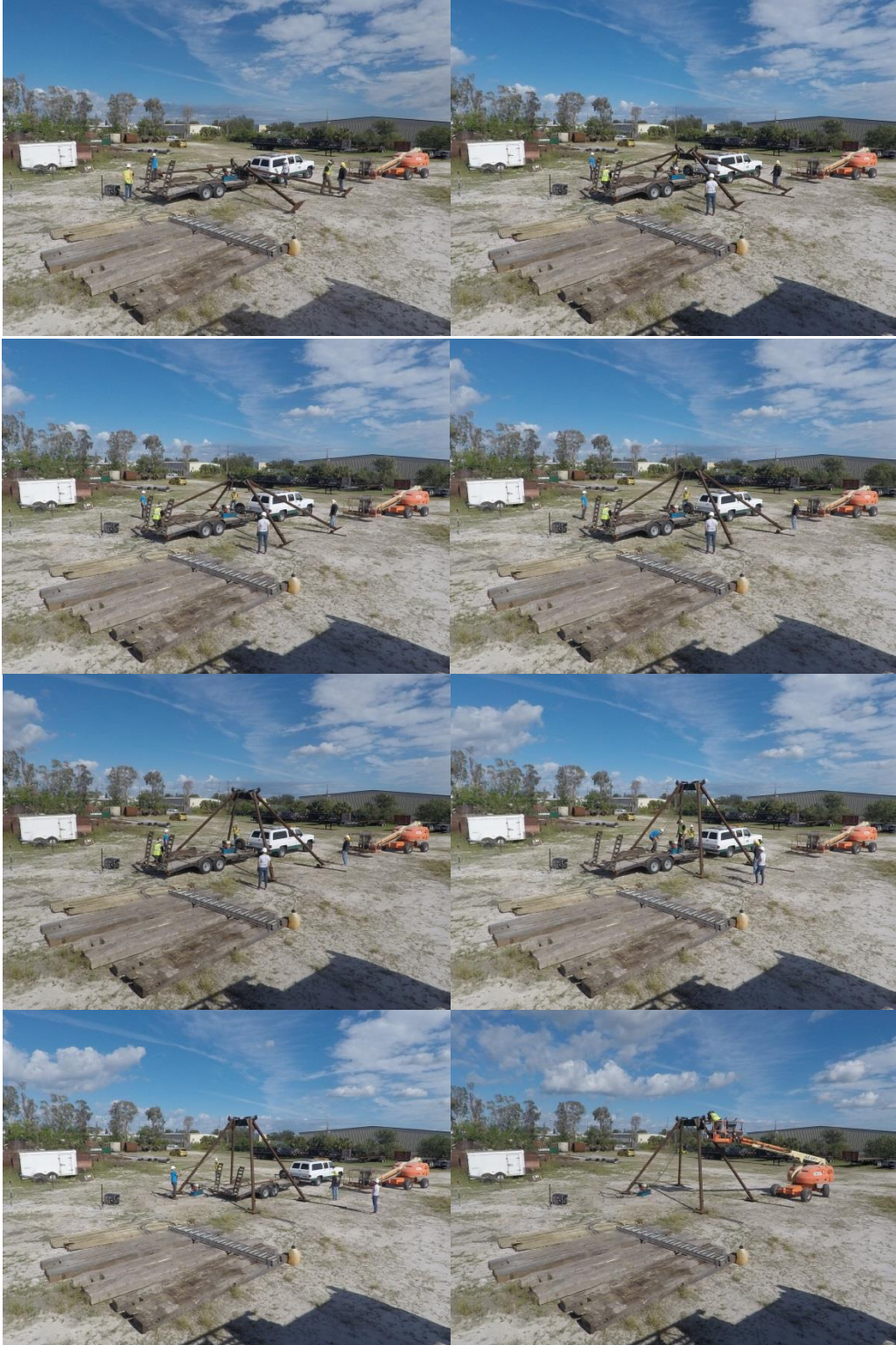
Figure 4.26 Self erecting load frame assembled on site.

Figure 4.27 Load testing in progress.

Figure 4.28 Shaft extraction.
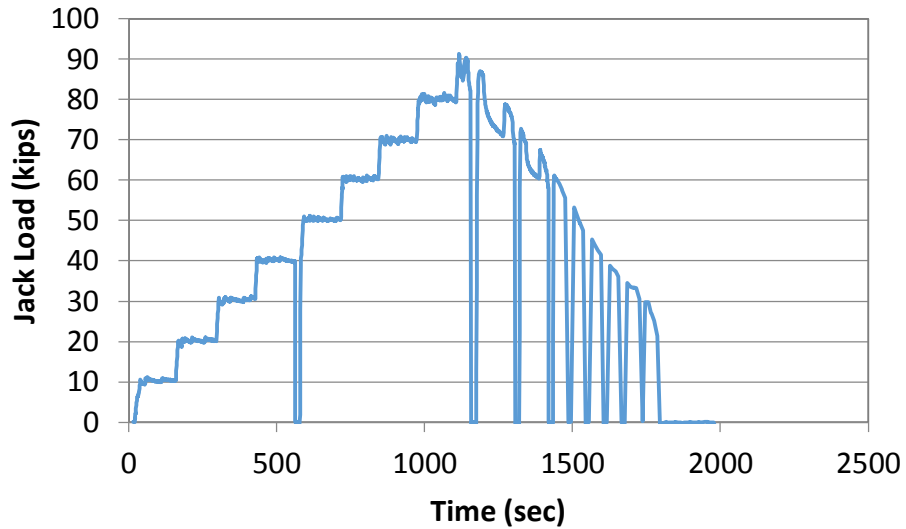
Figure 4.29 Load trace during testing and extraction procedures.

4.3.3 Dimension Measurements

Each shaft was set on wooden cribbing that allowed the sides of the shaft to be scraped down to the concrete surface and provided access for diameter measurements (Figure 4.30). Dimensioning involved cleaning off four locations on each side at 90 degree opposing positions and measuring the concrete diameter down the length of the shaft at 6in increments with a large specially designed caliper (Figure 4.31).

Figure 4.30 All five test shafts extracted and aligned for dimensional measurements.

159

Figure 4.31 Caliper used to take diameter measurements of each shaft.

The orthogonal diameter measurements (A and B locations) were then averaged to obtain the nominal shaft diameter as a function of depth (Figure 4.32). These values in turn were used to define the shaft length and surface area contributing to the side shear resistance. Table 4.4 show the shaft dimensions for all shafts.
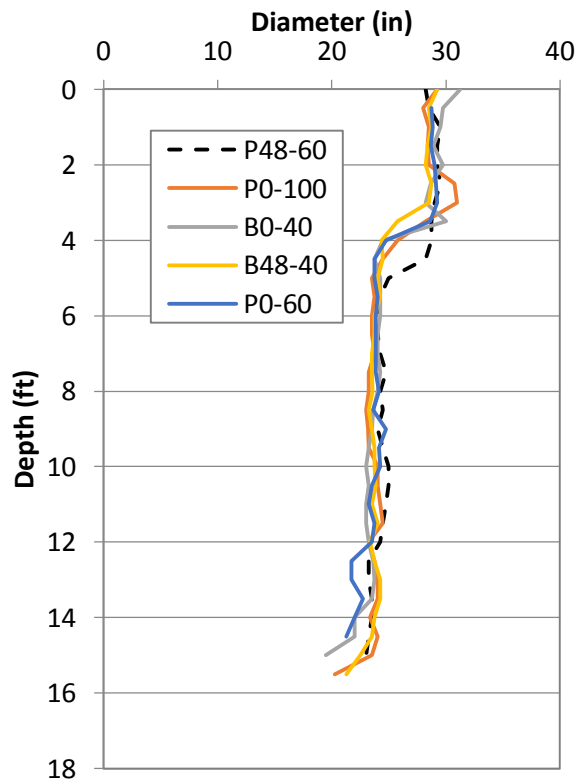
Figure 4.32 Average shaft dimensions from two orthogonal radial directions.

Table 4.4 Measured shaft dimensions.

Shaft ID	Length	Avg Diam	Surface Area	Conc Vol
	ft	in	ft^2	ft^3
P0-60	14	24.77	90.79	46.86
P48-60	15	25.67	100.80	53.91
B0-40	15.1	24.95	98.63	51.27
P0-100	15.5	24.85	100.85	52.79
B48-40	15.5	24.80	100.63	51.99

4.4 Results

As expected, the pull out capacity from each shaft position was affected by the local soil strength noted in Table 4.2. Coincidentally, both the bentonite shafts were located in the strongest soil profiles. In keeping with the lab scale approach (and that used in previous studies) the pull out capacity was normalized based on local soil strength. The trends were in line with the previous findings where shafts excavated with polymer slurry were slightly higher than bentonite-excavated shafts. Figure 4.33 shows the normalized pullout capacity of the five shafts.
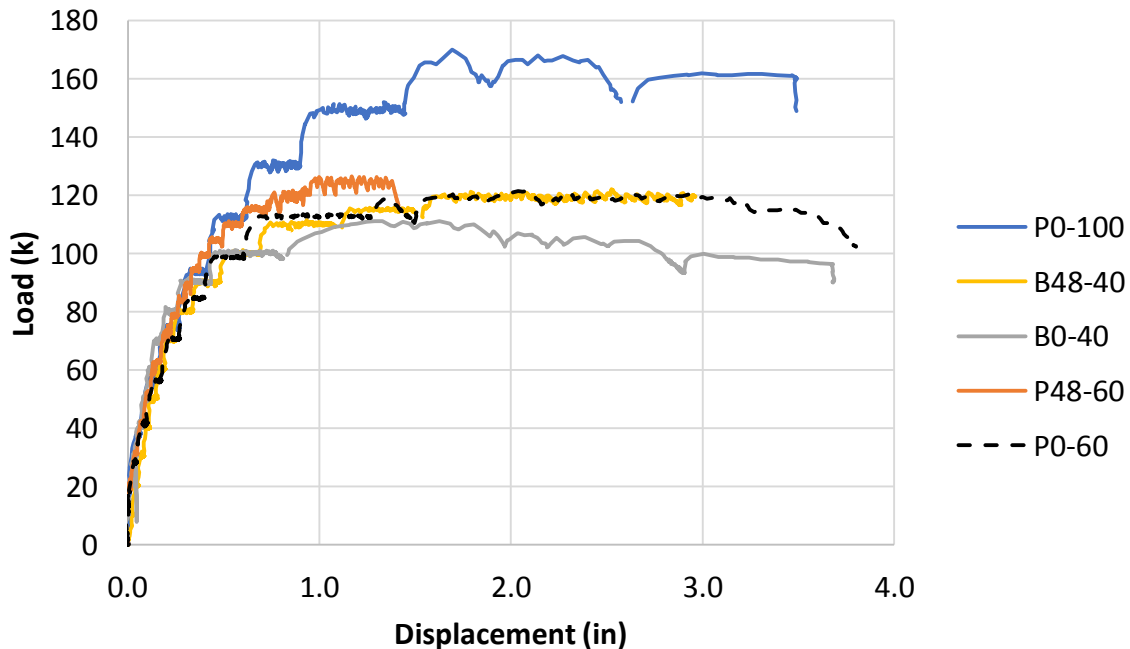
Figure 4.33 Pullout load normalized to the bentonite B0-40 shaft soil profile.

While the shaft dimensions shown in Figure 4.32 were similar among the various shafts, the subtle variations in shaft dimensions affected the resulting unit side shear (pullout force / surface area). Figure 4.34 shows the unit side shear response for the five test shafts.
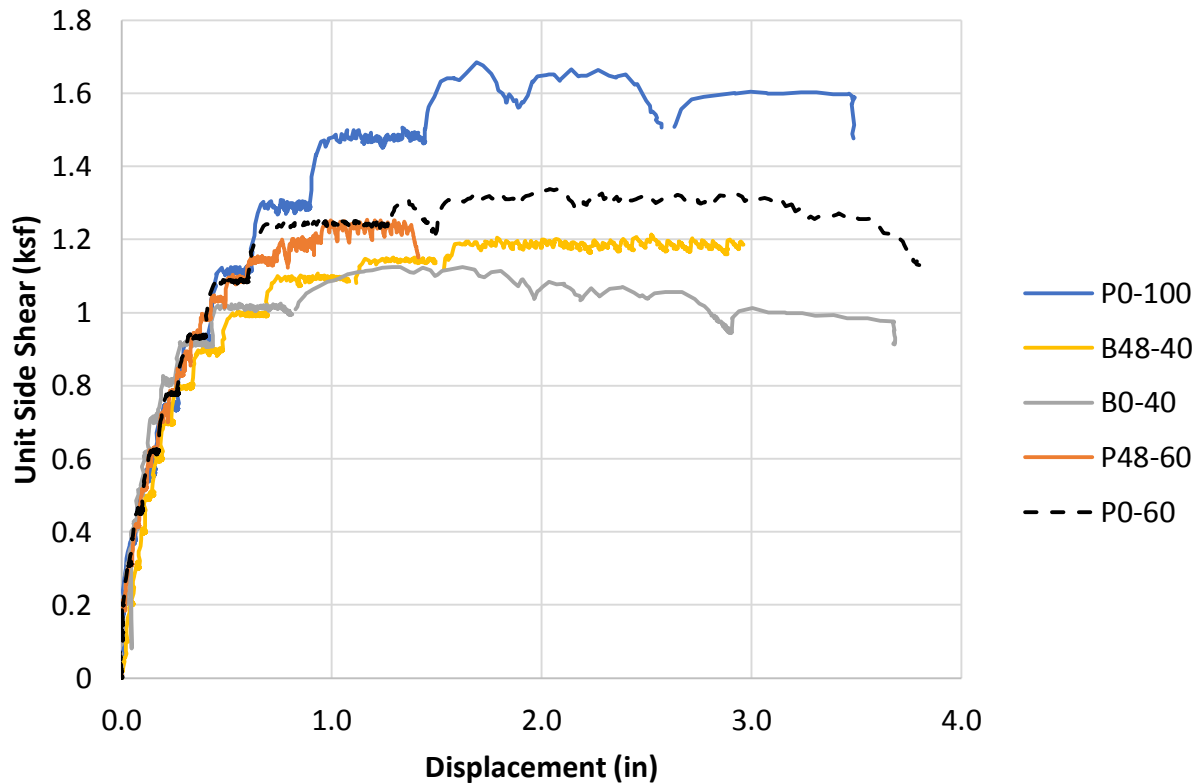
Figure 4.34 Unit side shear response for all test shafts.

Finally, when comparing the individual effects of slurry type and time of exposure, no appreciable variation was noted as a result of exposure time for polymer or mineral slurry (Figure 4.35). The shaft ID designations for 0hr are not really immediate with no exposure time. In reality, zero hour shafts were excavated starting at 3:00pm and concrete was completed by 6:00pm which was as close to 0hr as possible. Table 4.5 provides a timeline summary of the excavation and casting times as well as the average slurry viscosity over the exposure times.

Table 4.5 Exposure times and average viscosities.

Shaft ID	Average Viscosity (Sec/qt)	Commence Excavation	Concreting	Exposure Time (hr:min)
Shaft B48-40	43	2:55PM 10/16/17	5:59PM 10/18/17	48:04
Shaft P48-60	59	4:08PM 10/16/17	5:49PM 10/18/17	49:41
Shaft P0-60	62	5:05PM 10/18/17	5:37PM 10/18/17	0:32
Shaft P0-100+	109	2:56PM 10/18/17	5:44PM 10/18/17	1:48
Shaft B0-40	47	4:06PM 10/18/17	5:54PM 10/18/17	1:48

On the second day of drilling (0hr shafts), the B0-40 was excavated first using the premixed bentonite slurry. The remaining polymer slurry in the 1000 gal tank was used to refill P0-60 and then was bolstered to make the 100+ sec/qt polymer slurry. Immediately after shaft P0-100+ was excavated, fresh polymer slurry was prepared for the last shaft P0-60. This slurry was placed at a viscosity of 62sec/qt. Pullout bars were installed for the other four shafts during that time and concrete slump tests were performed during the cleanout period for the P0-60 shaft. As a result, the actual B0-40 exposure time was closer to 2 hours. In keeping with the small scale findings, the polymer excavated shaft performed better than the bentonite shafts (16%; l.25ksf vs 1.08ksf at 1in displacement, respectively). No change was noted in capacity as a result of prolonged exposures for either slurry type (i.e. from 2 to 48hrs).
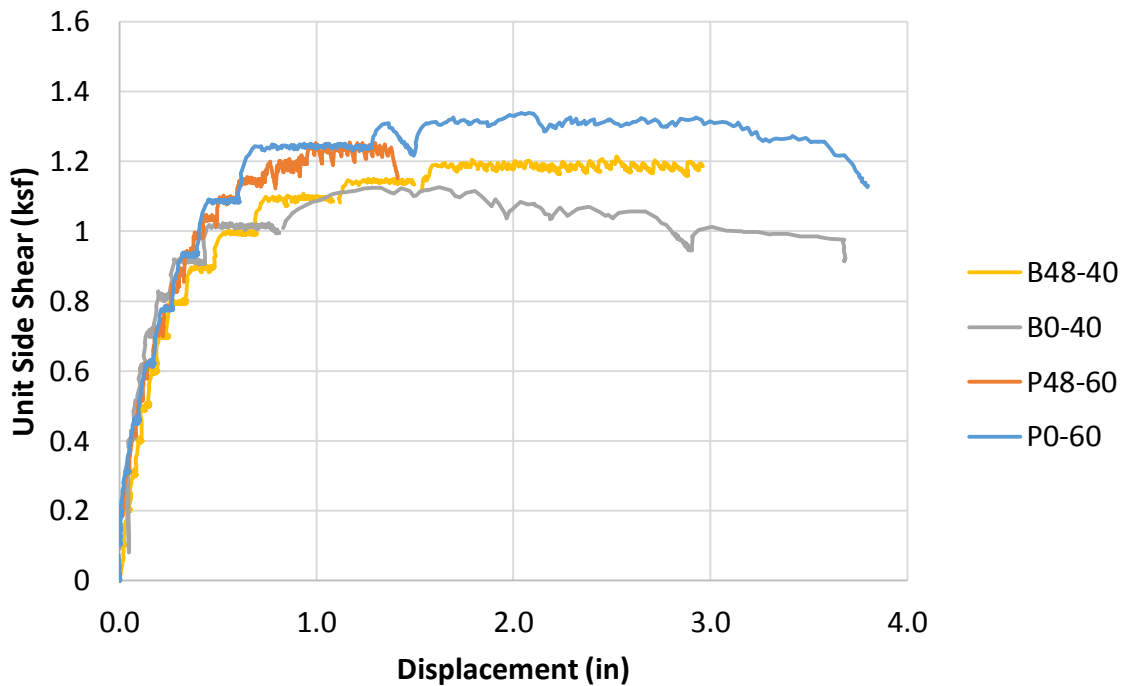
Figure 4.35 Effect of slurry exposure time on capacity.

4.5 Chapter Summary

As a means to verify the effects of slurry type and open-hole exposure time on shaft side shear resistance, full size shafts (although on small end of the shaft size range) were cast and exposed to both polymer and bentonite slurry for up to 48-49hrs. Similar shafts were also cast where the exposure was less than 2hrs. All shafts were load tested, exhumed, and measured. While the $1/10^{th}$ scale shaft testing program (Chapter 3) showed up 55% reduction in side shear for bentonite tested shafts, the larger shafts showed virtually no effects as a result of prolonged exposure. However, when compared to the shafts cast with polymer slurry, the bentonite shafts exhibited a 16% reduction in capacity.

The two testing programs varied in the aggressiveness of the concreting process where the small scale shaft concreting process imposed very little upward flow that could potentially scour the side walls from the low pressure head within the tremie. Further, the mortar used did not contain coarse aggregate which can aid is scour. In essence, the small scale concrete flow was largely radial escaping the 3in ID 3.5in OD tremie and pushing against the side walls 4.6in diameter excavation walls. However, upward flow outside a reinforcing cage whereby scouring can occur has been shown not to occur in reality, so the small scale tests may be more representative of the low energy conditions that occur outside a reinforcing cage under normal full scale field conditions. The larger diameter field tested shafts were cast with an aggressive upward concrete pumping flow up and around the central pullout/anchor bar. The more modest reduction in side shear 16% vs 55% is likely to be a by-product of this scour. As a result, the performance of the bentonite shafts may be optimistically high.

For the purpose of this study, the field results do confirm that no adverse effects result from prolonged exposure with polymer slurry, and just as important, the uniformity in shape of shafts cast with polymer slurry verified excavation stability.

Chapter Five: Conclusions and Recommendations

The primary objective of this project was to identify the effects, if any, of prolonged polymer slurry exposure on the concrete / soil interface around the perimeter of drilled shafts. Where bentonite slurry has been long understood to cause a poor interface stemming from a clay filter cake, polymer slurry is not known to develop any such detrimental interface. For bentonite slurry filter cakes that develop over an extended period (e.g. 24-36hrs), a common remedy is to scrape the sidewalls of an excavation thereby reaming the hole to a slightly larger diameter and removing the unwanted clay build-up. However, such a practice with polymer slurry supported excavations degrades the borehole stability and the excavation may collapse.

This study performed both small-scale and full-scale load testing of shafts cast with both mineral and polymer slurry where the exposure times were varied from 0 to 96 hours. In all, thirty seven shafts were cast, load tested, exhumed and physically measured to assess the comparative effects of slurry type and open-hole exposure time.

5.1   Small Scale Field Testing

Thirty-two small scale drilled shafts $(1/10^{th}$ scale) were constructed using four different commercial drilling slurry products used in practice (one bentonite and three polymers). Pull-out tests were performed for quantifying the effects the products might have on the side shear resistance. The shafts were, nominally, 4in diameter and 7ft to 8ft deep. The exposure time for each product ranged from 0h to 96h. All shafts were cast in sandy / silty sand soils.

Comparison of side by side load testing is always complex as no two shafts or piles can be constructed identically either due to variations in soil strata, shaft dimensions, or construction induced effects. The results from all test shafts were analyzed in different ways to address the above variables and showed a decrease in capacity with time in bentonite constructed shafts that was most pronounced within the first 8 hrs. Thereafter, only modest reductions were noted.

Polymer shafts showed no trends positive or negative with regards to capacity vs exposure time. However, when compared to bentonite shafts for the same exposure time, the average of all polymer products showed up to twice the bentonite capacity with an average increase of 26% over all times (Figure 5.1). The stiffness of all shafts showed similar trends (or lack thereof); stiffness was determined as the change in load within the first 0.1in of uplift (Figure 5.2).
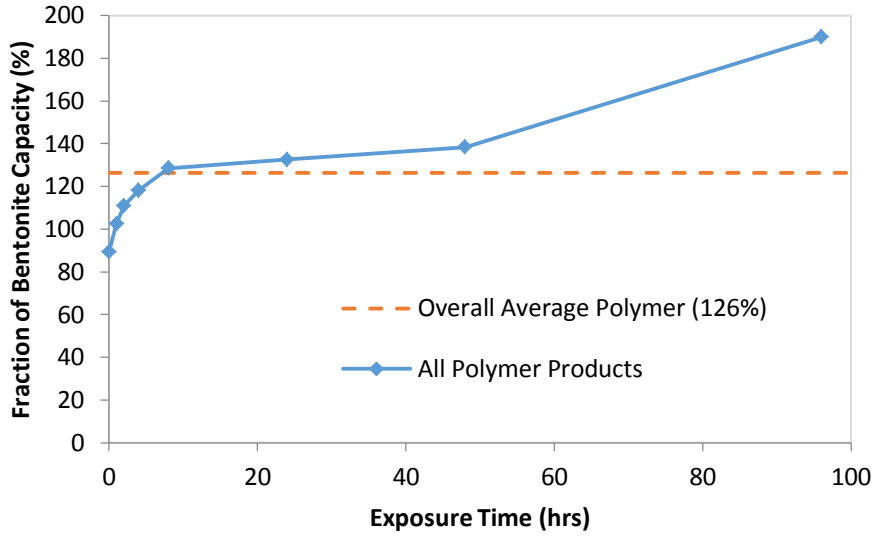
Figure 5.1 Polymer capacity relative to bentonite.
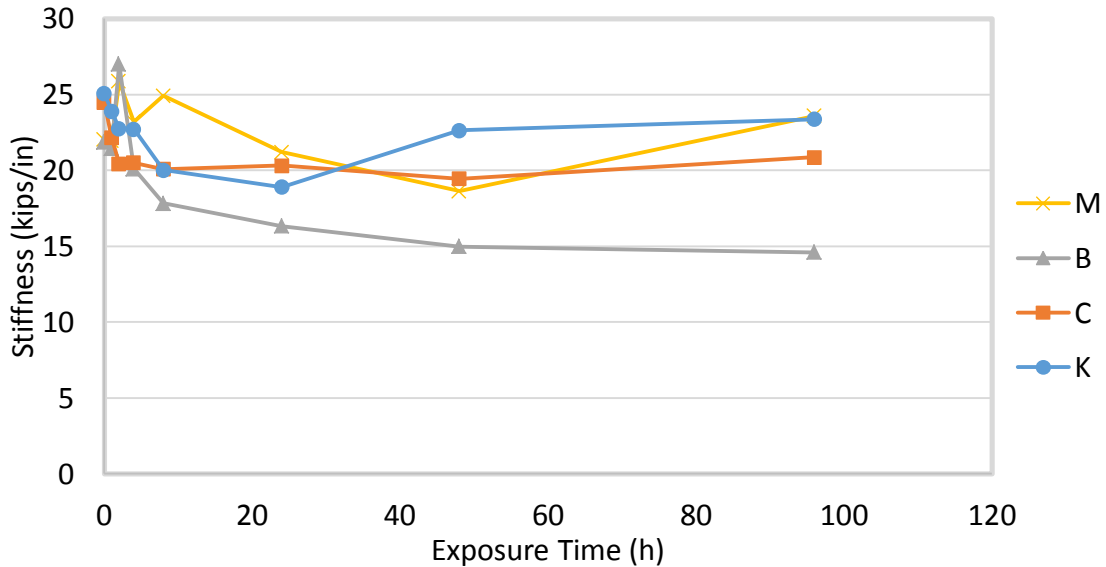
Figure 5.2 Change in stiffness as a function of slurry exposure time.

Considering only the bentonite shafts, Figure 5.3 and Table 5.1 show the comparative values for two methods of analyzing the data. Recall, length corrected assumes soils were uniform and only subtle changes in length account for unseen variations in the pullout capacity. CPT corrected accounts for both length differences and subtle variations in soil strength. The Principal Investigator considers the CPT corrected approach to be most valid, but both are shown for completeness. Additionally, using only the CPT corrected data set, the fraction of the 36hr capacity is shown on the second axis (Figure 5.3). This suggests a worst case 10% reduction

166

might be expected at 96hrs for open bentonite excavations that exceed the FDOT 36hr specification/limit.
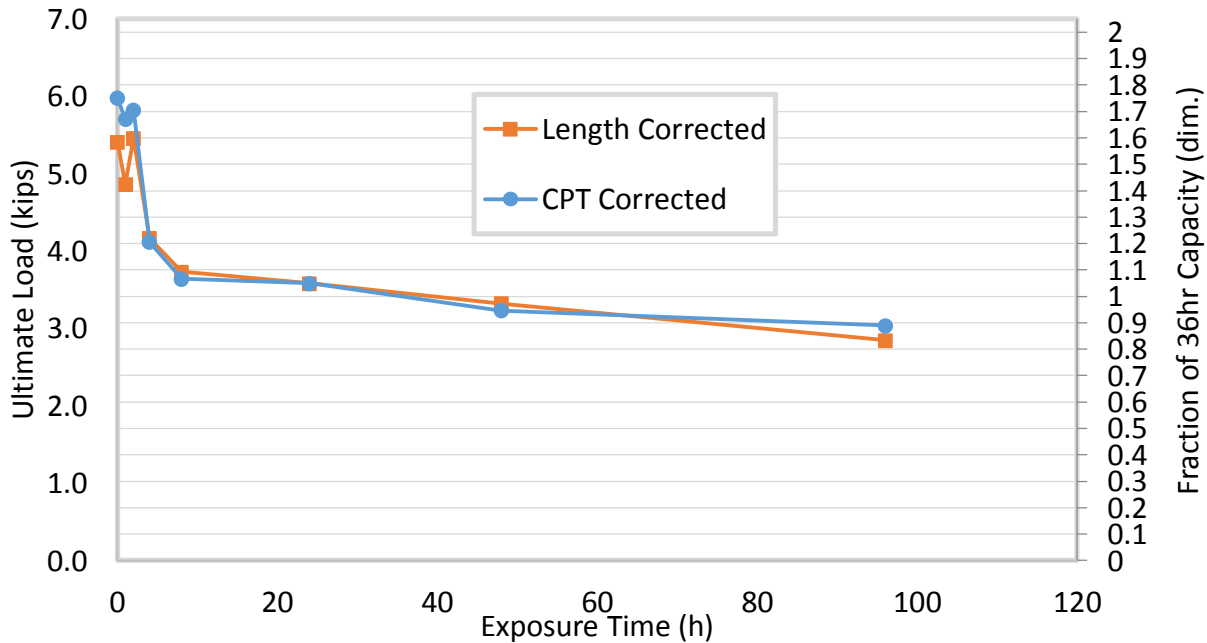
Figure 5.3 Bentonite shaft capacity comparisons.

Table 5.1 Bentonite shaft capacity values.

Shaft ID	Exposure[1] (hrs)	Stiffness (kips/in)	Ultimate Load	
			Length Corrected (kips)	CPT Corrected (kips)
B-0	0	21.85	5.41	5.98
B-1	1	21.43	4.86	5.71
B-2	2	26.99	5.46	5.82
B-4	4	20.10	4.17	4.12
B-8	8	17.82	3.73	3.64
B-24	24	16.32	3.58	3.58
B-48	48	14.97	3.32	3.23
B-96	96	14.59	2.85	3.04

[1]Time to beginning of concrete placement.

A side line study performed at the time of the small scale study involved tracking the fluid flow rate into the surrounding soil. The expectation was that bentonite slurry above the minimum 30 sec/qt viscosity would quickly slow to virtually zero flow and that polymer slurry would continue to flow but perhaps at progressively slower rates. Figure 5.4 shows the cumulative amount of volume added to several of the excavations performed and maintained for extended periods. Immediately apparent is the relationship between polymer viscosity and the amount of slurry required. While product brand was not a contributing factor (low viscosity = high flow rate and vice versa), C, M and K refer to Cetco, Matrix and KB International, respectively, and are noted for completeness. Similar to a previous study that defined the minimum viscosity for bentonite, this data can be used to show when polymer slurry becomes unstable in its ability to

167

maintain the borehole. Therein, inflow rate is also a measure of the outflow that can occur when the tool passes by the sidewalls and sets up a subtle reduction in outward pressure.
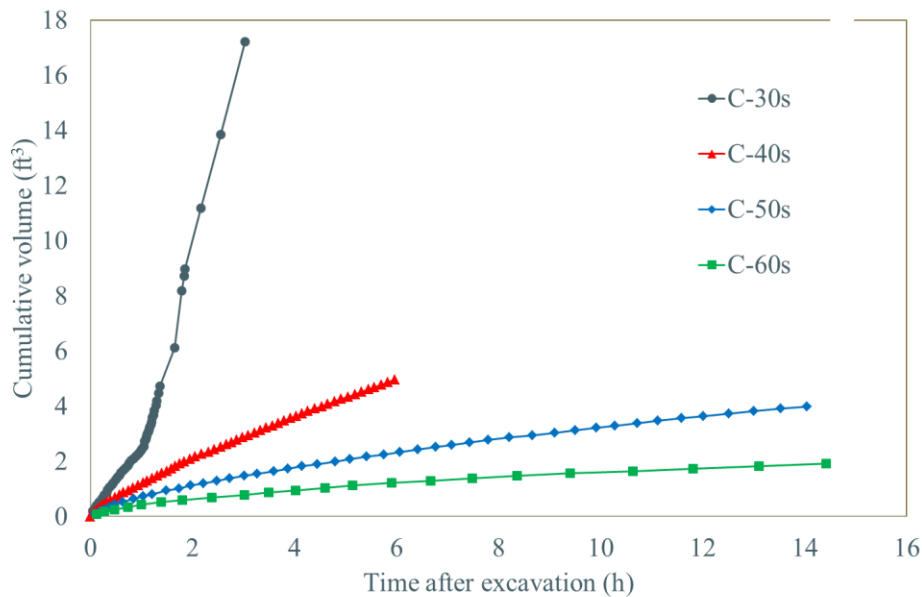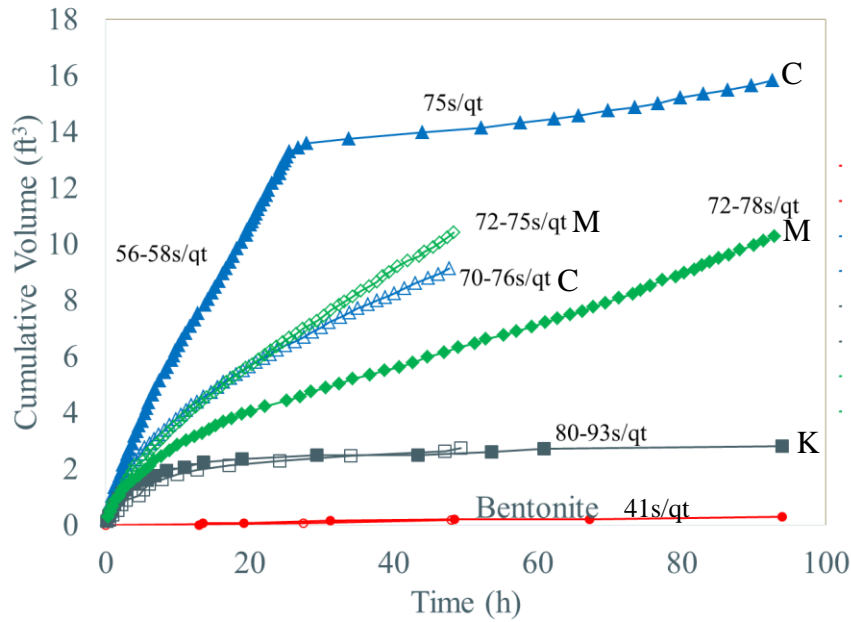
Figure 5.4 Cumulative flow as a function of time.

Figure 5.5 shows that as the viscosity approaches that of water (26sec/qt) the flow rate drastically increased. The magnitude of flow rates shown is based on an approximate shaft side wall area of 8.5 ft^2 from the small scale field tests for all polymer products tested; this can be directly extrapolated to the surface area of a production size shaft as the net hydrostatic pressure differential will be similar (4ft of head). Therefore, a 50ft long, 4ft diameter shaft cast in similar sandy soils could be expected to use around 80 cuft/hr (600 gal/hr) at a viscosity of 40sec/qt. Most manufacturers recommend in the range of 50 to 60 sec/qt for these soils which corresponds

to 20 cuft/hr, but personal observations in field by the PI have found this range is often not achieved.
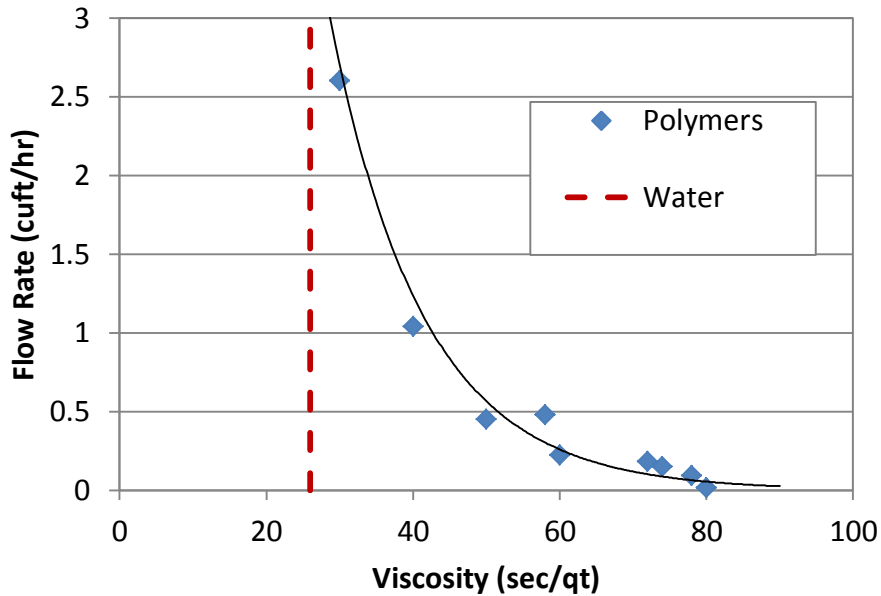
Figure 5.5 Polymer slurry flow rate as a function of Marsh funnel viscosity.

5.2 Large Scale Field Study

Five full size shafts (2ft diameter) were constructed using all traditionally used shaft construction equipment. Two were cast 48hr prior to the other three so that all concreting could be performed at one time and the effects of open excavation (slurry supported) could be assessed. The only variation from normal construction was no reinforcing cage was used; rather only a single centered anchor bar was cast into the shafts to provide for pullout testing. Similarly unusual when considering common construction practices, the anchor bar was sleeved with a standard 1.5in steel integrity access tubes such that the high strength threaded anchor bar could be removed for thermal integrity assessment. A brief summary of the load test results and thermal evaluation is presented.

Load test pullout forces were adjusted based on the local CPT soil strength profiles (as with small scale tests) and the exact surface area was determined from the extracted full size shafts. Unlike the small scale tests, no change was noted in the polymer or mineral slurry constructed shafts over a 2 to 48hr exposure timeframe in the full scale tests. Table 5.2 shows the ultimate and mobilized capacity (at 1in displacement) for each of the five shafts. The percent increase relative to bentonite is also presented. Some increase in capacity was noted for the shaft constructed with the higher viscosity polymer slurry.

Table 5.2 Full scale pullout test results.

Shaft ID	Exposure[1] (hrs)	Average Viscosity (sec/qt)	Unit Pullout Resistance		Relative Performance (% increase)
			Ultimate Side Shear (ksf)	Mobilized Side Shear @ 1in (ksf)	
B48-40	48	43	1.19	1.09	
P48-60	49	59	1.24	1.24	14.8
P0-60	0.5	62	1.33	1.24	14.8
P0-100+	2	109	1.68	1.47	36.1
B0-40	2	47	1.15	1.08	datum

[1]Time to beginning of concrete placement.

Thermal evaluation of the test shafts was performed using the Tsoil algorithm developed in a recent study (Mullins and Johnson, 2017). This method is best suited for center bar data of relatively small ACIP piles and in this case shafts. Figure 5.6 shows the measured and predicted shape of the five test shafts. The depth axis includes the tube stickup height which was 3.5-4.5ft.
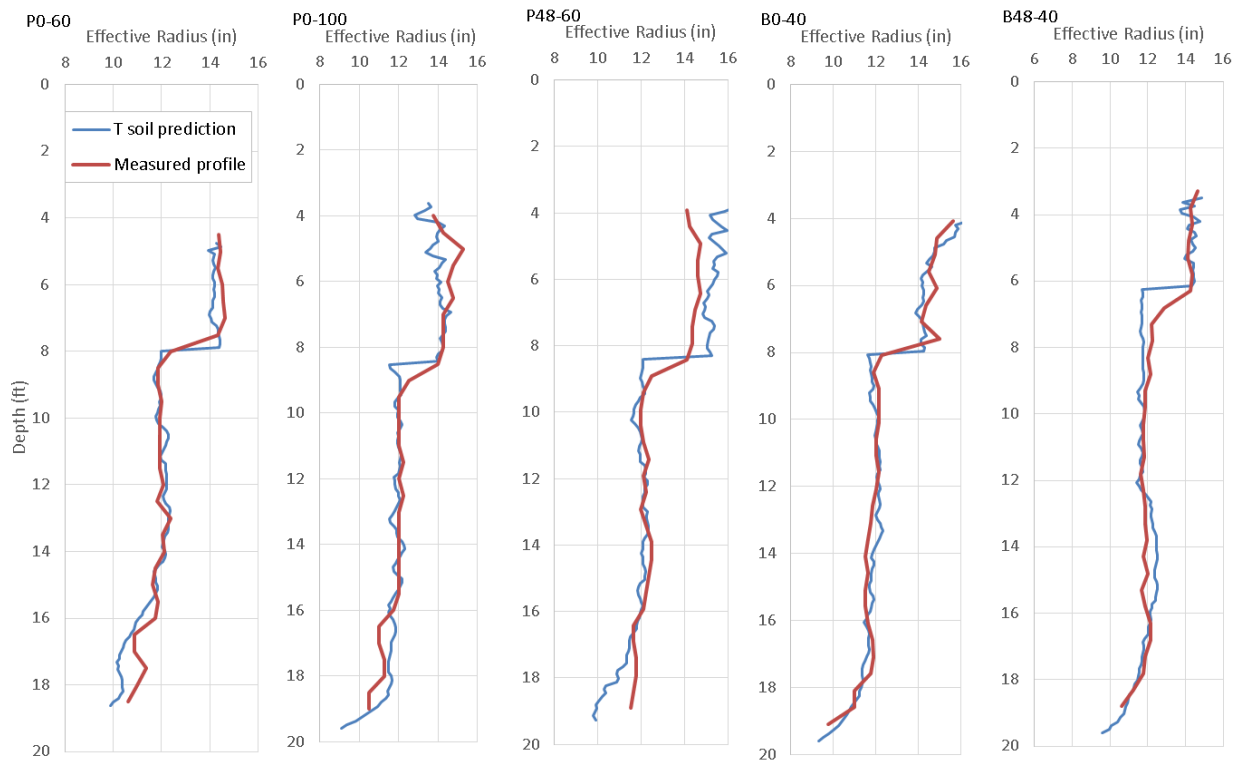

Figure 5.6 Measured vs predicted radius from thermal integrity evaluations.

5.3   Discussion

While decreasing trends in bentonite cast shaft capacity was evident, in the polymer shafts, no reduction from exposure was observed. Overall, polymer shafts performed up to 90% better than

bentonite shafts with prolonged exposure times of 96hrs. At more practical or specified time limits (i.e. 8 to 36hrs), the improvement ranged from 28 to 36%, respectively.

Differences in the small scale and full scale testing were noted to be a by-product of no scour vs scour, respectively. However, scale effects of the mortar aggregate size relative to the slurry cake thickness when compared to the aggregate of the concrete can also play a role.

5.3.1 Concrete Flow Effects

Radial flow through a conventional reinforcing cage with minimum longitudinal steel (1%) and appropriate tie / shear steel restricts upward flow of concrete in the cover region of the shaft. Past studies have clearly documented this effect and is the topic of on-going research worldwide to improve tremie placed concrete flow. As a result, scour does not occur with full reinforcing cages. The small scale tremie placement did not promote upward flow which more closely resembled radial through-cage concreting. Figure 5.13 shows the effects of concrete flow on the deposition of a bentonite clay layer that is not produced by infiltration (filter cake formation). In that study, each shaft was tremie placed in bentonite slurry with steel forms (no infiltration possible). The progression begins as concrete builds up head pressure within the cage and presses out radially until making contact with the excavation walls. Concrete squeezing through the cage pushes the bentonite slurry against the side walls and traps slurry that cannot be expelled. In the presence of sandy excavation walls the already present filter cake is then supplemented by the trapped slurry products.

This phenomenon also might explain the data in Figure 2.18 presented by Brown (2002) where side shear reductions were noted almost immediately with bentonite constructed shafts (relative to polymer constructed shafts) in low permeability/filter cake forming soil and only 1hr of exposure.

To this end, where the full scale testing (with no appreciable radial flow regime) showed polymer shafts were 14% higher in side shear at 48hrs of exposure, the small scale study (with no upward scour) showed 38% higher. Recall Brown (2002) showed a 29 to 99% increase in capacity from bentonite to polymer for dry and liquid polymers, respectively. Hence, the effect of entrapment and radial concrete flow may have even more effect on the resulting side shear with bentonite constructed shafts than demonstrated by this study.

Figure 5.7 Mechanisms in tremie placed concrete flow that promote slurry caking.

5.3.2 Slurry Infiltration Rates

The flow rate of slurry into the surrounding soil walls is a function of soil type, slurry type and slurry viscosity. This is reflected by manufacturer recommendations, but in general, lower permeability soils permit the use of lower slurry product concentrations (lower viscosity) than high permeability soils (Table 5.3). Where Figure 5.5 showed slurry usage/loss monitored during the Chapter 3 for polymer slurry in the sand / silty sand, the same trend is shown in Figure 5.8 for bentonite slurry (Mullins et al. 2005); a 30 sec/qt cutoff viscosity for bentonite was established on the basis of those findings.

Table 5.3 Manufacturer recommended polymer slurry viscosities.

Brands Tested	Viscosity (sec/qt)		
	sand	silt	clay
CETCO	60-75	45-55	35-50
KBI	75-100	65-100	60-75
MATRIX	60-70	40-55	40-45
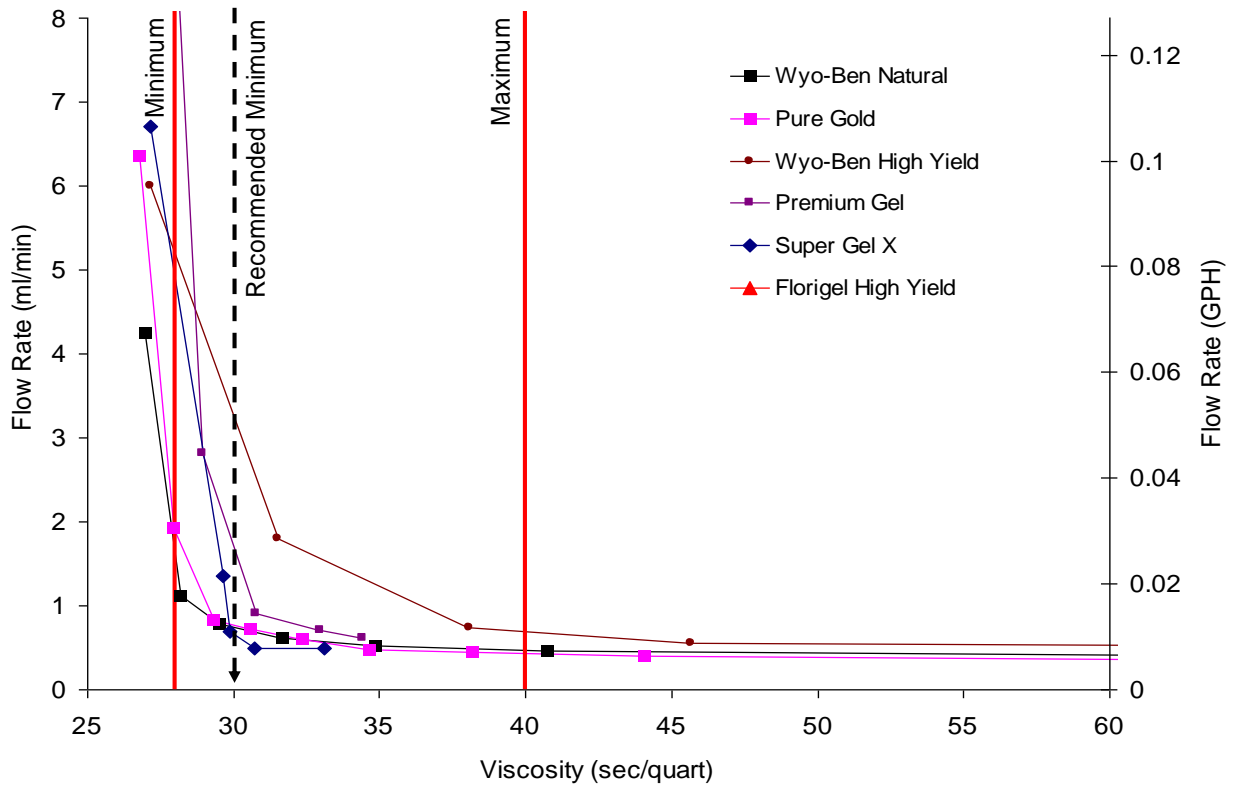
Figure 5.8 Effect of viscosity on flow rate for selected mineral slurry products.

Slurry testing performed at three sites in a concurrent study showed the effect of polymer slurry viscosity and mixing protocols on excavation stability. It also showed the importance of test spacing intervals with the length of the excavation.

At Site 1, slurry viscosity was 38 sec/qt which is below the recommended level. Viscosity vs depth profiles showed the slurry to be uniform (Figure 5.9). No noticeable accumulation was found at the bottom of the excavation when tested 15min after the design depth was encountered; hence, the bottom of excavation was located at the correct excavation depth. However, the automated downhole slurry testing unit showed significant amounts of debris on the top of the device upon extraction (approximately 10 minutes later).

At Site 2, viscosity was less at 32 sec/qt and uniform excepting the upper portion in the casing where a water truck was trickling in replacement fluid (water). Slightly higher viscosity was found near the bottom (Figure 5.10) and where approximately 1ft of sediment was found.

At Site 3, two shafts were excavated on subsequent days. On day 1, polymer slurry was mixed in the casing (in-hole) until slurry viscosity was approximately 50sec/qt. While excavating, water was added along with occasional scoops of dry powder polymer. Upon reaching the target depth slurry testing followed immediately while the cage was readied for installation. Before the downhole device could get to the bottom (6 minutes of testing), 3ft of sediment had accumulated (Figure 5.11). Average viscosity was between 27 and 30sec/qt for most of the shaft length increasing to 50sec/qt at the bottom where the inspector tested the slurry. The excavation was cleaned out, cage placed, and concreted. Slurry was captured and reused the second day. Despite a slight increase in viscosity to 33-34sec/qt, stability of the second excavation was even poorer where the accumulation at the bottom of the excavation was 6ft above the excavation depth indicating significant sidewall collapse. However, again the slurry was inspected at the bottom (54sec/qt) and accepted.

The viscosity results from all three sites were superimposed onto Figure 5.5 and replotted (Figure 5.12) to show the relative position of the three site values to the instability asymptote defined as the viscosity approaches that of water (26sec/qt). Technically, all sites did not comply with manufacturer recommendations with regards to viscosity and for Site 3, the poorly mixed slurry coupled with cleaner sandy soils failed to maintain the excavation stability.
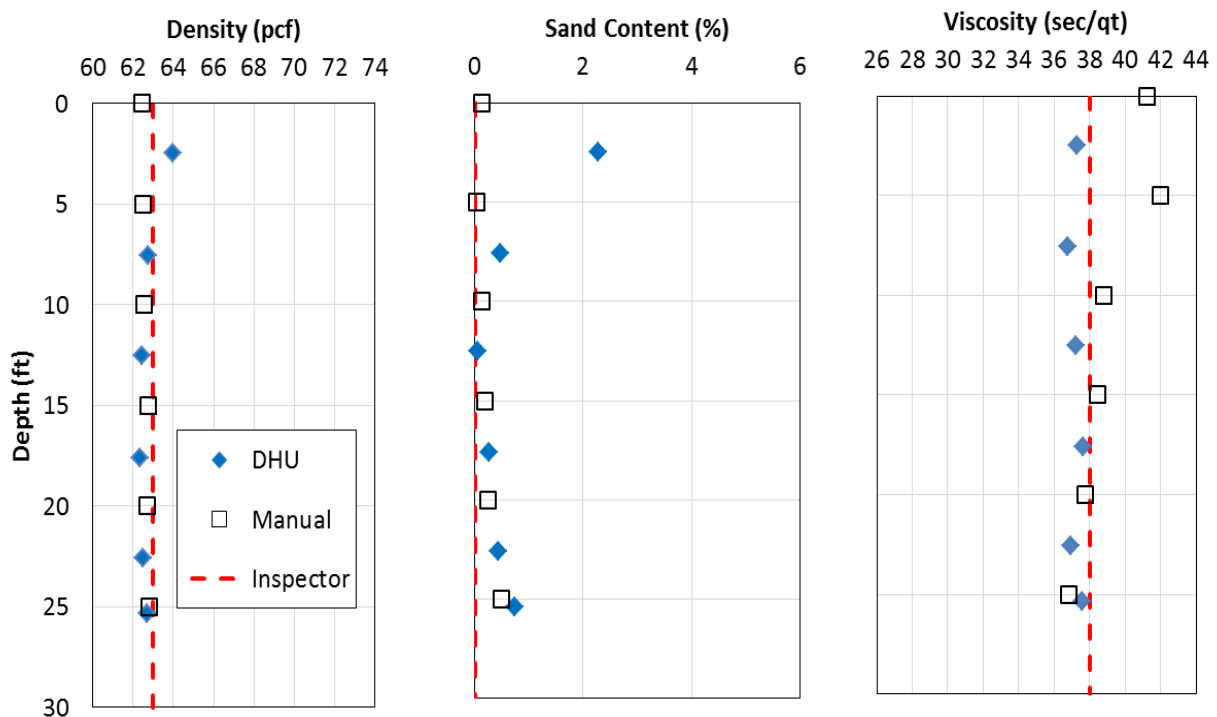

Figure 5.9 Site 1 slurry testing results.
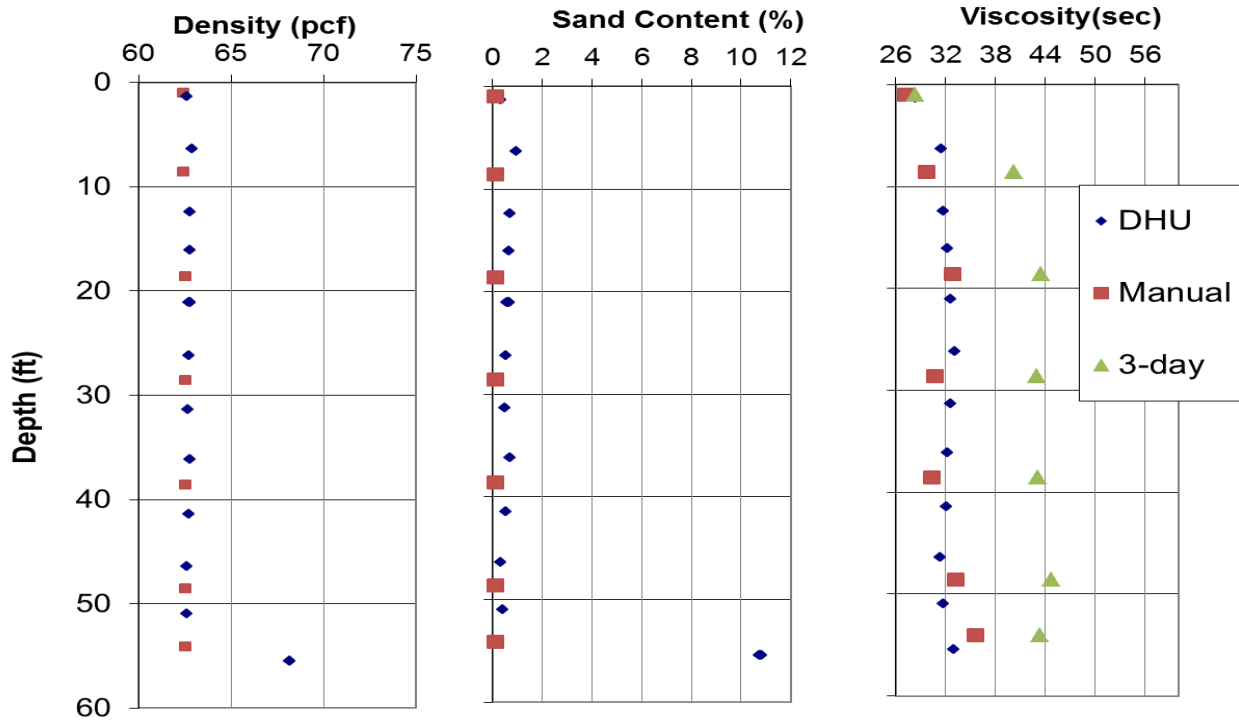
Figure 5.10 Site 2 slurry testing results.
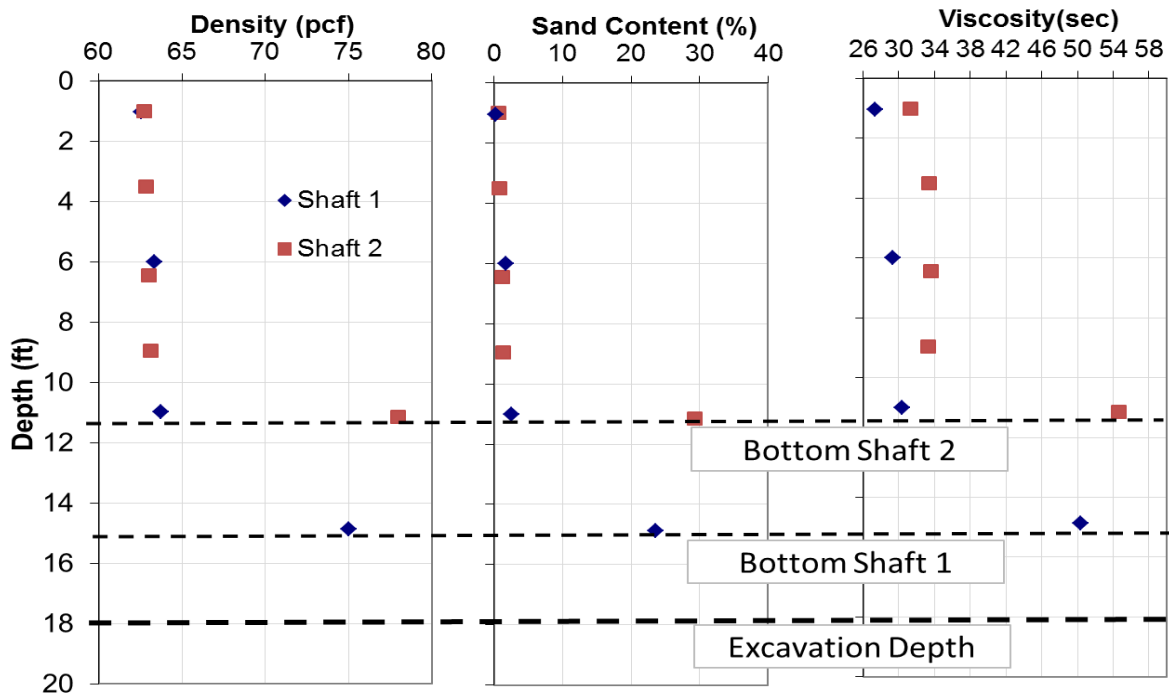
Figure 5.11 Site 3 slurry testing results.
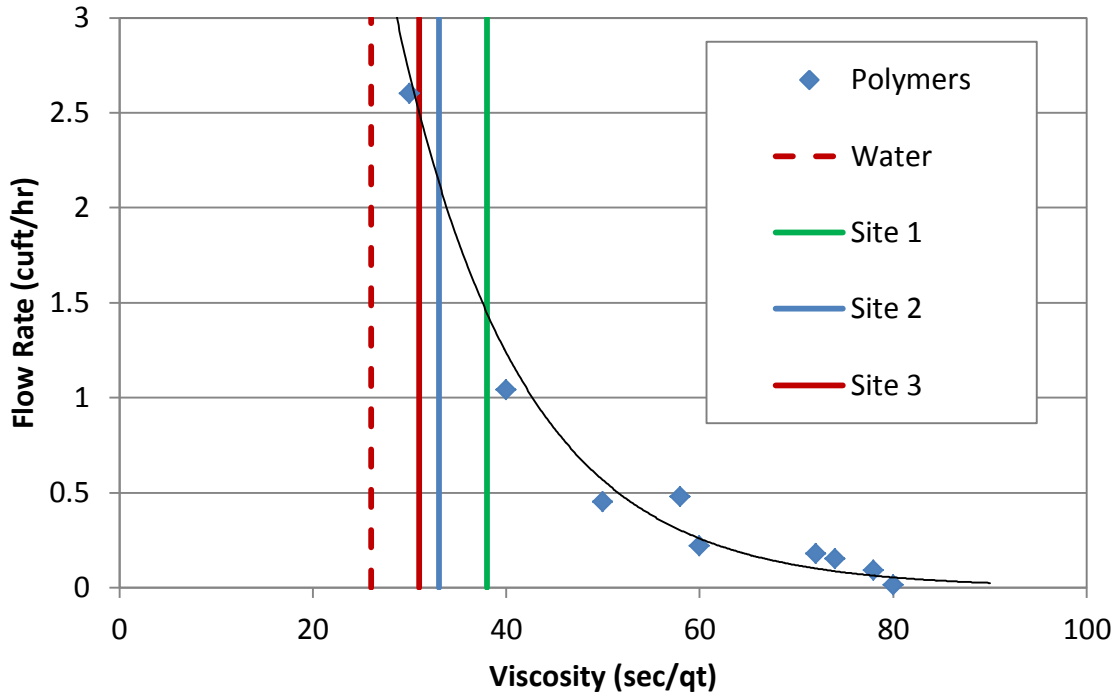
Figure 5.12 Site 1, 2 and 3 viscosities plotted on flow rate vs. viscosity curve.

5.4   Recommendations

The present Section 455-15.11.5 specification restricts open excavation times to 36hrs and the last 5ft of the excavation can only be open for 12hrs. A suggested change to the present specifications might remove limitations to open excavations times for polymer slurry supported excavations as no degradation in side shear with time was observed. Reaming should not be considered for polymer shafts. Further, use of sequential over sizing (larger and larger augers) with polymer slurry support as a means of using smaller equipment to excavate larger diameter holes should not be an acceptable excavation method as this produces the same degradation of the sidewall stability as reaming.

Open excavation times for bentonite showed a 10% ultimate reduction in side shear beyond the capacity associated with 36hr limit. The existing open excavation time limit of 36hrs for bentonite should remain. Future engineering review and analysis (EAR) documents could consider this 10% reduction when re-computing the resulting side shear capacity when this limit is inadvertently exceeded.

While present state specifications defer to slurry manufacturer recommendations for slurry viscosity, none of the sites discussed above met those specifications. This may have been the by-product of unclear recommendations. For instance, if clay is anticipated during an excavation then it is conceivable an interpretation might lead to the use of clay soil slurry recommendations even when sands are also present. In reality, the highest required viscosity for any soil layer

encountered should control. While variations in polymer slurry exist between manufacturers, it is reasonable to restrict use of any polymer for viscosity less than perhaps 50 or 60sec/qt. Higher values may be required for free flowing strata, but under no circumstances should it fall below the threshold. Further, the cost of slurry products is quite small relative to the cost of concrete and excavation (on the order of 0.1%) and the amount of slurry product required to increase slurry viscosity from 40 to 50sec/qt is insignificant (e.g. 1lb/1000gal).

Slurry testing frequency / depth intervals should be sufficient to monitor changes in slurry properties and for all portions of the shaft length. Present depth interval specifications have been updated to reflect these concerns (FDOT, 2018).

No data concerning the effects of slurry type on clayey soil was presented but should be considered for future review.

References

AASHTO (2012). "AASHTO LRFD Bridge Design Specifications", Customary U.S. Units. ISBN: 978-1-56051-523-4, Publication Code: LRFDUS-6.

AASHTO (2016). "AASHTO LRFD Bridge Construction Specifications", 3rd Edition, with 2010, 2011, 2012, 2014, 2015, and 2016 Interim Revisions. ISBN number: 978-1-56051-452-7.

AHTD (2014). "Standard Specification for Highway Construction". Arkansas State Highway and Transportation Department.

ALDOT (2012). "Standard Specifications for Highway Construction". State of Alabama Department of Transportation.

ADOT (2008). "Standard Specifications for Road and Bridge Construction". State of Arizona Department of Transportation.

AKDOT (2015). "Standard Specifications for Highway Construction". State of Alaska Department of Transportation.

Aurora, R. P., and Reese, L. C. (1976). "Behavior of Axially Loaded Drilled Shafts in Clay-Shales". Research Report No 176-4 – The Behavior of Drilled Shafts, Center for Highway Research, The University of Texas at Austin.

Baxter, C. D. P., Page, M., Bradshaw, A. S., and Sherrill, M. (2005). "Guidelines for Geotechnical Investigations in Rhode Island, Final Report". RIDOT – Rhode Island Department of Transportation.

Bernal, J. B., and Reese, L. C. (1983). "Study of the Lateral Pressure of Fresh Concrete as Related to the Design of Drilled Shafts". Research Report No 308-1F, Center for Transportation Research, The University of Texas at Austin.

Brown, D.A. and Vinson, J. (1998). "Comparison of strength and stiffness parameters for a Piedmont residual soil," Geotechnical Site Characterization, ISC'98, P.K. Robertson and P.W. Mayne, eds, Vol. 2, Balkema, Rotterdam, 1229-1234.

Brown, D.A. and Drew, C. (2000). "Investigation of Axial Capacity of Augered Displacement Piles at the Auburn University Test Site" New Technological and Design Developments in Deep Foundations, GSP 100, N.D. Dennis, R. Castelli, and M.W.O'Neill, eds., ASCE, New York, N.Y., pp. 397-403.

Brown, D. (2002). "Effect of Construction on Axial Capacity of Drilled Foundations in Piedmont Soils." Journal of Geotechnical and Geoenvironmental Engineering, Vol. 128, No. 12, pp. 967-973, (doi: http://dx.doi.org/10.1061/(ASCE)1090-0241(2002)128:12(967)).

Caliari de Lima, L. (2008). "Analyzes of static load tests in micropiles used in the foundation reinforcement of a historical bridge in Downtown Recife-PE, Brazil." Master thesis, Federal University of Pernambuco, Brazil, 187p.

CALTRANS (2010). "Standard Specifications". State of California, Business, Transportation and Housing Agency, Department of Transportation.

Camp, W.M., Brown, D.A., and Mayne, P.W. (2002). "Construction Methods Effects on Drilled Shaft Axial Performance." Deep Foundations 2002, Geotech Spec. Publ. 116, M.W. O'Neill and F. C. Townsend, eds., ASCE, Reston, VA, pp. 193-208.

CDOT (2011). "Standard Specifications for Road and Bridge Construction". State of Colorado Department of Transportation.

Cernak, B. (1976), "The Time Effect of Suspension on the Behavior of Piers." Proceedings. Sixth European Conference on Soil Mechanics and Foundation Engineering, 1.1, Vienna, March, pp. 111-114.

Chang, M. and Zhu, H. (2004). "Construction Effect on Load Transfer along Bored Piles." Journal of Geotechnical and Geoenvironmental Engineering, American Society of Civil Engineers, 130(4), 426–437.

Chen, YJ, and Kulhawy, F. H. (1994). "Case History Evaluation of Behavior of Drilled Shafts Under Axial & Lateral Loading". Report TR-104601, EPRI, Palo Alto.

Chen, YJ, and Kulhawy, F. H. (2002). "Evaluation of Drained Axial Capacity for Drilled Shafts". Deep Foundations 2002: pp. 1200-1214. doi: 10.1061/40601(256)86.

Clayton, C. R. I., and Milititsky, J. (1983). "Installation effects and the performance of bored piles in stiff clay". Ground Engineering, 16, (2), 17-22.

ConnDOT (2005). "Geotechnical Engineering Manual". State of Connecticut Department of Transportation.

ConnDOT (2009). "Drilled Shafts Guide and Specifications". State of Connecticut Department of Transportation. www.ct.gov/dot/lib/dot/documents/dsoils/ConnDOTGuideDrilledShaftSpec.pdf

Cooke, R.W. (1979). "Load Transfer from Bored, Cast-in-Situ Piles in London Clay,"Behavior of Deep Foundations, STP 670, ASTM, Philadelphia, PA, pp. 250-263.

Darley, H. C., and Gray, G. R. (1988), "Composition and Properties of Drilling and Completion Fluids". Fifth Edition, Gulf Publishing Company, Houston, TX, 643 pp.

Day, R. W. (2010). "Foundation Engineering Handbook: Design and Construction with the 2009 International Building Code, Second Edition". Edition: 2nd ed. New York. The McGraw-Hill Companies, Inc., ASCE Press, ISBN: 978-0-07-174010-4, MHID: 0-07-174010-4.

Deese, G. G. (2004). "Slurry sand content and concrete interaction in drilled shaft construction." Master thesis, University of South Florida, Tampa, FL, 117p.

DelDOT (2001). "Standard Specifications for Road and Bridge Construction". The Delaware Department of Transportation.

DOTD (2006). "Standard Specifications for Roads and Bridges". State of Louisiana Department of Transportation and Development.

Engeling, D. E., and Reese, L. C. (1974). "Behavior of Three Instrumented Drilled Shafts Under Short Term Axial Loading". Research Report No 176-3 – The Behavior of Drilled Shafts, Center for Highway Research, The University of Texas at Austin.

FDOT (2007). "Standard Specifications for Road and Bridge Construction". State of Florida Derpartment of Transportation, 2007.

FDOT (2009). "Standard Specifications for Road and Bridge Construction". State of Florida Derpartment of Transportation, 2009.

FDOT (2014). "Standard Specifications for Road and Bridge Construction". State of Florida Derpartment of Transportation, 2014.

Fleming, W. K., and Sliwinski, Z. J. (1977). "The use and influence of bentonite in bored pile constuction." Report PG3, Construction Industry Research and Information Association, London, England.

FHWA (2010). "Drilled Shafts: Construction Procedures and LRFD Design Methods," NHI Course No. 132014, FHWA-NHI-10-016, FHWA GEC 010, U.S. Department of Transportation, Federal Highway Administration.

Frizzi, R. P., Meyer, M. E. and Zhou, L. (2004). *"Full scale field performance of drilled shafts constructed utilizing bentonite and polymer slurries"*. Proceedings, GeoSupport Conference 2004, Orlando, FL, American Society of Civil Engineers, pp. 573-586.

GDOT (2013). "Section 524 – Drilled Caisson Foundations". Special Provision, Department of Transportation, State of Georgia.

Hegazy, Y. A., Cushing, A. G., and Lewis, C. J. (2004). "Driven Pile Capacity in Clay and Drilled Shaft Capacity in Rock from Field Load Tests". Proceedings of the Fifth International Conference on Case Histories in Geotechnical Engineering, April 13-14, 2004, New York.

Holden, J.C. (1984). "Construction of Bored Piles in Weathered Rock, Part 4: Bentonite Construction Procedures," Technical Report No.6, Road Construction Authority of Victoria, Australia.

HIDOT (2005). "Standard Specifications and Special Provisions". State of Hawaii Department of Transportation – Highways.

IDOT (2012). "Standard Specifications for Road and Bridge Construction". State of Illinois Department of Transportation.

INDOT (2015). "Standard Specifications". State of Indiana Department of Transportation.

Iowa DOT (2012). "Standard Specifications for Road and Bridge Construction". State of Iowa Department of Transportation.

ITD (2012). "Standard Specifications for Highway Construction". Idaho Transportation Department.

KSDOT (2015). "Standard Specifications for State Road and Bridge Construction". State of Kansas Department of Transportation.

Kulhawy, F. H., and Hirany, A. (1989). "Interpretation of Load Tests on Drilled Shafts, Pt. 2: Axial Uplift". Foundation Engineering: Current Principles & Practices (GSP 22), Ed. FH Kulhawy, ASCE, New York, 1150-1159.

Kulhawy, F. H., Trautmann, C. H., Beech, J. F., O'Rourke, T. D., McGuire, W., Wood, W. A., and Capano, C. (1983). "Transmission Line Structure Foundations for Uplift-Compression Loading". Report EL-2870, EPRI, Palo Alto.

KYTC (1997). "Special Note 11C – Drilled Shafts". Kentucky Transportation Cabinet, http://transportation.ky.gov/Construction/Special%20Notes%20and%20Special%20Provisions/SPECIAL%20NOTE%2011C%20DRILLED%20SHAFTS.doc

Lam, C., Jefferis, S., and Martin, C. M. (2014). "Effects of polymer and bentonite support fluids on concrete–sand interface shear strength." Geotechnique 64, No. 1, 28–39 [http://dx.doi.org/10.1680/geot.13.P.012].

Lam, C. and Jefferis, S. (2015). "Performance of Bored Piles Constructed Using Polymer Fluids: Lessons from European Experience." J. Perform. Constr. Facil., 10.1061/(ASCE)CF.1943-5509.0000756 , 04015024.

Maine DOT (2014). "Standard Specifications". State of Maine Department of Transportation.

Mayne, P.W. (2007). NCHRP Synthesis 368: "Cone Penetration Testing", Transportation Research Board, National Research Council, Washington, D.C., 117 p.

Majano, R. E. (1992). "*Effect of mineral and polymer slurries on perimeter load transfer in drilled shafts,*" Ph.D. dissertation, University of Houston, TX, 388p.

MassDOT (2012). "Supplemental Specifications to the 1988 English Standard Specifications for Highways and Bridges and the 1995 Metric Standard Specifications for Highways and Bridges". State of Massachusetts Department of Transportation, Highway Division.

MDT (2014). "Standard Specifications for State Road and Bridge Construction". State of Montana Department of Transportation.

MDOT (2012). "Standard Specifications for Construction". State of Michigan Department of Transportation.

MDOT (2008). "Standard Specifications for Construction and Materials". Maryland Department of Transportation, State Highway Administration.

MDOT (2004). "Mississippi Standard Specifications for Road and Bridge Construction". State of Mississippi Department of Transportation.

MNDOT (2014). "Standard Specifications for Construction". Department of Transportation, St. Paul, Minnesota.

MODOT (2011). "Specification Book for Highway Construction". State of Missouri Department of Transportation.

Mullins, A. G., Winters, D., Bowen, J., Johnson, K., DePianta, V., Vomacka, J., and Mullins, M. (2013). "Defining the Upper Viscosity Limit for Mineral Slurries Used in Drilled Shaft Construction." Final Report, FDOT BDK84 977-24.

Mullins, A. G. (2012) Load Testing of Drilled Shafts Constructed with CETCO Polymer Slurry, Final Report, 65 pp.

NCDOT (2012). "Standard Specifications for Roads and Structures". North Carolina Department of Transportation.

NDDOT (2014). "Standard Specifications for Road and Bridge Construction". North Dakota Department of Transportation.

NDOR (2014). "Bridge Office of Policies and Procedures – BOPP". Nebraska Department of Roads, Bridge Divison.

NDOT (2014). "Standard Specifications for Road and Bridge Construction". State of Nevada Department of Transportation.

NHDOT (2010). "Standard Specifications for Road and Bridge Construction". State of New Hampshire Department of Transportation.

NJDOT (2007). "Standard Specifications for Road and Bridge Construction". Updated 2007 Standard Specifications for Road and Bridge Construction, 2015. State of New Jersey Department of Transportation.

NMDOT (2014). "Standard Specifications for Road and Bridge Construction". New Mexico State Department of Transportation.

NYSDOT (2008). "Standard Specifications". State of New York Department of Transportation.

ODOT (2009). "Standard Specifications". Oklahoma Department of Transportation.

Ohio DOT (2013). "Construction and Material Specifications". State of Ohio Department of Transportation.

O'Neill, M. W. (1981). "Drilled Piers and Caissons". Proceedings of a session sponsored by the Geotechnical Engineering Division at the ASCE National Convention, St. Louis, Missouri. ISBN 0-87262-285-1.

O'Neill, M. W., and Hassan, K. M. (1994). "Drilled Shafts: Effects of Construction on Performance and Design Criteria." Proceedings: International Conference on Design and Construction of Deep Foundations. Volume I, Keynote Papers. US Federal Highway Administration (FHWA), pp 137-187.

O'Neill, M. (2000). "National Geotechnical Experimentation Site: University of Houston." National Geotechnical Experimentation Sites, American Society of Civil Engineers: pp. 72-101. doi: 10.1061/9780784404843.ch04.

O'Neill, M.W., and Reese, L. C. (1970). "Behavior of Axially Loaded Drilled Shafts in Beaumont Clay, Part One – State of the Art". Research Report No 89-8 – Soil Properties as Related to Load-Transfer Characteristics of Drilled Shafts, Center for Highway Research, the University of Texas at Austin.

O'Neill, M.W., and Reese, L. C. (1970). "Behavior of Axially Loaded Drilled Shafts in Beaumont Clay, Part Four – Design Inferences and Conclusions". Research Report No 89-8 – Soil Properties as Related to Load-Transfer Characteristics of Drilled Shafts, Center for Highway Research, the University of Texas at Austin.

O'Neill, M.W., and Reese, L. C. (1978). "Load Transfer in a Slender Drilled Pier in Sand". Preprint 3141, ASCE Spring Convention and Exhibit, April 24-28, 1978, Pittsburgh, Pennsylvania.

O'Neill, M. W., and Reese, L. C. (1999). Drilled Shafts: Construction Procedures and Design Methods. DTFH6 1-96-2-0005, Report Number FHWA-IF-99-025.

O'Neill, M. W. (2001). "Side Resistance In Piles and Drilled Shafts." J. Geotech. Geoenviron. Eng., 127(1), 3–16. 34th Terzaghi Lecture.

O'Neill, M. W. (1998). "Project 89 Revisited". Proceedings of the ADSC Drilled Shaft Foundation Symposium held to honor Dr. Lymon C. Reese, January 30, 1998, Austin, Texas.

Oregon DOT (2015). "Standard Specifications for Construction". Oregon Department of Transportation.

Owens, M. J., and Reese, L. C. (1982). "The Influence os a Steel Casing on the Axial Capacity of a Drilled Shaft". Research Report No 255-1F, Center for Transportation Research, The University of Texas at Austin.

PennDOT (2008). "Construction Manual". Commonwealth of Pennsylvania Department of Transportation.

Quiros, G. W., and Reese, L. C. (1977). "Design Procedures for Axially Loaded Drilled Shafts". Research Report No 176-5F – The Behavior of Drilled Shafts, Center for Highway Research, The University of Texas at Austin.

Reese, L. C., and Hudson, W. R. (1968). "Field Testing of Drilled Shafts to Develop Design Methods". Research Report No 89-1 – Soil Properties as Related to Load-Transfer

Characteristics of Drilled Shafts, Center for Highway Research, the University of Texas at Austin.

Reese, L. C, O'Neill, M. W., and Touma, F. T. (1973). "Bored piles installed by slurry displacement." Proc, 8th International Conference on Soil Mechanics and Foundations Engineering, Moscow, U.S.S.R.

Reese, L. C., and O'Neill, M. W. (1971). "Criteria for the Design of Axially Loaded Drilled Shafts". Research Report No 89-11F – Soil Properties as Related to Load-Transfer Characteristics of Drilled Shafts, Center for Highway Research, The University of Texas at Austin.

Reese, L. C., and O'Neill, M. W. (1988a). "Drilled Shafts: Construction Procedures and Design Methods". US Department of Transportation, FHWA, Office of Implementation, McLean, Virginia.

Reese, L. C., and O'Neill, M. W. (1988b). "Field Load Tests of Drilled Shafis," in Proceedings, International Seminar on Deep Foundations on Bored and Auger Piles, Van Impe (ed.), Balkema, Rotterdam, June, pp. 145-192.

Reese, L. C., and Wright, S. J. (1977). "Drilled Shaft Design and Construction Guidelines Manual", Volume I. US Department of Transportation, FHWA, Offices of Research and Development, Implementation Division, Washington, D.C.

Reynaud, P., and Riviere, P. (1981). "Mesure des Pressions Developpees Dans une Paroi Moulee en Cours de Betonnage". Bulletin Maiso Laboratoire des Ponts et Chaussees, No. 113, Mai/Juin, Paris, France, 1981, pp 135 through 138.

Saye, S. R., Brown, D. A., and Lutenegger, A. J. (2013). "Assessing Adhesion of Driven Pipe Piles in Clay Using Adaptation of Stress History and Normalized Soil Engineering Parameter Concept". Journal of Geotechnical and Geoenvironmental Engineering, ASCE, 2013.139:1062-1074.

SCDOT (2007). "Standard Specifications for Highway Construction". South Carolina Department of Transportation.

SDDOT (2015). "Standard Specifications for Roads and Bridges". South Dakota Department of Transportation.

Shakyr, R. R., and Zhu, J. (2010). "An examination of the mechanical interaction of drilling slurries at the soil-concrete contact." Journal of Zhejiang University-Science, Applied Physics & Engineering, 2010 11(4):294-304.

Stas C.V., and Kulhawy F.H. (1984). "Critical evaluation of design methods for foundations under axial uplift & compression loading". Report EL-3771, Electric Power Research Institute, Palo Alto.

Tabsh, S. W., O'Neill, M. W., and Nam, M. S. (2005). "Shear strength of drilled shafts with minor flaws". Engineering Structures, Volume 27, Issue 5, April 2005, Pages 736–748.

TDOT (2015). "Standard Specifications for Road and Bridge Construction". Tennessee Department of Transportation.

Tomlinson, M. J. (1957). "The Adhesion of Piles Driven in Clay Soils". Proceedings of the Fourth International Conference on Soil Mechanics and Foundation Engineering, Volume II. August 12-24, 1957, London, England.

Touma, F. T. (1972). "The Behavior of Axially Loaded Drilled Shafts in Sand". Ph.D Dissertation, the University of Texas at Austin, December, 1972, Austin, Texas.

Touma, F. T., and Reese, L. C. (1972). "The Behavior of Axially Loaded Drilled Shafts in Sand". Research Report No 176-1 – The Behavior of Drilled Shafts, Center for Highway Research, the University of Texas at Austin.

Turner, J. P. (1992). *"Constructability for Drilled Shafts"*. Journal of Construction Engineering and Management, American Society of Civil Engineers, 10.1061/(ASCE)0733-9364(1992)118:1(77), 77-93.

TXDOT (2014). "Standard Specifications for Construction and Maintenance of Highways, Streets, and Bridges". Texas Department of Transportation.

UDOT (2012). "Standard Specifications for Road and Bridge Construction". Utah Department of Transportation.

VDOT (2007). "Road and Bridge Specifications". Virginia Department of Transportation.

Vermont DOT (2011). "Standard Specifications for the Construction Book". Vermont Agency of Transportation.

WisDOT (2015). "2016 Standard Specifications". Wisconsin Department of Transportation.

WisDOT (2013). "Drilled Shaft Foundation, Special Provision 0090." wisconsindot.gov/dtsdManuals/strct/spec-provs/drldshft.doc

Wooley, J. A., and Reese, L. C. (1974). "The Behavior of an Axially Loaded Drilled Shaft Under Sustained Loading". Research Report No 176-2 – The Behavior of Drilled Shafts, Center for Highway Research, The University of Texas at Austin.

WSDOT (2014). "Standard Specifications for Road, Bridge and Municipal Construction". Washington State Department of Transportation.

WVDOH (2010). "Standard Specifications – Roads and Bridges". West Virginia Division of Highways.

WYDOT (2010). "Standard Specifications for Road and Bridge Construction". State of Wyoming Department of Transportation.